Trapping Efficiencies for the BLH-84, Helley-Smith, Elwha, and TR-2 Bedload Samplers

John Robert Gray

Dissertation submitted to the faculty of the Virginia Polytechnic Institute and State University in partial fulfillment of the requirements for the degree of

Doctor of Philosophy
in
Civil Engineering

Committee Chair: Panayiotis Diplas
Committee Co-Chair Adil N. Godrej
Jonathan A. Czuba
Kyle B. Strom

(May 13, 2019)
Manassas, Virginia

Keywords: bedload, bedload transport, sediment transport, total load, bedload sampler, bedload sampler calibration, bedload sampler trapping efficiency

Trapping Efficiencies for the BLH-84, Helley-Smith, Elwha, and TR-2 Bedload Samplers

John Robert Gray

ACADEMIC ABSTRACT

Bedload-trapping efficiencies for four types of pressure-difference bedload samplers – a standard Helley-Smith (intake-nozzle width and height of 76.2 mm x 76.2 mm), BLH-84 (76.2 mm x 76.2 mm), Elwha (203 mm x 102 mm) and Toutle River-2 (TR-2; 305 mm x 152 mm) were calculated from data collected during the StreamLab06 Phase I and II experiments in the St. Anthony Falls Laboratory Main Flume during January-March 2006. A sampler's trapping coefficient quantifies its bedload-trapping efficiency. A technically supportable coefficient is divided into a raw trapping rate measured by a sampler to correct for sampling bias. For example, a coefficient of 1.5 would result in a sampler capturing 50-percent more bedload than would have transited in the sampler's absence.

A key factor influencing a sampler's trapping efficiency is its nozzle-flare ratio: the area of the nozzle's outlet divided by its inlet area. The BLH-84, Elwha, and TR-2 each have nozzle-flare ratios of 1.4. That for the Helley-Smith is 3.22.

Six combinations of sampler and bed types were tested at steady flows during Phases I and II of the StreamLab06 experiments: the BLH-84, Elwha, and Helley-Smith samplers were deployed atop a sand bed (D_{50} = 1.0 mm) during five flows ranging from 2.0-3.6 m^3/s. The BLH-84, Elwha, and TR-2 were deployed atop a gravel bed (D_{50} = 11.2 mm) at four flows ranging from 4.0-5.5 m^3/s.

Thirty-seven trials – each comprised of repeated manual at-a-point deployments of a bedload sampler for a given steady flow and bed type – took place. Trapping coefficients were calculated for each sampler and bed type in which it was deployed. Ergo, two of the samplers – the BLH-84 and Elwha – were each assigned two trapping efficiencies for sampling on a sand versus a gravel bed.

These data were evaluated using four analytical methods as follows:

Ratio of Averages: This relatively simple and straight-forward method calculated averages of untransformed bedload-transport rates derived for each of the 37 trials for a given bedload sampler and the nine combinations of weigh drums and time windows.

Average of Ratios: This more complex method, based on untransformed data, developed average transport rates from data produced by the weigh drums for each of the 2,030 bedload samples. Running-average transport rates were calculated for the drums at intervals equal to the duration of a single at-a-point bedload measurement, which ranged from 15-180 seconds. Ratios (trapping coefficients) were calculated by dividing each single-sample trap rate by the respective interval average from one or a combination of weigh drums. Those ratios were averaged to produce a single trapping coefficient for a trial which, in turn, were combined to derive a single coefficient for each combination of bedload sampler and bed type.

Modified Thomas and Lewis Model (1993): The Thomas-Lewis Model was revised to operate using untransformed data in addition to cube-root transformed data (thus, the third and fourth analytical methods used, respectively), and to use nine pan-window combinations to calculate trapping coefficients. The original 3-step model required first regressing cube root-transformed sampler data on time-window averaged pan transport rates. The second step squared the regression residuals from the first step on the variance of the cube root of the interval-mean transport rate for the time window. The predicted values from the second-step regression were inverted and used as weights to re-estimate the first-step regression. This model was considered to produce the most reliable coefficient values.

Generalized trapping-coefficients were computed using each analytical method. Those relying largely on coefficients from the modified Thomas and Lewis (1993) model in real space follow:

- BLH-84 Sampler: A 0.83 sand-bed trapping coefficient and 0.87 gravel-bed coefficient, which are suggested to be averaged to a single coefficient of 0.85.
- Elwha Sampler: A 1.67 sand-bed trapping coefficient and 1.54 gravel-bed coefficient, which are suggested to be averaged to a single coefficient of 1.6.
- Helley-Smith Sampler: The 3.11 sand-bed trapping coefficient could be applied as such or reasonably simplified to a value of 3.0, and
- TR-2 Sampler: The gravel-bed trapping coefficient equaled 1.70.

The data produced, and analysis subsequently performed as part of these experiments consistently infer – under the conditions in which the samplers were tested – that the Elwha (sand and gravel), and TR-2 (gravel) trap bedload at least 50-percent super-efficiently; and that the Helley-Smith traps sand about 300-percent super-efficiently. In contrast, the BLH-84, with a mean sand-and-gravel coefficient of 0.85, was the sole sampler to trap bedload close to unity, albeit sub-efficiently.

The coefficients generated through the Phases I and II of the StreamLab06 experiments may also be applied, albeit provisionally, to raw bedload-transport data from the BLH-84, Elwha, and TR-2 samplers deployed atop riverbeds coarser or finer than those in which each sampler was deployed during StreamLab06 Phases I and II, and (or) at flow velocities differing substantially from those in which these bedload samplers were tested. However, the validity of applying these bias-correction coefficients under conditions differing from those in which the samplers were tested may be inferred but not verified based on the results of the StreamLab06 experiments.

The data and analytical results described herein support the conclusion that raw (uncorrected) bedload-transport rates produced by three of the four samplers tested – the Elwha, TR-2 and Helley-Smith samplers – under the conditions in which each was tested during the StreamLab06 experiments – produce substantially positively biased results that unequivocally require correction for inherent sampler bias to produce results consistent with ambient riverine bedload-transport rates. The raw data produced by the BLH-84 would also benefit from correction for sampling bias. Stated otherwise, there is no technically supportable reason refrain from applying bias-corrections coefficients to the raw data produced by any of these samplers given the availability of selected, technically supportable sampling coefficients produced by bedload-sampler calibration experiments performed in the St. Anthony Falls Laboratory Main Flume.

GENERAL AUDIENCE ABSTRACT

Bedload-trapping efficiencies for four types of pressure-difference bedload samplers – a BLH-84 (intake-nozzle width and height of 76.2 mm x 76.2 mm), Helley-Smith, BLH-84 (76.2 mm x 76.2 mm), Elwha (203 mm x 102 mm) and Toutle River-2 (TR-2; 305 mm x 152 mm) – were calculated from data collected during the StreamLab06 experiments in the St. Anthony Falls Laboratory Main Flume during January-March 2006. A sampler's trapping coefficient quantifies its bedload-trapping efficiency. A technically supportable coefficient is divided into a raw trapping rate measured by a sampler to correct for sampling bias. For example, a coefficient of 1.5 would result in a sampler capturing 50-percent more bedload than would have transited in the sampler's absence.

A sampler's trapping coefficient quantifies its bedload-trapping efficiency. A technically supportable trapping coefficient is divided into raw trapping rate measured by the sampler to produce a "true" bedload-transport rate. For example, a coefficient of 2.0 would result in the sampler capturing double that which would have passed in the absence of the sampler.

A key factor influencing a sampler's trapping efficiency is its nozzle-flare ratio: the area of the nozzle's outlet divided by its inlet area. The BLH-84, Elwha, and TR-2 each have nozzle-flare ratios of 1.4. That for the Helley-Smith is 3.22.

Six combinations of sampler and bed types were tested at steady flows during Phases I and II of the StreamLab06 experiments: the BLH-84, Elwha, and Helley-Smith samplers were deployed atop a sand bed (D_{50} = 1.0 mm) during five flows ranging from 2.0-3.6 m^3/s. The BLH-84, Elwha, and TR-2 were deployed atop a gravel bed (D_{50} = 11.2 mm) at four flows ranging from 4.0-5.5 m^3/s.

Thirty-seven trials – each comprised of repeated manual at-a-point deployments of a bedload sampler for a given steady flow and bed type – took place. Trapping coefficients were calculated for each sampler and bed type in which it was deployed. Ergo, two of the samplers – the BLH-84 and Elwha – were each assigned two trapping efficiencies for sampling on a sand versus a gravel bed. These data were evaluated using four analytical methods:

Ratio of Averages: This relatively straight-forward and simple method used untransformed data to derive trapping coefficients from averages of bedload-transport rates for the bedload samplers and selected combinations of time intervals ("windows") and weigh pans.

Ratio of Averages: This relatively simple and straight-forward method calculated averages of untransformed bedload-transport rates derived for each of the 37 trials for a given bedload sampler and the nine combinations of weigh drums and time windows.

Average of Ratios: This more complex method, based on untransformed data, developed average transport rates from data produced by the weigh drums for each of the 2,030 bedload samples. Running-average transport rates were calculated for the drums at intervals equal to the duration of a single at-a-point bedload measurement, which ranged from 15-180 seconds. Ratios (trapping coefficients) were calculated by dividing each single-sample trap rate by the respective interval average from one or a combination of weigh drums. Those ratios were averaged to produce a single trapping coefficient for a trial which, in turn, were combined to derive a single coefficient for each combination of bedload sampler and bed type.

Modified Thomas and Lewis Model (1993): The Thomas-Lewis Model was revised to operate using untransformed data in addition to cube-root transformed data (thus, the third and fourth analytical methods used, respectively), and to use nine pan-window combinations to calculate trapping coefficients. The original 3-step model required first regressing cube root-transformed sampler data on time-window averaged pan transport rates. The second step squared the regression residuals from the first step on the variance of the cube root of the interval-mean transport rate for the time window. The predicted values from the second-step regression were inverted and used as weights to re-estimate the first-step regression. This model was considered to produce the most reliable coefficient values.

Generalized trapping-coefficients were computed using each analytical method. Those relying largely on coefficients from the modified Thomas and Lewis (1993) model in real space follow:

- BLH-84 Sampler: A 0.83 sand-bed trapping coefficient and 0.87 gravel-bed coefficient, which could be averaged to a single coefficient of 0.85.
- Elwha Sampler: A 1.67 sand-bed trapping coefficient and 1.54 gravel-bed coefficient, which could be averaged to a single coefficient of 1.6.
- Helley-Smith Sampler: The 3.11 sand-bed trapping coefficient could be applied as such or reasonably simplified to a value of 3.0, and
- TR-2 Sampler: The gravel-bed trapping coefficient equaled 1.7.

The coefficients generated through the Phases I and II of the StreamLab06 experiments may also be applied, albeit provisionally, to raw bedload-transport data from the BLH-84, Elwha, and TR-2 samplers deployed atop riverbeds coarser or finer than those in which each sampler was deployed during StreamLab06 Phases I and II, and (or) at flow velocities differing substantially from those in which these bedload samplers were tested. However, the validity of applying these bias-correction coefficients under conditions differing from those in which the samplers were tested may be inferred but not verified based on the results of the StreamLab06 experiments.

The data produced, and analysis subsequently performed as part of these experiments consistently infer – under the conditions in which the samplers were tested – that the Elwha (sand and gravel), and TR-2 (gravel) trap bedload at least 50-percent super-efficiently; and that the Helley-Smith traps sand about 300-percent super-efficiently. In contrast, the BLH-84, with a mean sand-and-gravel coefficient of 0.85, was the sole sampler to trap bedload close to unity, albeit sub-efficiently.

The data and analytical results described herein support the conclusion that raw (uncorrected) bedload-transport rates produced by three of the four samplers tested – the Elwha, TR-2 and Helley-Smith samplers – under the conditions in which each was tested during the StreamLab06 experiments – produce substantially positively biased results that unequivocally require correction for inherent sampler bias to produce results consistent with ambient riverine bedload-transport rates. The raw data produced by the BLH-84 would also benefit from correction for sampling bias. Stated otherwise, there is no technically supportable reason refrain from applying bias-corrections coefficients to the raw data produced by any of these samplers given the availability of selected, technically supportable sampling coefficients produced by bedload-sampler calibration experiments performed in the St. Anthony Falls Laboratory Main Flume.

DEDICATION

The "Saga" of the author's Ph.D. program, for which data collection took place in 2006, owes its origins to Virginia Tech's Dr. Tom Grizzard, then-Director of the Occoquan Water Monitoring Laboratory in Manassas, Virginia. Ironically, it was Tom's untimely and tragic demise in 2017 that provided the impetus for the successful closure of this "Saga."

In spite of our relatively small difference in age, Tom was a mentor in addition to a most-valued colleague and friend. This dissertation and the Virginia Tech Ph.D. in Civil Engineering conferred upon me are dedicated to the memory of this most-valued colleague and friend.

ACKNOWLEDGEMENTS

This dissertation would not exist but for the encouragement and support of many. These include:

- **Present Committee Members**: Co-chairs Panayiotis Diplas (Lehigh University) and Adil Godrej; and Jonathan A. Czuba and Kyle Strom (Virginia Tech), whose support, insights, collaboration, and encouragement were fundamental toward the success of this project.

- **Past Committee Members**: Peter Wilcock (presently at Utah State University, formerly at Johns Hopkins University) and Gregory Schwarz (U.S. Geological Survey; "USGS") in addition to Tom Grizzard. The former two graciously resigned as committee members in 2017 due to institutional committee representation rules.

- **Primary Collaborator**: The statistical expertise and seemingly infinite patience of the USGS's Gregory Schwarz were instrumental in producing the analyses and results in this dissertation. It was through our dozens of convocations that the four analytical techniques that produced the results herein were developed. His participation and support defined the word, "collegial," and will never be forgotten.

- **Bedload-Data Collection**: The 2,030 bedload samples that were used in this analysis were collected through a selfless, collaborative effort, led by the USGS with the considerable involvement of the Federal Interagency Sedimentation Project. In addition to the author, the following personnel participated in bedload-data collection: Broderick Davis and Johnny McGregor, Federal Interagency Sedimentation Project; Robert Hilldale, Bureau of Reclamation; John Pitlick, University of Colorado; Smokey Pittman and Wes Smith, Graham Matthews and Associates; and Sarah Johnson, St. Anthony Falls Laboratory. Jeff Marr, Chris Ellis, and David Dean of the St. Anthony Falls Laboratory in 2006 provided the oversight and support for the collection of the "ground truth" bedload data from the Main Flume. The over-arching support of the St. Anthony Falls Laboratory and National Center for Earth-Surface Dynamics were fundamental to the initiation and execution of the StreamLab06 experiments.

- **Dissertation Support**: The training, statistical assessments, and (or) help in generating plots provided by Joel Groten, David Dean, Gregory Noe, Harry Jenter, and Annette Goode (USGS) and Michael McDonnell (volunteer, USGS) are greatly appreciated. Kristin Bunte, Colorado State University, provided her usual keen insights that helped to explain some of the findings herein. Babette Welch and Darien Brost provided invaluable editorial support toward submission of this document to the Virginia Tech Graduate School.

- **Technical Foundation**: My 37-year USGS career – the last 17 years of which were served as the National Sedimentologist in the Office of Surface Water, National Center, Reston, Virginia – provided the professional foundation that enabled my conception, implementation, and oversight of the bedload-sampler calibration experiments described herein. I am proud to continue my association with the USGS as a Scientist Emeritus.

  William Emmett, USGS (retired), protégé' of the USGS's Luna Leopold, provided my initial bedload-sampling techniques training in at the Army Corps of Engineers Rock Island District, Illinois, in 1978. To this day, he remains a mentor and most valued colleague.

  The mentorship of and collaboration with G. Douglas Glysson, USGS – a protégé of the Federal Interagency Sedimentation Project's first leader, Paul Benedict – that started in 1978 in Illinois was as timely as it was invaluable in my eventual career path and later career in sedimentology.

  I had the good fortune to collect bedload data from Washington's Elwha River with the developer of the Elwha bedload sampler, the USGS's Dallas Childers, albeit using a hand-held Helley-Smith sampler deployed from an anchored boat. I was his understudy as leader of the USGS training course, "Sediment-Data Collection Techniques," before his 1990s retirement. I also had the good fortune to "talk sediment" with David Hubbell of the USGS in 1986. I cannot overstate my appreciation and sense of good fortune in learning the intricacies of fluvial-sediment science from these and myriad other stalwart sedimentologists.

  Ben Chie Yen, Civil Engineering professor and my academic advisor, University of Illinois at Urbana-Champaign, led my initial graduate academic training that substantially augmented my field experience in sedimentology and resulted in my receiving a M.S. in Civil and Environmental Engineering from that institution.

  Others too numerous to name influenced my career. All those cited above provided the strong shoulders on which I metaphorically stood as I became immersed in the science and art of fluvial sedimentology. They share my perpetual gratitude.

- **Non-Technical Foundation**: Finally, I would be grossly remiss to exclude recognition of the patience and support of the mother of my two children who doubles as loving wife of 41-and-counting years – Heather Marie Gray. She stood by me with unwavering support through the thick-and-thin of this "Saga." From my heart with everlasting gratitude…

TABLE OF CONTENTS

SELECTED NOMENCLATURE

A number of terms used in this dissertation are either unique to the StreamLab06 bedload-sampler trapping efficiency experiments or may be arcane to some readers. Following are explanations for selected terms used in this dissertation:

- **Bedload**: That part of the total-sediment load that is transported by rolling, skipping, or sliding on the bed of the channel. Along with suspended sediment, it constitutes a watercourse's operationally defined total sediment load.

- **Bedload Sampler**: A device for collecting bedload. Those hand-deployed versions used in this study – the BLH-84 ("BL-84" when cable suspended), Helley-Smith, Elwha, and Toutle River-2 (TR-2) – are based on the pressure-difference principle designed to equalize the rate of streamflow through the sampler with the ambient flow rate. The Helley-Smith, with a nozzle exit area divided by its inlet area – its intake-flare ratio – of 3.22, was named after its developers, Ed Helley and Wink Smith of the U.S. Geological Survey in Sacramento, California.

  The Elwha sampler was named by its developer, Dallas Childers of the USGS Cascades Volcano Observatory, after Washington's Elwha River in which he deployed the sampler. The Toutle River-2 (TR-2) was developed for deployment in Washington's Toutle River and tributaries to enable collection of larger clasts than the other samplers described herein. The latter two samplers – and the BLH-84 (Bedload, Handheld, 1984) endorsed by the Federal Interagency Sedimentation Project– are 1.4-flare ratio variants of the Helley-Smith.

  Each of the aforementioned bedload samplers have hand- and cable-deployed versions. Only the cable-suspended version of the BLH-84 – the BL-84 – is uniquely designated among the four samplers. The key component of each sampler – the nozzle – is identical for a hand-deployed versus cable-suspended version of a given pressure-difference bedload sampler.

- **Bedload-sampler at-a-point deployment (or similarly phrased):** Placing a bedload-sampler on the channel bed for a recorded duration before its retrieval and transfer of its contents to a sample bag for subsequent weighing and in some cases size-distribution analysis.

- **Bedload-sampler cross-section deployment:** A series of at-a-point sampler deployments at the centroids of equal one-fifth-width intervals across the 2.74-meter-wide Main Flume at a location 8.5 meters (m) upstream from the flume slot and sub-surface weigh pans

- **Bedload-sampler trial:** A series of at-a-point sampler deployments, either at a single location or at several points in a cross-section, during a single steady-state discharge over a sand or gravel bed.

- **Data Transformations – Cube Root versus Real Space**: The bedload-trapping coefficient analyses were performed using cube root-transformed bedload-transport rates (consistent with those use by Hubbell and others (1987) and Thomas and Lewis (1993)), and non-transformed transport rates, also referred to somewhat redundantly as data "in real space."

- **Grave**l: The bed in Streamlab06 Phase II was composed of sediments ranging from 1–32 mm median diameters, with a D_{50}=11.2 mm median diameter. This distribution is usually referred to as simply as “medium gravel” or simply as “gravel” even though it is technically a medium-sand to medium-gravel distribution.

- **Run:** A given steady-state discharge in the Main Flume either continuous in time or including intervals of the steady-state discharge around flow stoppages, over a sand or gravel bed.

- **Sand**: The bed in Streamlab06 Phase I was composed of sediments ranging from 0.6-1.8 mm median diameters, with a median diameter of 1.0 mm. This distribution is usually referred to as “coarse sand” or simply as “sand” even though it is technically a medium-to-coarse sand distribution.

- **Set:** Compilation of bedload-transport and ancillary statistics associated with a given bedload sampler for all runs over a sand or gravel bed.

- **Time Window**: An interval of the time-series bedload-trapping data produced at approximately 1.1-second intervals during a given run selected for use in the bedload-trapping tests. Each of three time intervals was indexed to the duration that a bedload sampler was deployed on the bed using the at-a-point scheme to represent relatively short, medium, and long durations for bedload-sampler coefficient computations.

- **Weigh Pan (Drum)**: Each of five 0.55-m-wide pans (alternatively referred to as “drums”), contiguously arrayed within and across the entire width of the slot. Each pan – connected to a load-cell transducer – automatically, independently, and continuously trapped and weighed accumulating bedload. Upon attainment of a preset sediment mass, each pan individually and episodically dumped its contents into the bottom of the slot for automatic removal and recirculation to an upstream section of the flume.

Trapping Efficiencies for the BLH-84, Helley-Smith, Elwha, and TR-2 Bedload Samplers

John Robert Gray

1. Introduction

A study of sediment transport logically begins with theories of bedload movement because the discharge of bedload provides a basis for the computation of bed-material discharge and is also closely related to processes of erosion and deposition (Colby, 1963). Bedload – that part of the total sediment load that is transported by rolling, skipping, or sliding along the streambed (ASTM International, 1998) – provides the major process link between the hydraulic and material conditions that govern river-channel morphology. An understanding of bedload-transport mechanisms and what constitutes reliable data describing bedload-transport rates is important to engineers, scientists, managers, and others interested in the causes and consequences of changes in channel form and to make informed and technically supportable management decisions that affect a river's function (Gomez, 2006).

Information on bedload-transport rates can be obtained indirectly from empirical or theoretical equations, inferred directly from bedload-surrogate monitoring technologies, and (or) measured by physical samplers. The reliability and accuracy of riverine bedload-transport data obtained from empirical equations or surrogate technologies cannot be quantified, let alone verified, in the absence of demonstrably reliable ground-truth data. Thus, all technically supportable bedload-transport data are predicated on—that is, directly or indirectly derived from—physical bedload measurements from certifiably accurate and properly deployed bedload samplers. Hence, absent comparative, reliable physical bedload measurements, few if any bedload-transport data derived from empirical equations or from surrogate technologies can be considered unequivocally valid (Gray and Simões, 2008; Gray and others, in press).

As part of the 2003 Federal Interagency Sediment Monitoring Instrument and Analysis Research Workshop (Gray, 2005) sponsored by the Federal Interagency Sedimentation Project (FISP, 2019), a workgroup led by Ryan and others (2005) recognized an "overarching need for more thorough testing of the accuracy of existing [bedload samplers]," along with, "…better documentation of existing samplers, including information on limitations and uncertainty of the data obtained."

In May 2000, the author and colleague Larry Schmidt—acting in their capacities as U.S. Geological Survey (USGS) and U.S. Forest Service members, respectively, of the FISP Technical Committee—and Basil Gomez of Indiana State University, visited the St. Anthony Falls Laboratory (SAFL, University of Minnesota, Minneapolis) to ascertain the potential for the FISP to use the SAFL Main Flume to calibrate the bedload-trapping efficiency of the Elwha and other selected bedload samplers. This threesome was disappointed to learn that the Main Flume data-acquisition systems had fallen into disrepair and would require some $1.5 million (about $2.2 million in 2019 dollars) to renovate the facility and produce a dataset enabling the derivation of bedload-trapping coefficients for as many as four bedload samplers. This funding level was some two orders of magnitude beyond the financial means of the FISP. The concept was shelved.

But luck was with the FISP. In 2005, as part of the National Center for Earth-surface Dynamics's (NCED, 2017) investment in community-wide experimental earth-surface dynamics research, several improvements were made to the Main Flume. The goal of the NCED—funded by the National Science Foundation as a Science and Technology Center—was to equip the Main Flume with state-of-the-art flow- and sediment-transport monitoring technologies and make the facility available for use by the broader community for advancing science and practice of river ecohydromorphodynamics. The upgrades—completed in time for the initiation of Phase I of the StreamLab06 experiments in January 2006—included enhancements to the flow-control and sediment-recirculation systems; a state-of-the-art sediment-flux monitoring system; and ancillary monitoring upgrades (Singh and others, 2013).

The considerable costs associated with refurbishing the Main Flume, plus its operation as part of StreamLab06 Phases I and II experiments in January-March 2006, were borne by the NCED and the SAFL. These capital investments enabled the participating organizations and researchers in StreamLab06 to participate in segments of the bedload-sampler trapping-efficiency Phase I and II experiments using personnel and relatively affordable resources from their respective organizations.

The bedload-sampler trapping-coefficient experiments were but one of several such experiments taking advantage of the StreamLab06 Phase I flows over a coarse-sand bed, and Phase II flows over a medium-gravel bed (Singh and others, 2013). The competing needs of other researchers coupled with the inability for personnel to be available to deploy bedload samplers during all of the controlled flows unfortunately precluded the deployment of the bedload samplers during some of the more influential (medium-to-high) flows.

No universally agreed-upon method exists for calibrating portable bedload samplers (Gray and Simóes, 2008). However, given appropriate deployment gear, portable pressure-differential samplers can be deployed by hand-held rod or suspension cable from a variety of platforms including bridges, cableways, or boats without the need for pre-existing on-site support equipment.

The above factors – and Ryan and others (2005) statement of need that echoing the sentiment of FISP and the broader fluvial-sediment science community for the need for technically supportable sampling efficiencies of manually deployed pressure-difference bedload samplers – led to the StreamLab06 bedload-sampler trapping-efficiency experiments. Four pressure-difference bedload samplers: the BLH-84[1], Helley-Smith, Elwha, and Toutle River-2 (TR-2) were tested. All but the TR-2 were deployed during five steady flows over a sand bed (1.0-mm median diameter[2]), and all but the Helley-Smith were deployed during four steady flows over a gravel (11.2-mm) bed. Descriptions of the samplers, research facilities, experimental design, data-collection procedures, and analytical techniques follow, and precede the presentation of the experimental results.

2. Overview of Pressure-Difference Bedload Samplers

Bedload samplers can be classified according to one or a combination of the following types: box or basket, pan or tray, vortex tube, trough or pit, or pressure-difference bedload samplers (Hubbell, 1964). All four of the bedload samplers deployed during the StreamLab06 experiments operated on the pressure-difference principle (Helley and Smith, 1971; Tacconi and Billi, 1987; Kuhnle, 1991, 2008; International Standards Organization, 1992; Carey, 2005; Gray and others, 2010; Gray and others, in press).

A pressure-difference bedload-sampler is composed of a nozzle, mesh collection bag, and a means for supporting the trailing end of the bag. Cable-deployed versions include a supporting frame terminating in a stabilizing tail fin and a bag fastener. Rod-deployed versions typically are equipped with a narrow-diameter horizontal rod extending rearward from the bottom of the deployment rod with the mesh bag attached to its trailing end.

The sampler's key component—the nozzle—is a single feature composed of an upstream-oriented intake and a downstream-oriented outlet to which the mesh collection bag is affixed. Figure 1 is a schematic of the original Helley-Smith sampler nozzle with a 3.22 nozzle-flare ratio (Helley and Smith, 1971; Druffel and others, 1976). The rearward expansion of the nozzle is a defining and influential feature of a pressure-difference bedload sampler.

The pressure-difference-type bedload sampler was designed to equalize or moderately increase the velocity of the flow entering the sampler's nozzle with that which would have occurred in the same section of the bed in the absence of the deployed sampler (Hubbell, 1964; Helley and Smith, 1971; Carey, 2005; Gray and others, in press). This quest for a nozzle flow-through velocity roughly equaling or slightly exceeding the ambient flow velocity incident on the deployed sampler is important because, in general,

[1] The BLH-84 is a rod-deployed version of the cable-suspended BL-84. They share identically configured nozzles. Hereafter, referral to the BLH-84 can be construed as also being relevant and applicable to the BL-84 – and vice versa – unless otherwise stated.
[2] Hereafter reported particle-diameter values implicitly refer to their median (D_{50}) values unless otherwise qualified.

increases or decreases in ambient flow velocities typically result in concomitant changes in time-averaged bedload-transport rates.

Equalization of the flow velocity at the intake with respect to the ambient velocity is approximated through the creation of a pressure drop at the nozzle outlet by constructing walls that diverge rearward from the intake nozzle (Hubbell, 1964) (figure 1). The cross-sectional area of the outlet divided by that of the smaller inlet is the nozzle's "flare ratio" or "expansion ratio." The flare ratio is a fixed quantity for a given bedload sampler. In addition to the 1.4- (BLH-84, Elwha, TR2) and 3.22-flare ratio (Helley-Smith) nozzles of the pressure-difference bedload samplers used in the StreamLab06 experiments (figure 2 shows three of the four samplers used in the StreamLab06 experiments; figure 3 shows cable-suspended versions of the four sampler types), versions of these four pressure-difference samplers have been constructed with nozzle-flare ratios of 1.0, 1.11, 1.13, 1.66, 1.96, and 2.62, (Druffel and others, 1976); 1.1, and 3.07 (Hubbell and others, 1987); and possibly others.

Bedload samplers have been constructed with varying dimensions to measure particles as small as fine sand (0.125–0.25 mm) or as large as cobbles (<200 mm) (Hubbell, 1964). There is evidence that even slight design modifications can impinge on sampler performance; Ryan and Porth (1999) have shown that a thin-wall Helley-Smith, such as that shown in figure 2 (the Helley-Smith sampler shown in figure 2 was not used in the StreamLab06 bedload-calibration experiments; a standard thick-wall version was used in the experiments), can infer transport rates of approximately double those of the standard (thicker-walled) Helley-Smith. Although the accuracy of data produced by a pressure-difference bedload sampler can be influenced by numerous factors even discounting vagaries associated with improper deployment techniques (Hubbell and Stevens, 1986; William Emmett, U.S. Geological Survey, oral communication, 1978), key determinants with respect to a bedload-sampler's trapping efficiency is its nozzle's flair ratio; the geometry and dimensions of its intake; and potential back-pressure caused by an overfilled and (or) otherwise clogged collection bag.

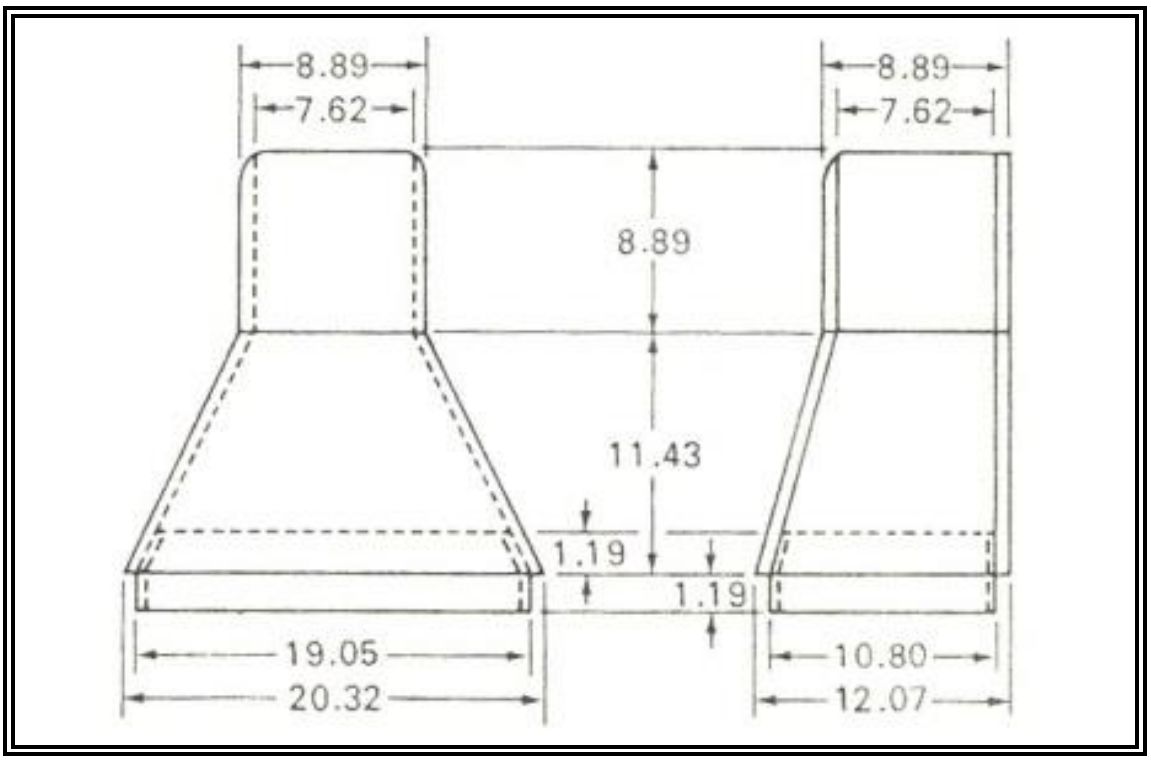

Figure 1. Schematic of a Helley-Smith (Helley and Smith, 1971) upward-facing 7.62-mm-square intake nozzle with a 3.22 nozzle-flair ratio. From Druffel and others, 1976. The dimensions are in centimeters.

A bedload sampler nozzle with equal intake and outlet dimensions increases resistance to flow. Consequently, the rate of flow through the nozzle (sampler) is reduced with respect to the ambient flow velocity. Reductions in shear stress concomitant with lower sub-ambient flow velocities result in spurious reductions in bedload captured by the sampler. This is due to the accumulation of particles in the nozzle entrance and others being diverted away from the intake (Kuhnle, 2008, p. 340-341). Alternately, an increase in shear stress concomitant with acceleration of the ambient flow into the nozzle can result in spurious increases in bedload capture by the sampler due to a vacuuming effect on the bed in the vicinity of the intake nozzle. Thus, a bedload sampler's hydraulic efficiency is a key determinate of its trapping efficiency.

The hydraulic efficiency of a given sampler is determined by a combination of factors. These include the sampler's nozzle-flare ratio; intake-nozzle configuration, dimensions, and area; ambient flow velocity incident on the nozzle; bag mesh pore size; and factors related to mesh bag backpressure (percentage that the collection bag is filled; and bag clogging by inorganic or organic material).

Historical assessments of pressure-difference bedload sampler hydraulic efficiencies included those by Druffel and others (1976), who determined that filling the sampler bag less than about 40 percent had no measurable effect on the hydraulic efficiency of the

standard Helley-Smith sampler. Hubbell and others (1985; 1987) assign a hydraulic efficiency of 1.54 to the standard Helley-Smith. Those listed for the BLH-84 and TR-2 are 1.35 and 1.40, respectively, both of which were qualified as "estimated."

Hydraulic-efficiency tests of the BLH-84 and TR-2 (in addition to the Elwha, the hydraulic characteristics of which theretofore were unquantified) conducted by Bunte and others (2017) produced markedly different results than those shown reported by Hubbell and others (1985; 1987). In general, a sampler's hydraulic efficiency may vary with the duration that the sampler rests on the bed, ambient transport rates, and the size of material in transport. More specifically, its hydraulic efficiency is a function of the ambient flow velocity, nozzle-flare ratio, nozzle-inlet size and area, and the through-flow velocity. The latter is a function of potential backpressure created by a decline in the effective flow-through area of the net resulting from overfilling the mesh bag, and (or) by the clogging of the mesh pores by debris.

Given the number of variables that may impinge on a sampler's hydraulic efficiency, deriving a single reliable hydraulic efficiency under a single – let alone range -- of ambient flow and bedload-transport conditions would be difficult at best. Ergo, any attempt to derive a bedload-trapping efficiency based solely on a sampler's hydraulic efficiency would be unlikely to produce definitive and demonstrably reliable results. Regardless, within these contexts, hydraulic and bedload-trapping efficiencies remain positively correlated, and are relevant to comparisons of the trapping efficiencies derived for the tested bedload samplers.

Bunte and others (2017) report that hydraulic efficiencies measured for the BLH-84 ranged from 0.93 (at a mean velocity of 0.45 m/s) to 1.03 (mean velocity of 1.07 m/s). Those for the Elwha (for which no previous hydraulic or trapping-efficiency data are available) ranged from 1.01 to 1.10; and 1.08 to 1.15 for the TR-2. They observed that,

1. "In order to use multiple bedload samplers interchangeably, all samplers should have the same hydraulic efficiency, and ideally, that [coefficient] value should be near [1.0] for a wide range of sampler bag configurations," and

2. A high hydraulic efficiency more likely causes pronounced oversampling under specific conditions when: (a) suspended sand is sucked into the sampler, (b) sandy bed material is scoured at the sampler entrance and then sucked into the sampler, and (c) gravel particles are sucked into the sampler after dislodgement when the sampler is set on the bed.

Their test results indicated that flow was sucked (or "vacuumed") into the hydraulically super-efficient Elwha and TR-2 samplers for all target velocities and net configurations – even for a clogged net. On the other hand, they determined that the hydraulic efficiency of the BL-84 ranged from moderately sub-efficient to near unity (i.e., near a value of 1.0).

Bunte and others' (2017) hydraulic-efficiency determinations for the BLH-84 dand TR-2 are considered more reliable than the substantially larger values reported by Hubbell and others (1987). This conclusion was drawn from the fact that Bunte and others (2017) had the advantage of use of advanced flow-through measurement technologies and relatively modern analytical methods for their measurements, and because the BL-84 and TR-2 hydraulic efficiencies reported by Hubbell and others (1987) are qualified as "estimated." Hence, only the hydraulic efficiency values reported by Bunte and others (2017) are used in the analysis section of this dissertation.

Figure 2. Photograph of four types of hand-deployed pressure-difference bedload samplers tested in the St. Anthony Falls Laboratory Main Flume, January–March 2006. All but the Helley-Smith sampler shown were those used in the tests. A standard Helley-Smith with thicker walls was used instead of that shown. From left to right: BLH-84, Helley-Smith, Elwha, and Toutle River-2 (TR-2, without collection bag). All but the Helley-Smith sampler (flare ratio = 3.22) have flare ratios of 1.4. Photograph courtesy of Kurt Swingle, Ft. Collins, Colorado, May 2006. From Gray and others, in press.

Figure 3. Photographs of cable-suspended versions of the four pressure-difference bedload samplers tested in the St. Anthony Falls Laboratory Main Flume, January–March 2006 (hand-deployed versions are shown in figure 2). Clockwise from top left: a BL-84, Helley-Smith, TR-2, and an Elwha atop a TR-2 (the latter lacking a mesh bag).

3. Historical Pressure-Difference Bedload Sampler Trapping-Efficiency Comparisons and Calibrations

3A. Factors and Challenges

The capacity to collect a representative sample of any medium—that is, to obtain a sample that proportionally reflects the presence of an attribute of interest—is a fundamental prerequisite of any credible sampling scheme. Assuming the proper selection and deployment of a bedload sampler using approved guidelines (USGS, 1990; Edwards and Glysson, 1999) in a channel in which the ambient flow, bed, and bedload-transport conditions are all within the sampler's operating range, the capacity to obtain a representative bedload sample is determined by the sampler's sediment-trapping efficiency: the ratio resulting from the dry mass of bedload captured by the sampler divided by that which otherwise would have passed the intake-nozzle section in the sampler's absence (Hubble, 1964; USGS, 1990). For example, a trapping efficiency of 1.5 indicates that the bedload mass captured by the sampler is 50 percent greater than the

mass that would have passed the section of the streambed occupied by the intake nozzle for the same duration but in the absence of the deployed bedload sampler.

Quantifying a bedload sampler's bedload-trapping efficiency – or "calibrating the bedload sampler" – is of fundamental importance in the collection of quality-assured, certifiably reliable bedload-transport data. Samplers with unknown trapping coefficients produce technically unsupportable data. Samplers with known trapping coefficients produce raw bedload-transport data that require division by the trapping coefficient to derive unbiased bedload-transport data.

Ascertaining reliable bedload-sampler trapping efficiencies is complicated by an innate inability to quantify the rate of bedload transport that would have occurred in the absence of a bedload sampler deployed at the same time and location on the streambed unless the efficiency of the deployed bedload sampler is known. According to Hubbell (1964), "Needless to say, truly representative sampling efficiencies for [bedload] samplers are extremely difficult, if not impossible, to determine," but that, "they can be determined most easily and accurately through tests in a [properly equipped] laboratory flume."

The StreamLab06 bedload-sampler trapping-efficiency tests (Marr and others, 2010a, 2010b), took advantage of the relative accuracy of an automatic system that produced a dense bedload-transport data time series by continuously collecting and weighing bedload captured in a slot across a sediment-recirculating flume. These measurements represented ground-truth bedload-transport data for calculating absolute bedload-trapping efficiencies for each of four types of portable pressure-difference bedload samplers, and to quantitatively compare the relative performances among the samplers.

The efficiency with which a sampler traps bedload can be described in relative (comparative) or absolute terms. Relative efficiencies are derived from simultaneous bedload measurements in adjacent or otherwise proximate parts of the riverbed with two or more bedload samplers, or from sequentially alternating bedload samplers deployed as part of an at-a-point[3] sampling scheme. Such comparisons yield potentially useful information on any differences in trapping efficiencies among co-deployed samplers, particularly to give data users a sense of the variance and potential bias associated with the performance of one type of sampler versus another.

Sampler comparisons can be informative and, in some cases, useful. However, data describing reliable bedload-transport rates can be derived only if the sampler's trapping efficiency, otherwise referred to as its calibration coefficient, is known. Thus, bedload-sampler comparisons—although inferentially indicative of differences in trapping efficiencies among bedload samplers and potentially useful from a general, relative perspective—cannot alone produce reliable bedload-transport data.

[3] References in the literature to sampling bedload "at a point" is a common misnomer; more specifically and correctly, at-a-point bedload sampling involves deploying the bedload sampler in a discrete segment of a channel where the "point" is the area formed by the geometry of an upstream-oriented intake nozzle resting on the bed.

Absolute trapping efficiencies are calculated using bedload-sampler data in conjunction with known bedload-transport rates such as from a river or flume equipped with an adequate bedload-metering system. Such tests are performed to identify the ratio, or range of ratios, that quantifies the presence or absence of bias in data produced by a bedload sampler and may enable subsequent mathematical bias corrections.

Thus, data produced by a bedload sampler, the trapping efficiency for which has been calibrated against ground-truth data, meet the requisite requirement for correcting raw-data bias that, in turn, enables computing technically supportable bedload-transport rates. Alternately, trapping efficiencies inferred from sampler comparisons may yield useful information but cannot be used to produce certifiably reliable bedload-transport data.

3B. Synopsis of Previous Research on Bedload-Sampler Trapping Efficiencies

Numerous studies have been conducted, mostly in field settings, to compare the trapping efficiencies of pressure-difference bedload samplers. Gray and others (in press) cite six examples of such comparative studies: (Childers (1999); Gray and others (1991); Ryan and Porth (1999); Vericat and others (2006); Bunte and Abt (2009); and Bunte and others (2010). It is worth reiterating that trapping efficiencies inferred from sampler comparisons may yield information useful for comparative purposes but cannot address or otherwise resolve the fundamental need for obtaining certifiably reliable bedload-transport data.

Due to a fundamental need for reliable ground-truth data, most bedload-sampler trapping efficiency tests have taken place in settings where bedload-transport rates can be controlled, or at least measured, with a quantifiably acceptable degree of accuracy to produce absolute (as opposed to comparative) trapping coefficients. Sediment-recirculating flumes such as the Main Flume at the SAFL meet this criterion. However, at least two problems impinge on the usefulness of recirculating flume bedload-sampler calibrations: the often-substantial temporal and spatial variabilities in bedload-transport rates that are consistent with those occurring in natural settings.

Even with a comparatively stable mean transport rate, the instantaneous rate at a given location in a stream or flume can vary widely about the mean (Hamamori, 1962; Hubbell and others, 1985; Gomez and others, 1990; Gray and others, 1991; Carey, 2005; Gray and Simões, 2008). Feinberg and others (2010) observed that mean bedload-transport rates decreased with increasing sampling time at moderate flows “in agreement with results reported in field studies.” Singh and others (2009) found the same outcome for low transport rates. However they noted that mean rates increased with sampling time at higher-transport conditions. Bunte and Abt (2005), using data from bedload traps in a montane gravel-bed stream, found that bedload-transport rates decreased with sampling time near incipient motion, but increased with time at moderate flows. Consistent among the aforementioned studies is the theme of dependence between sampling duration and measured transport rate.

In addition to the temporal dependence in bedload measurements, sampler calibrations also are hampered by the oft considerable spatial variability in bedload movement. Transport rates in the section of a flume – such as SAFL Main Flume – in which the bedload sampler is deployed (with respect to the distances from the sidewall, the slot, and the individual slot weigh pan) may differ from those at the flume ground-truth measuring location. Spatial variability can be a factor:

- laterally and longitudinally, depending on where the bedload sampler is deployed,
- with increasing distance between the bedload-sample measuring section and the ground-truth measuring location (which, in turn, leads to uncertainties in the temporal bedload-transport characteristics), and
- with the presence or absence of bedforms and other factors related to the bedload-transport process.

One solution to the previously mentioned challenges imposed by the spatial and temporal variability in bedload movement was to construct a concrete trough across the bed of the East Fork River near Pinedale, Wyoming, bedload slot sampler (Leopold and Emmett, 1976, 1997; Emmett,1980, 1981; Leopold and Emmett, 1997). A conveyor belt inside a cross-channel concrete slot transferred captured bedload to a bank-mounted continuous sediment-weighing system. This system was used to collect bedload data from 1973 to 1979 and to field calibrate a rod-deployed Helley-Smith. Emmett (1980) concluded, for bedload particle sizes between 0.5–16 mm (medium-sand to pebble-size material), that the Helley-Smith's trapping efficiency was "near-perfect" (i.e., close to unity). The Helley-Smith was determined to trap material finer than 0.5 mm with an efficiency somewhat greater than unity; however, this departure from calibration was partly attributed to the entry of suspended sand into the sampler. Bedload larger than 16 mm was determined to be trapped with sub-unity efficiency.

The aforementioned East Fork River bedload-sampler trapping efficiency effort is notable for its considerable success in quantifying the bedload characteristics of the East Fork River and quantifying the Helley-Smith's range in trapping efficiencies under the measurement conditions, as well as highlighting the difficulties and considerable time and expense of obtaining reliable bedload data.

Recognizing that the previously described trapping-efficiency characteristics of the Helley-Smith warranted further research and that a bedload sampler capable of collecting larger clasts was sought by the FISP member agencies, Hubbell and others (1985; 1987), Hubbell and Stevens (1986), and Hubbell (1987) deployed six pressure-difference-type bedload samplers in the St. Anthony Falls Hydraulic Laboratory (now called the SAFL) Main Flume in 1977 to derive calibration curves (as opposed to single-value trapping-efficiency coefficients) for each sampler

The Main Flume was operated at various combinations of flow rates and bed-material size compositions ranging from 2.1 to 23.5 median diameter material for 60–80 hours

before the bedload samplers were deployed. Masses of sediment collected on 6-second intervals were automatically measured at each of the seven weigh pans imbedded in the flume slot. The bedload samplers were suspended by chain hoist from points 3–8 m upstream from the slot. A tether line (Childers, 1999, p. 12) connected the sampler to the ceiling over the flume several meters upstream from the deployment section. The tether line stabilized the sampler and prevented it from being swept downstream by the force of the flow.

The samplers were deployed at three lateral stations in the first four series of tests and at the center station only during the last two series of tests. The tests were performed sequentially with three distributions of 2.1-, 6.5-, and 23.5-mm material composing the bed and lastly with a logarithmic mixture of these size fractions. Dunes were present during all tests.

Because such calibrations are hampered by an inability of making matched individual sampler and trap measurements of sediment transport at the same time and place, two methods for developing calibration curves for the six bedload samplers were used:

1. Comparing sampled rates with corresponding estimated true rates computed from relations between bed elevation at the sampling point and rates at the bedload trap, and

2. Matching probability distribution functions for sampled bedload-transport rates with respect to rates measured at the bedload trap, which entailed comparing sampler and trap averages under a range of steady-flow conditions.

Hubbell, and others (1985), and Hubbell and Stevens (1986) concluded that the close agreement between the curves obtained by the two methods demonstrated that accurate calibration curves can be defined by the probability-matching method. Calibration curves, defined in this way with data from different experimental runs, can be characterized by a single composite curve for a given bed-material size composition.

The objective of Hubbell and others (1985; 1987) and Hubell and Stevens (1986) was to develop composite curves to correct bedload-transport rates inferred from bedload-sampler deployments to obtain true bedload-sampler rates. Their work has had a legacy in that it served as the basis for acceptance of the 1.4-flare-ratio version of the Helley-Smith – the BL-84 and BLH-84 – as the only bedload sampler type endorsed for collecting bedload data by the Technical Committee that oversees the FISP. The USGS, a member of the FISP Technical Committee, formally supports this position but continues to accept standard Helley-Smith bedload data for storage in its national database “until additional calibration work is performed” (Edwards and Glysson, 1986; 1999).

Subsequent to the above, the probability matching technique used by Hubbell and others (1985, 1987) and Hubbell and Stevens (1986) was criticized as invalid by Thomas and Lewis (1993) because it:

1. implicitly assumes that neither trap nor sampler bedload-transport rates have associated measurement or sampling error, observing that errors are present in all physical measurements,

2. gives biased and highly variable results, and

3. does not contain information for determining which independent variables to include and exclude from a regression equation.

Thomas and Lewis (1993) developed a new model (hereafter, the "T-L" model) for bedload-sampler calibrations that matches unobservable trap rates to normally distributed populations of cube-root transformed trap transport rates with individual rates measured by manually deployed bedload samplers. The model requires at-a-point bedload-sampler data that correspond to trap data at a given downstream weigh pan. The model "regresses transformed individual sampler measurements on daily means of transformed trap data and incorporates within-day variation in trap rates to explain part of the sampler variation" (Thomas and Lewis, 1993). The parameters are estimated by maximum likelihood using a nonstandard regression model to account for the physical inability of matching individual trap versus bedload-sampler measurements in time and space.

The T-L model was used to develop calibration curves using data from Hubbell and others (1987), even though one of the requirements for the model's calibration—collecting a large number of bedload samples from at a single point—was not always met (many of the sample runs were made using three-point measurements laterally across the flume). The cube-root curves for the coarsest material tested over the full range of transport (8 kg/m x s) —23.5 mm — indicated moderately sub-unity collection efficiencies of about 0.75 for both the BL-84 and TR-2. The cube-root curves for the coarse-sand and fine-gravel size material — 2.1 mm — indicate back-transformed (real space) trapping coefficients of about 0.8 for the BL-84, and about 0.9 for the Helley-Smith. However, an anomalously small value of 0.03 was computed for the TR-2 atop the 2.1 mm bed (Thomas and Lewis, 1993, table 3 and figure 8). The results for the 6.5-mm-size class were moderately super-efficient for the BL-84, and considerably super-efficient for the TR-2 with a value of about 1.6.

4. Rationale for the StreamLab06 Bedload Sampler Calibration Experiments

Deficiencies associated with traditional instruments and techniques used to quantify bedload-transport rates, and potential solutions to address those deficiencies, were identified as part of two workshops sponsored by the Advisory Committee on Water Information's Subcommittee on Sedimentation (2017): The Federal Interagency Sediment Monitoring Instrument and Analysis Research Workshop (Gray, 2005; Ryan and others, 2005) and the International Bedload-Surrogate Monitoring Workshop (Gray

and others, 2010). Both workshops described a fundamental need for ground-truth data to:

- quantify the accuracy of manually deployed bedload measurements, and
- enable the verification or adjustment of bedload-transport-rate estimates derived from surrogate technologies that may provide a continuous time series of the data.

The following list summarizes the impetuses for performing bedload-sampler trapping-efficiency tests as part of Phases I and II of the StreamLab06 experiments:

1. Unlike the other three bedload samplers tested, the trapping efficiency of the Elwha bedload sampler had never been empirically resolved. This reason alone was considered sufficient by the FISP and USGS to take advantage of the ground-truth bedload-transport data from the Main Flume during controlled flows over a bed of sand, and of gravel.

2. The justification for the FISP's 1985 provisional endorsement of the BL-84 (BLH-84) was only partly consistent with the graphical data supporting its endorsement (Hubbell and Stevens, 1986); thus, the BLH-84 was deemed worthy of additional testing.

3. The FISP's previously mentioned "provisional" endorsement of the BL-84 (BLH-84) in 1985—reiterated in 1990 and in 1995 as a "tentative" endorsement by the FISP—remained unchanged in 2006 when the StreamLab06 experiments took place. By 1990, the USGS endorsed use of samplers "with the 1.4-flare ratio" (for example, the BL-84 and BLH-84). That endorsement remained unchanged as of 2019 even though the trapping efficiency of the 1.4-nozzle flare Elwha sampler had yet to be investigated.

4. The USGS's endorsement of the BL-84 (BLH-84) is inconsistent with Edwards and Glysson's (1986) guidance to continue to use the Helley-Smith until the BL-84 was "tested further and [became] available for use," given there is no evidence of additional ground-truth testing of the BL-84 between 1985 and 2006. Eliminating confusion between the FISP's and USGS's tentative or unqualified endorsements of the BL-84 (BLH-84) was another potential outcome for the StreamLab06 bedload-sampler experiments.

5. Thomas and Lewis (1993) not only raised doubts of the statistical treatment of bedload data in Hubbell and others (1987), but they provided an alternate statistically based "new model" for calibrating bedload samplers that warranted application with StreamLab06 data.

6. Inclusion of a bedload-sampler comparison component as part of the requisite calibrations was anticipated to increase the usefulness of the experiments. Any potentially unique characteristics related to use of the Main Flume for producing ground-truth data to calibrate bedload samplers presumably would have a common effect on all of the samplers tested.

7. The refurbished SAFL Main Flume with state-of-the-art monitoring capabilities offered unprecedented precision and data-storage capabilities to automatically produce ground-truth bedload-transport time-series data.

8. The considerable costs associated with refurbishing the Main Flume, plus its operation as part of StreamLab06 Phases I and II experiments, were borne by the NCED and SAFL. These up-front capital investments enabled the participating organizations and researchers to afford to participate in the StreamLab06 experiments.

5. The StreamLab06 Bedload-Sampler Trapping-Efficiency Experiments

5A. St. Anthony Falls Laboratory Main Flume

5Ai. Physical and Operational Description

The Main Flume, located on the ground floor of the SAFL, is capable of conveying field-scale flows from the adjacent Mississippi River and recirculating known quantities of introduced sediments ranging from sand- to medium-gravel size for days at a time. These characteristics, along with the automatic bedload weighing and recirculating capability, led the FISP to use the flume for advancing sediment-transport research and bedload-monitoring technologies beginning in the late 1970s (Hubbell and others, 1985, 1987; Hubbell and Stevens, 1986), and again as a collaborative effort in 2006 as part of the StreamLab06 experiments.

The Main Flume (figures 4 and 5) is composed of an open rectangular concrete channel with flow- and stage-controlling devices. Water from the Mississippi River upstream from St. Anthony Falls is diverted through a screened intake to the flume's entrance, taking advantage of the static head differential created by the falls. A sluice gate controls flow to the headwater of the flume at steady-state rates ranging up to 8.5 m^3/s. The diverted flow courses through the flume and returns to the Mississippi River (that is, the flow is not recirculated) downstream from the falls.

The 80-m-long flume is 2.74 m wide with sidewalls that rise vertically 1.8 m from the level concrete floor. The horizontal flume bed culminates with a sharp-crested weir, the elevation of which is adjustable to control flow stage. Stage and the weir elevations are automatically measured, and coupled with a theoretical stage-discharge relation, are used to continuously meter water discharge. Sand-size (January–February 2006) and gravel-

size material (March 2006) were laid atop the concrete bed for StreamLab06 Phases I and II tests, respectively.

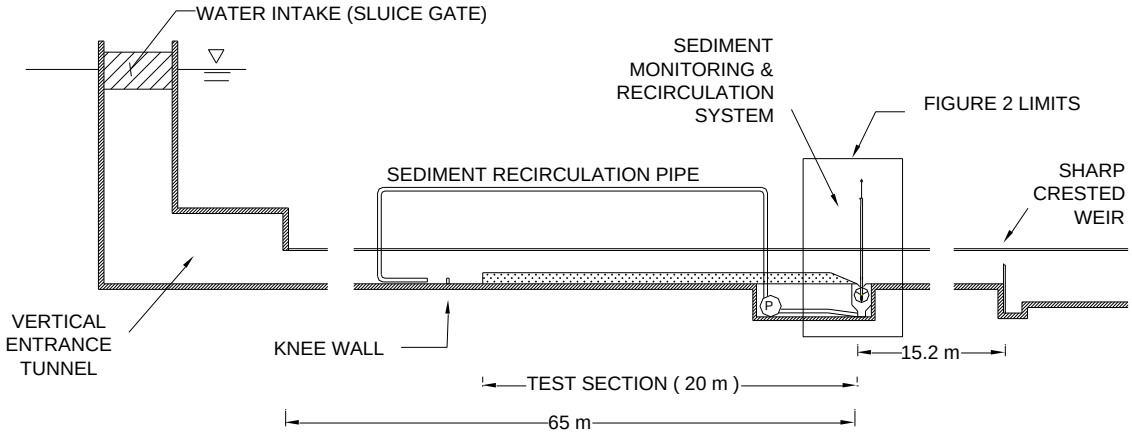

Figure 4. Side-view schematic of the St. Anthony Falls Laboratory Main Flume showing the entire facility from the water intake to the tailwater of the sharp-crested weir.

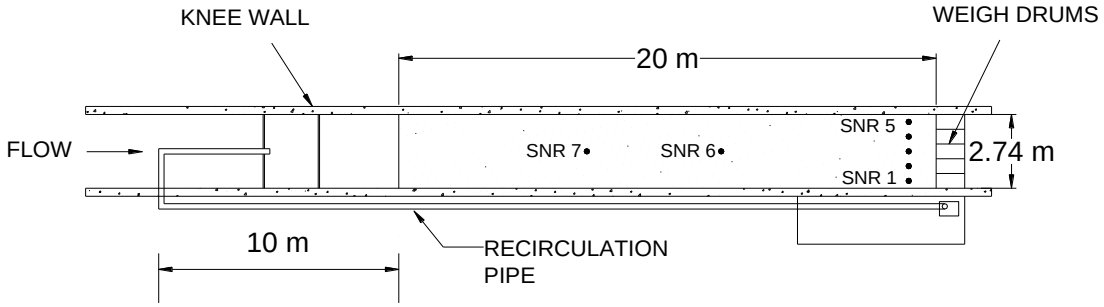

Figure 5. Plan-view schematic of the St. Anthony Falls Laboratory Main Flume showing the section in which bedload is captured by the weigh pans (drums) and recirculated to the approach section upstream from a knee wall. SNR refers to locations of sonar bed-elevation sensors.

A key attribute of the Main Flume in sediment-transport studies is the Sediment Monitoring and Recirculation System (SMRS). Located approximately 65 m downstream from the flume entrance and 15.2 m upstream from the sharp-crested weir (figure 4), the SMRS is capable of continuously monitoring bedload flux during flows over introduced sediment covering the flume bed.

The SMRS, capable of continuously measuring and recording the rate of captured bedload up to about 76-mm, has the following principal components:

1. A 2.74-meter bedload slot (trap) spanning the width of the Main Flume into which bedload particles fall,

2. A sediment-monitoring component that collects and weighs the captured bedload in pans (drums) located inside the slot (figures 6, 7 and 8). Each of the weigh pans automatically and independently dumps accumulated sediments exceeding a preset value of mass. Mass-accumulation data are stored at approximately 1.1-second intervals for each of the five pans.

3. A horizontally imposed auger (figure 8) at the base of the slot that conveys captured, weighed, and dumped sediments to a pumping system next to the auger, and

4. A pump operated by an auger motor (figure 8) capable of transporting sediments up to 76-mm long diameter via an overhead pipe about 30 m upstream from the slot for return to the flume.

A submerged 0.3-m-high knee wall weir spanning the width of the flume 1 m downstream from the outlet pipe was designed to dissipate the large-water and -entrained sediment velocities exiting the recirculation pipe. Based on bathymetric surveys, asymmetries in bed configuration in the 3- to 5-m reach of the flume downstream from the knee wall were attributable to water and sediment discharges from the return pipe (Marr and others, 2010a). The bedload samplers were deployed about 15 m downstream from the knee wall.

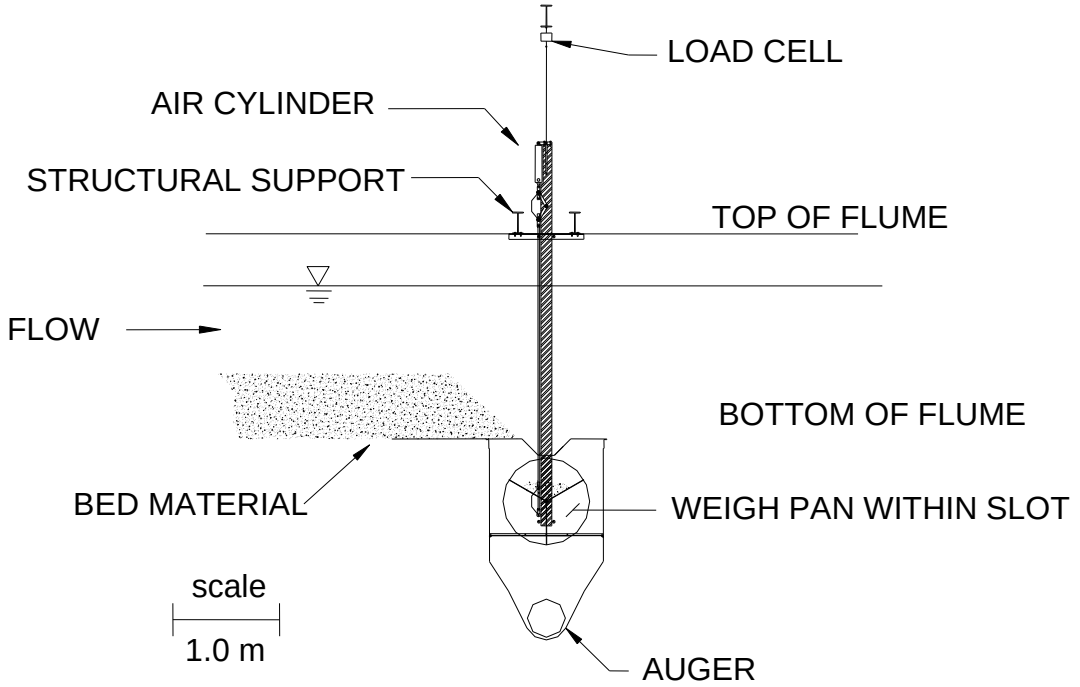

Figure 6. Schematic of the Sediment Monitoring and Recirculation System, showing the right-most of the five weigh pans (drums) in the cross-channel slot over the auger in the bottom of the slot. The view is from the right side of the flume proper to the slot.

Figure 7. Photographs of the Main Flume sediment-flux monitoring component of the Sediment Monitoring and Recirculation System. Left, the slot at low- or zero-flow; center, the non-submerged part of the weigh-pan apparatus; right, the partially submerged apparatus during an experimental run.

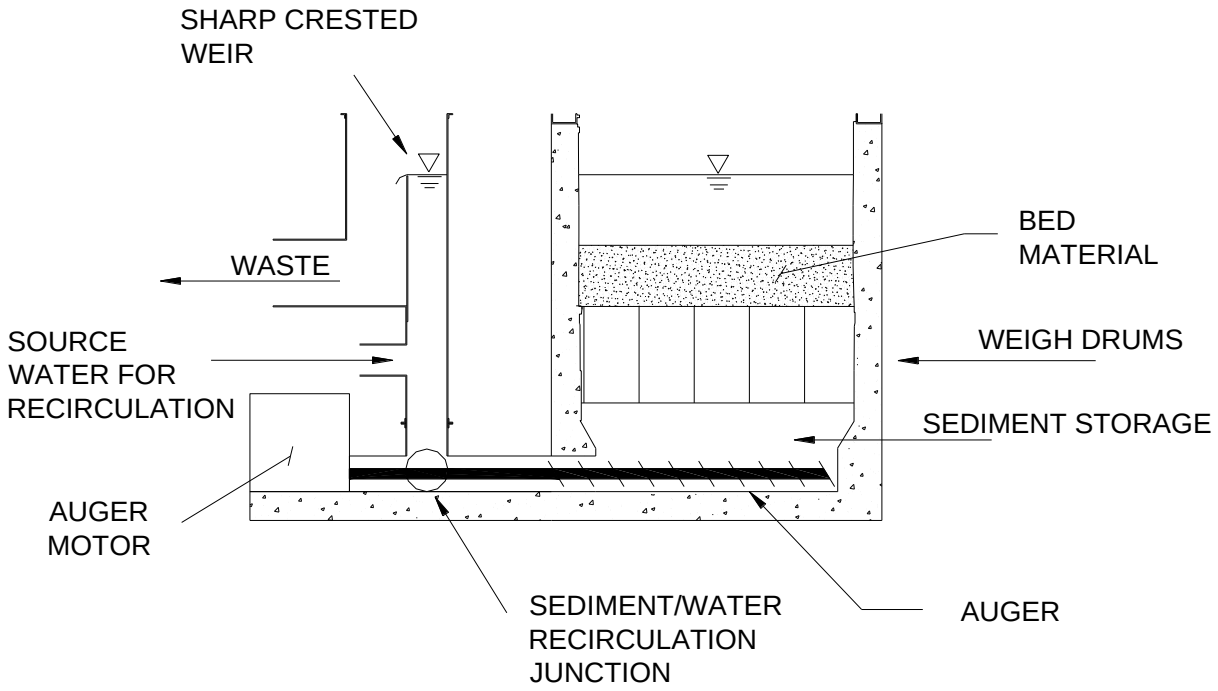

Figure 8. Schematic of the Sediment Monitoring and Recirculation System, showing the five weigh pans (drums) in the cross-channel slot over the auger in the bottom of the slot. Municipal water is used for recirculation. The view is upstream.

The submerged weights of each pan were measured continuously by the respective load cell and used by the central data-acquisition (CDAQ) system to control the evacuation of each pan. The bedload-transport data acquired and stored by the CDAQ system were accompanied by ancillary data, which included flow rates, water-surface elevations, and water temperatures.

The pan weigh data are used to estimate bedload mass fluxes by calculating the rate of change of the submerged weight of sediment trapped in each pan. Marr and others (2010a) and Gray and others (in press) describe the operation of SMRS in greater detail.

5Aii. Experimental Conditions During StreamLab06 Phases I and II

The 2006 StreamLab06 bedload-sampler trapping-efficiency experiments took place during nine steady-state water discharges (combinations of Main Flume flows and bed compositions), each of which is referred to as a "run." Bedload samplers were deployed during five Phase I runs in the sand-bedded Main Flume on January 31–February 14. Four runs over a gravel bed were sampled during Phase II on March 3–27.

Table 1 summarizes selected characteristics germane to each of the nine runs. Appendix 1 consists of plots of weigh-pan bedload-transport rates in kilograms/(seconds × meter) for each of the StreamLab06 Phase I sand and Phase II gravel runs during which bedload samplers were deployed.

Table 1. Summary of Main Flume experimental conditions as part of nine StreamLab06 bedload-sampler trapping-efficiency runs. From Marr and others (2010a) [Abbreviations: gm, grams; hr, hours; m^3, cubic meters; °C, degrees Celsius; m, meters; ND, not determined; s, seconds]

Qw, design (m^3/s)	Bed type	Time, total (hr)	Time, eq (hr)	Temp, mean (°C)	Qw, mean (m^3/s)	qs, mean[1] (gm/(m×s)-dry)	qs-equil, mean (gm/(m×s)-dry)
2.0	sand	12.3	11.7	0.4	2.02	13	13
2.5	sand	15.8	14.2	0.5	2.7	45	47
2.9	sand	34.3	22.3	2.3	2.95	77	77
3.2	sand	8.5	ND	0.6	3.20	126	ND
3.6	sand	11.6	10.3	1.0	3.69	180	176
4.0	gravel	56.0	43.0	2.2	4.01	3	2
4.3	gravel	36.3	13.0	3.5	4.32	11	15
4.9	gravel	33.9	24.2	4.7	4.90	161	168
5.5	gravel	29.0	28.2	2.7	5.51	785	782

Table column headers (variables) explained:

Qw, design: design water discharge for the run

Bed: bed material type

Time, total: total duration of time at the design discharge including equilibration period

Time, eq: total duration of time at equilibrium bed condition

Temp, mean: mean water temperature

Qw, mean: mean water discharge

qs, mean: mean sediment transport rate computed over total duration

qs-equil, mean: mean sediment transport rate computed for period after equilibration was reached

Footnote: [1] The variable "qs, mean" is computed using a 90-second moving-average window.

The sand introduced to the Main Flume for the Phase I tests consisted of well-sorted siliceous material in a range of 0.6-1.8 mm and a D_{50} of 1.0 mm. Upon completion of the Phase I tests, the sand was removed and replaced with a comparatively broad distribution of mostly gravel-size material (1–32 mm; D_{50}=11.2 mm) for the Phase II tests (Marr and others, 2010a). The sieved grain-size distributions for the sand-bed and gravel-bed materials are shown in Figure 9.

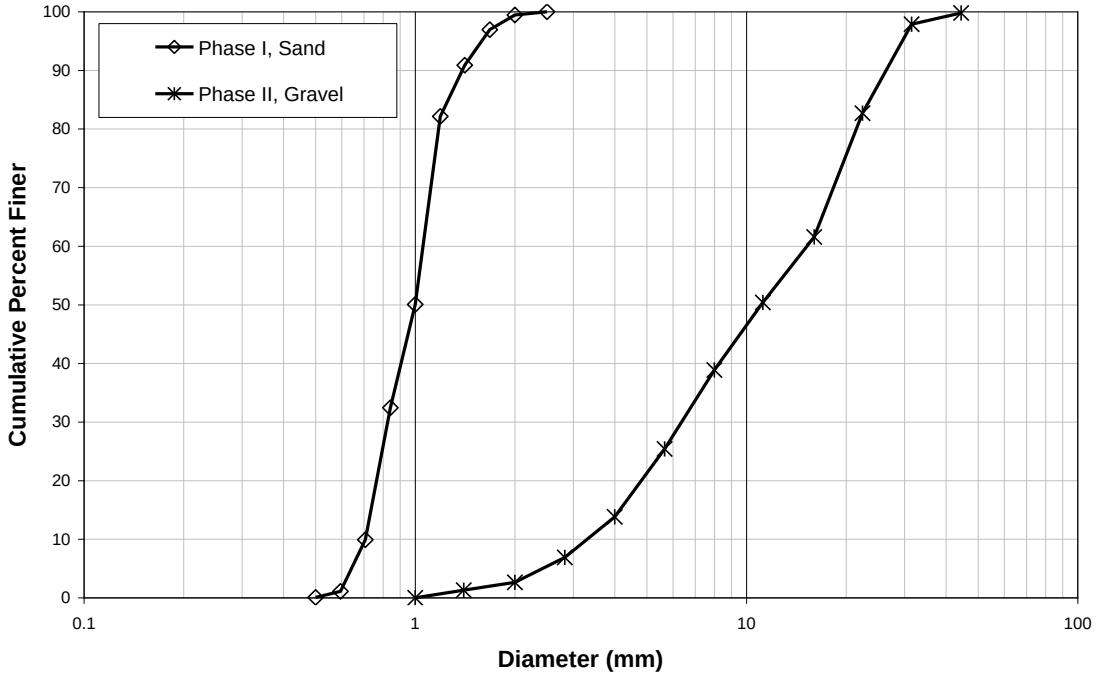

Figure 9. Grain-size distributions of the original sand- and gravel-bed material used in StreamLab06 Phase I (left) and II (right) tests.

Figure 10 shows the Main Flume in three periods: Left-to-right, after flow cessation in the sand- and gravel-bedded channel; and during a flow of 5.5 m^3/s over a gravel bed.

Figure 10. Three downstream views of the St. Anthony Falls Laboratory Main Flume, 2006; left, dunes in the drained sand-bedded flume after a test run (undated, either January or February); center, from near the bedload-sampler deployment section showing the vertical stanchions of the sediment-flux weighing-system assembly after a gravel-bed test run on March 10; and right, from the flume headwater during a 5.5 m^3/s gravel-bed test run on March 11, 2006.

For each experimental discharge and for a shorter period of time at the beginning of each sampling session, it was necessary to operate the flume and recirculation system to establish a dynamic bed equilibration. Achievement of dynamic equilibrium in bedload-transport rates was inferred by observing stabilization of the computed 60-minute mean sediment-flux rates. The 60-minute mean bedload-rate value was continuously computed and displayed by CDAQ software.

5B. Pressure-Difference Bedload Samplers Used During Streamlab06

5Bi. Description of Samplers and Deployment Methods

Data for calculating the bedload-trapping efficiencies of manually deployed versions of the Helley-Smith, BL-84 (BLH-84), Elwha, and TR-2 were collected as part of Phases I and II of the StreamLab06 experiments. Table 2 describes selected characteristics of these types of pressure-difference samplers (figure 2).

Table 2. Selected characteristics of bedload samplers used in the StreamLab06 Phase I and II experiments and the median bed-material grain sizes, in millimeters, atop which each bedload sampler was deployed (also see figure 2).

Sampler type	Nozzle dimensions; width (mm) x height (mm)	Nozzle outlet-to-inlet area ratio	Bag mesh size (mm)	Bed composition (mm)
BLH-84	76.2 x 76.2	1.4	0.25	Sand, D_{50} = 1.0
Elwha	203 x 102	1.4	0.5	Sand, D_{50} = 1.0
Helley-Smith	76.2 x 76.2	3.22	0.25	Sand, D_{50} = 1.0
US BLH-84	76.2 x 76.2	1.4	0.25	Gravel, D_{50} = 11.2
Elwha	203 x 102	1.4	0.5	Gravel, D_{50} = 11.2
Toutle River-2 (TR-2)	305 x 152	1.4	0.5	Gravel, D_{50} = 11.2

A single bedload sampler was deployed at a given time by hand-held rod (figure 2) as part of a trial. The key element of a rod- or cable-deployed bedload sampler—the nozzle—is the same for a given sampler designation regardless of deployment method.

The hand-deployed bedload sampler was composed of a nozzle with a bag affixed to the outlet; a deployment rod affixed to the top of the nozzle normal to the nozzle's base; and a narrower-diameter rod extending from the deployment-rod base horizontally to the end of the collection bag. The deployment rod was graduated in decimeters indexed to the base of the sampler to indicate the water depth for subsequent recording when the sampler rested on the bed.

Each deployed sampler was connected by a tether line of several meters length that extended from the base of the deployment rod to an upstream ceiling structural beam. The tether line kept the sampler from being swept downstream at higher flow velocities and enabled the sampler to rest at a consistent longitudinal location in the measurement cross section while deployed.

The pressure-difference bedload samplers were deployed in a cross section 8.5 m upstream from the weigh pans in one or more of five lateral locations in a cross section ("sections"): 0.27, 0.82, 1.37, 1.92, and 2.47 m from the left (viewed downstream) flume wall. Thus, the center of a deployed bedload sampler rested directly upstream from the center of a given weigh pan (figure 11). The large majority of bedload samples were repeatedly collected "at-a-point" from sections 0.82 or 1.92. The BLH-84 was deployed sequentially during some later runs at all five sections using the multiple-equal-width-increment method [Edwards and Glysson, 1999] to identify and quantify potential cross-section skew in mean bedload-transport rates.

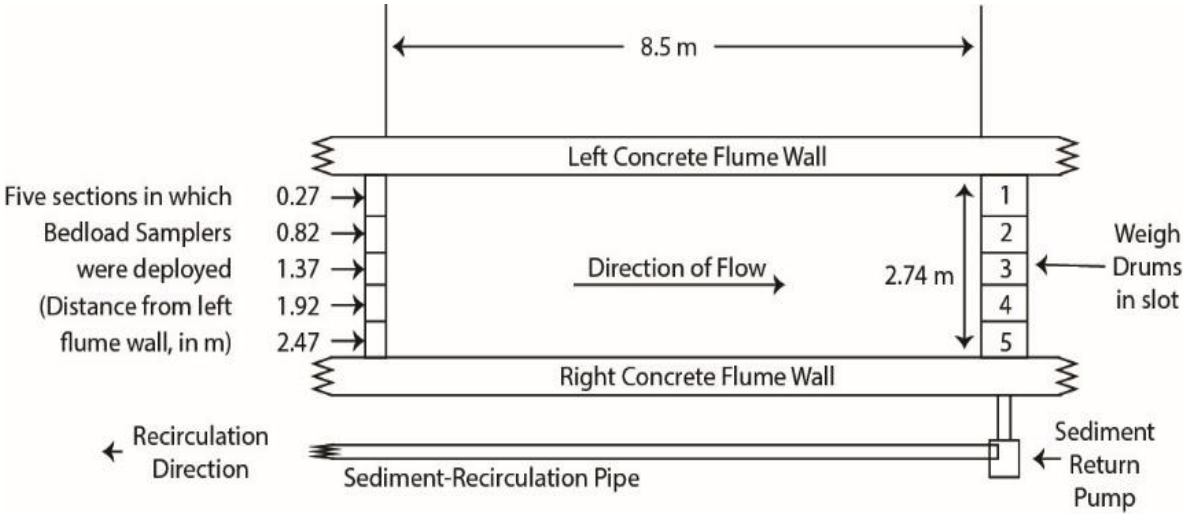

Figure 11. A plan-view schematic of the section of the Main Flume showing the cross section in which the pressure-difference bedload samplers were manually deployed to the weigh pans (drums) within the cross-channel slot. The schematic is approximately to scale.

Sections located 0.27-, 0.82-, 1.37-, 1.92-, and 2.47-m from the left flume wall were selected for at-a-point sampling for the following reasons:

1. Application of the Thomas-Lewis (1993) model required single at-a-point sample sets,

2. The Hubbell and others (1987) bedload-transport data included a large number of at-a-point sample sets, and some value was presumed to be gained from consistency with previous bedload-sampler calibrations in this flume, and

3. Based on an unpublished project summary (Dave Hubbell, USGS, written commun., undated but probably in the late 1970s or early 1980s), bedload-transport rate minima averaged over four test runs were measured in the exterior pans, and maximum values in the interior pans. This "sidewall" drag effect was anticipated to recur during the StreamLab06 experiments.

Bedload-sampler deployments in sections 0.82 m or 1.92 m from a side wall were hypothesized to yield data most closely approximating mean-transport rates in the cross section. This hypothesis was based on expected minimum mean transport rates at the two pans adjacent to the sidewalls due to sidewall-drag effects; and a hypothetical maximum mean rate for the center section farthest from the sidewalls. These hypotheses were supported by hydraulic theory and by unpublished data from the 1980s (Gray and others, in press). Neither potential condition was considered optimal for the bedload-sampler tests. Thus, the large majority of the StreamLab06 at-a-point sequential bedload samples (as opposed to cross-section samples) were collected 0.82 m or 1.92 m from the sidewalls.

Each trial involved repeatedly deploying a given bedload sampler to remain stationary on the bed for one of the following durations: 15, 30, 45, 60, 90, 120 or 180 seconds (at least 2,023 of the 2,030 discrete bedload sampler deployments were took place in this manner; the remaining seven also likely so). The duration that the sampler rested on the bed was, with rare exception, constant for a given trial, and was selected to minimize the potential for the volume of trapped bedload to exceed about half of the mesh bag's capacity.

A crew of 2–3 hydrographers deployed, retrieved, and emptied the sampler. One hydrographer deployed the bedload sampler from a platform spanning the flume. Each successive deployment included setting the sampler on the bed, measuring the water depth on the graduated deployment-sampler rod, and retrieving the sampler upon elapse of the pre-determined time on the bed.

The retrieved bedload sampler was transferred in a nozzle-up orientation to the flume-side hydrographer, with the deployment hydrographer retaining a firm grip on the deployment rod. A sample bag was placed over the intake nozzle; the rod was rotated 180 degrees resulting in a nozzle-down orientation; and the contents of the mesh bag and residual material in the sampler nozzle were dumped into the sample bag while vigorously shaking and snapping the mesh bag. A small amount of residual material usually remained in the sampler in successive deployments (i.e. an inconsequential percentage of the residual material remained in the sampler after each deployment). Each sample bag was labeled with the information relevant to the single bedload sample that it contained. Figure 12 shows photographs of the bedload-sampler deployment-and-emptying sequence.

Figure 12. Sequence of deploying a bedload sampler in the gravel-bedded Main Flume, St. Anthony Falls Laboratory, March 6, 2006. Left, a hydrographer holds a graduated rod affixed to a BLH-84 resting on the bed of the Main Flume 0.82 m from the left wall and 8.5 m upstream from the weigh-pan slot; center, after recording the water depth, the BLH-84 is retrieved upon elapse of a pre-determined duration on the bed; and right, the young, bespectacled author empties the contents of the BLH-84 bag for weighing.

Smaller-volume samples were immediately wet-weighed using a method described by Carey (1984). This method involved suspending the bagged samples from a hanging scale and submerging the sample bag in a bucket of river water, taking care to ensure that no air remained in the bag. Larger-volume samples were dry-weighed on a floor scale.

The submerged mass was recorded in an Excel spreadsheet, and the dry mass of the trapped bedload was calculated according to equation 1:

$$W_{ds} = \frac{SG_s}{SG_s - 1} * W_{ss} \qquad (1)$$

Where:

W_{ds} is the dry mass of bedload trapped by the pressure-difference bedload sampler, in grams,
W_{ss} is the submerged (wet) mass measured by the scale, in grams, and
SG_s is the mean specific gravity of the sediment material (for example, 2.65 for quartz).

Samples subsequently were stored. Some eventually were dried and sieved to derive grain-size distribution statistics[4] (Gray and others, in press). Several samples that had been wet-weighed were oven-dried to compare the actual dry weight to the computed dry weight from the wet-weigh process. Dry-weight comparisons to same-sample values computed by equation 1 confirmed that the Carey (1984) wet-weighing system was deemed to be quite accurate.

The dry mass of a captured bedload was used with ancillary data to compute the bedload-transport rate by equation 2:

[4] All bedload samples collected during StreamLab06 Phases I and II have been discarded.

$$BL_q = W_{ds} / ((W_{sampler}) \times (T_{on\ bed})) \quad (2)$$

Where:

BL_q	is the transport rate measured by the bedload sampler, in grams per meter per second,
W_{ds}	is the dry mass of bedload trapped by the pressure-difference bedload sampler, in grams,
$W_{sampler}$	is the width of the bedload sampler, in meters, and
$T_{on\ bed}$	is the duration that the sampler rested on the bed, in seconds.

5Bii. Summary of Bedload-Sampler Trial Deployments

A total of 2,030 bedload samples were collected from the SAFL Main Flume as part of 37 bedload-sampler trials. Table 3 provides selected statistics from the 19 trials that took place during five steady flows of 2.0, 2.5, 2.9, 3.2, and 3.6 m^3/s over a sand bed. Table 4 summarizes those statistics for the 28 gravel-bed trials during four steady flows of 4.0, 4.3, 4.9, and 5.5 m^3/s.

Table 3. Summary statistics for bedload-sampler trapping-efficiency trials in flows over a sand bed (D_{50} = 1.0 mm) during Phase I of the StreamLab06 experiments. The pressure-difference bedload samplers were deployed at selected points in a cross section 8.5 meters upstream from the weigh-pan slot spanning the 2.74-m-wide SAFL Main Flume.

Bedload Sampler Designation	Sand-Bed Trial ID	Mean Bedload Transport Rate (g/(m*s))	Mean Water Discharge (m^3/s)	Mean Flow Velocity (m/s)[1]	Mean Depth at Sampler (m)2	Range in Depth at Sampler (m)[2]	Froude Number ((v/(gd)1/2)	Distance of Center of Sampler from Left Wall (m)	# of Samples Collected	Mean Water Temp (°C)[4]	Duration on Bed #:time (s)	Date 2006	Trial Start-End Central Standard Time (h:m:s)
BLH-84	S1	39.2	2.95	0.74	1.46	1.65-1.35	0.200	1.92	75	2.3	90	31-Jan	14:25:57 20:19:05
Helley-Smith	S2	235	2.95	0.85	1.27	1.35-1.15	0.241	0.82	42	1.8	90	1-Feb	12:45:25 16:35:20
Elwha	S3	173	2.95	0.87	1.24	1.30-1.15	0.249	1.92	42	1.8	30	1-Feb	12:39:02 16:31:15
BLH-84	S4	85.7	2.95	0.78	1.38	1.5-1.25	0.212	0.27	30	2.3	90	2-Feb	14:03:27 19:27:51
BLH-84	S5	48.9	2.95	0.79	1.36	1.5-1.25	0.216	0.82	30	2.3	90	2-Feb	14:05:47 19:51:25
BLH-84	S6	63.9	2.95	0.79	1.36	1.5-1.3	0.216	1.37	30	2.3	90	2-Feb	14:08:35 19:53:39
BLH-84	S7	82.5	2.95	0.79	1.36	1.5-1.25	0.216	1.92	30	2.3	90	2-Feb	14:10:40 19:55:44
BLH-84	S8	63.9	2.95	0.77	1.40	1.5-1.25	0.208	2.47	30	2.3	90	2-Feb	14:12:54 19:57:54
BLH-84	S9	207	3.62	0.94	1.41	1.55-1.3	0.25	1.92	80	2.0	45	3-Feb	15:55:30 17:57:20
Elwha	S10	311	3.62	0.98	1.34	1.45-1.25	0.273	1.92	49	0.5	15	4-Feb	11:18:32 14:01:48
Helley-Smith	S11	631	3.62	0.96	1.37	1.25-1.45	0.262	0.82	50	0.5	15	4-Feb	11:20:29 14:03:36
BLH-84	S12	9.3	2.02	0.52	1.42	1.49-1.32	0.139	1.92	60	0.34	120	6-Feb	16:00:22 18:53:46
Elwha	S13	16.1	2.02	0.53	1.39	1.42-1.37	0.144	1.92	50	0.34	60	7-Feb	10:33:18 17:38:00
BLH-84	S14	5.8	2.02	0.53	1.40	1.47-1.37	0.14	1.37	50	0.34	120	7-Feb	10:35:40 17:46:20
Helley-Smith	S15	41.9	2.02	0.52	1.41	1.48-1.38	0.140	0.82	50	0.34	120	7-Feb	10:38:40 17:43:39
BLH-84	S16	24	2.5	0.66	1.39	1.48-1.31	0.179	variable	122	0.6	114: 120s 6: 121-126s	8-Feb	12:02:00 17:18:34
Elwha	S17	37.3	2.5	0.67	1.36	1.41-1.29	0.183	1.92	56	0.4	45	9-Feb	9:49:25 12:47:57
Helley-Smith	S18	88.8	2.5	0.64	1.43	1.49-1.29	0.171	0.82	50	0.4	60	9-Feb	9:51:20 12:37:26
BLH-84	S19	113	3.2	0.87	1.34	1.47-1.25	0.188	1.92	74	0.4	60	9-Feb	14:54:24 16:59:49

[1]Mean velocity computed as a produce of mean of depths measured at the sampling vertical(s) during each bedload sample collection and the flume width of 2.74 meters.

[2]Depth from bottom of the bedload sampler resting on the bed to the water surface as indicated on the graduated deployment rod.

[3]Froude Number = mean flow velocity divided by the square root of the product of the acceleration of gravity and mean depth of flow.

[4]Water temperatures over the duration of a trial rarely varied more than 0.2°C from the mean value, and never by more than 0.5°C.

Table 4. Summary statistics for bedload-sampler trapping-efficiency trials in flows over a gravel bed (D_{50} = 11.2 mm) during Phase II of the StreamLab06 experiments. The pressure-difference bedload samplers were deployed at selected points in a cross section 8.5 meters upstream from the weigh-pan slot spanning the 2.74-m-wide SAFL Main Flume.

Bedload Sampler Designation	Gravel Trial ID	Mean Bedload Transport Rate (g/(m*s))	Mean Water Discharge (m^3/s)	Mean Flow Velocity (m/s)[1]	Mean Depth at Sampler (m)[2]	Range in Depth at Sampler (m)[2]	Froude Number[3]	Distance of Center of Sampler from Left Wall (m)	# of Samples Collected	Mean Water Temp (°C)[4]	Duration on Bed #:time (s)	Date 2006	Trial Start-End Central Standard Time (h:m:s)
Elwha	G1	501	5.5	1.64	1.22 (5	1.25-1.15	0.474	var	6	4.6	5: 15 s 1:	11-Mar	10:55:00
BLH-84	G2	599	5.5	1.68	1.19	1.30-1.05	0.492	0.27	28	4.7	3: 30 s	11-Mar	10:55:00
BLH-84	G3	897	5.5	1.7	1.18	1.34-1.05	0.5	0.82	28	4.7	3: 30 s	11-Mar	11:03:00
BLH-84	G4	829	5.5	1.69	1.19	1.35-1.00	0.495	1.37	28	4.7	2: 30 s	11-Mar	11:07:00
BLH-84	G5	767	5.5	1.69	1.19	1.35-1.03	0.495	1.92	28	4.7	2: 30 s	11-Mar	11:13:00
BLH-84	G6	757	5.5	1.72	1.17	1.34-1.00	0.508	2.47	28	4.7	2: 30 s	11-Mar	11:16:00
Elwha	G7	1130	5.5	1.73	1.16	1.3-0.99	0.513	1.92	66	3.7	15	12-Mar	12:33:00
BLH-84	G8	842	5.5	1.65	1.21	1.48-1.03	0.479	0.82	75	3.7	15	12-Mar	12:18:00
BLH-84	G9	515	5.5	1.6	1.26	1.38-1.08	0.452	x-sect.	25	1.9	15	13-Mar	12:56:00
TR-2	G10	1009	5.5	1.67	1.2	1.4-1.00	0.487	1.92	40	1.8	15	13-Mar	13:41:00
BLH-84	G11	1026	5.5	1.73	1.16	1.28-1.04	0.513	x-sect.	25	0.8	15	14-Mar	12:32:00
BLH-84	G12	702	5.5	1.65	1.22	1.40-1.05	0.477	x-sect.	25	1.25	15	14-Mar	15:47:00
TR-2	G13	1042	5.5	1.66	1.21	1.30-1.05	0.482	1.92	22	1.1	15	14-Mar	14:46:40
BLH-84	G14	18.7	4.0	1.31	1.12	1.14-1.08	0.395	x-sect.	25	1.2	120	16-Mar	12:57:00
TR-2	G15	18.0	4.0	1.17	1.25	1.28-1.20	0.334	1.92	40	1.5	120	17-Mar	8:32:00
Elwha	G16	12.7	4.0	1.15	1.27	1.28-1.25	0.378	1.92	40	2.1	120	17-Mar	13:02:30
BLH-84	G17	5.5	4.0	1.19	1.23	1.26-1.20	0.342	x-sect.	25	2.8	180	18-Mar	13:35:00
BLH-84	G18	4.9	4.0	1.21	1.21	1.23-1.16	0.251	x-sect.	25	2.6	180	22-Mar	8:37:00
BLH-84	G19	6.3	4.0	1.22	1.19	1.21-1.17	0.357	x-sect.	25	3.2	180	22-Mar	10:29:00
TR-2	G20	23.8	4.0	1.23	1.19	1.19-1.81	0.36	1.92	51	3.2	120	22-Mar	10:24:00
Elwha	G21	24.4	4.0	1.24	1.18	1.19-1.16	0.364	0.82	51	3.6	120	22-Mar	18:25:00
BLH-84	G22	9.1	4.3	1.35	1.16	1.18-1.14	0.4	x-sect.	25	3.3	180	24-Mar	10:09:00
BLH-84	G23	4.8	4.3	1.34	1.17	1.20-1.13	0.396	x-sect.	25	3.3	120	24-Mar	09:02:00
TR-2	G24	38.1	4.3	1.32	1.18	1.22-1.15	0.388	1.92	55	3.6	120	24/25-Mar	13:08:00
Elwha	G25	33.3	4.3	1.33	1.18	1.21-1.15	0.391	1.92	55	3.6	120	24/25-Mar	13:50:00
BLH-84	G26	148	4.9	1.51	1.18	1.23-1.12	0.444	x-sect.	25	4.7	60	27-Mar	10:50:00
Elwha	G27	322.7	4.9	1.53	1.17	1.03-1.24	0.452	1.92	70	4.8	30	27/28-Mar	12:19:00
TR-2	G28	340.4	4.9	1.53	1.17	1.07-1.25	0.452	1.92	70	4.7	30	27/28-Mar	12:50:00

[1]Mean velocity computed as a produce of mean of depths measured at the sampling vertical(s) during each bedload sample collection and the flume width of 2.74 meters.

[2]Depth from bottom of the bedload sampler resting on the bed to the water surface as indicated on the graduated deployment rod.

[3]Froude Number = mean flow velocity divided by the square root of the product of the acceleration of gravity and mean depth of flow.

[4]Water temperatures over the duration of a trial rarely varied more than 0.2°C from the mean value, and never by more than 0.5°C.

6. Data and Methods to Derive Bedload-Sampler Trapping Efficiencies

6A. Overview of Bedload-Transport Data Sources and Quality

Two primary sources of bedload-transport data produced in units of grams per seconds per meter of width were used to calculate trapping efficiencies for the bedload samplers deployed during Phases I and II of the StreamLab06 experiments:

1. Time-series data collected from each of the five Main Flume weigh pans, and

2. Discrete data produced from samples collected by the four pressure-difference bedload samples deployed 8.5 meters upstream from the weigh pans.

Selected characteristics and the quality of these data are described as follows:

6Ai. Main Flume Pan Time-Series Data

Most if not all recirculating flumes have unique characteristics that might affect the quality of the data produced and subsequent analyses. A number of factors associated with the SAFL Main Flume Facility during the StreamLab06 experiments warrant description for those considering use of the derived data, including the following:

1. Pan masses were recorded at approximately at 1.1-second intervals for the duration of the nine runs, totaling approximately 3.8-million time-series individual weigh-pan measurements. These data were corrected for brief periods of load-cell instability resulting from turbulence that occurred when a given pan tipped and dumped its accumulated sediments to the bottom of the slot. The time-series data were converted to bedload-transport rates (Marr and others, 2010a) for purposes of this analysis and for potential use by other researchers. These corrected episodes of load-cell instability constituted an insignificant part of the overall time-series dataset and are unlikely to be of any consequence in the computation of the bedload-sampler trapping coefficients produced from the StreamLab06 experiments.

2. The entrance condition into the Main Flume test section near the discharge end of the recirculation pipe was altered several times at the beginning of the Phase I sand runs. Jet plumes and secondary flow circulation resulted in bed scour adjacent to the sidewalls in the upper 3–5 m over the 20-m test section length. Because the bedload samples were collected 11.5 m downstream from the knee wall, the effect of sediment scour near the sidewalls was unlikely to be a factor that far downstream from the sampler-deployment cross section.

3. Several temporal gaps exist in the pan data but were determined to represent an inconsequential (with respect to trapping-coefficient analyses) proportion of the

dataset used in the trapping-efficiency experiments. Additionally, a number of instances of insignificant magnitude decreases in captured sediment masses based on ensuing measurements resulted in inferences of negative transport rates. Given no plausible explanation for such a bedload-transport phenomenon, these data were considered spurious, and each negative value was converted to zero.

4. The sand and gravel at the end of the test section terminated in a slope at an angle of repose at the front lip of the slot. Movement of sediment down this sloping face often was episodic, occurring as sloughing events that were asynchronous with respect to the rate of bedload transport immediately upstream from the lee face of the slope. Similar observations were made during the Hubbell and others (1987) experiments. Compensation for this problem in the bedload-trapping analysis relied on use of relatively large time intervals of at least 12.5 minutes of pan bedload-transport data.

5. The flume was operated at a constant flow rate for at least a half hour prior to sampler deployments as part of a bedload-sampler trial to enable development of dynamic equilibration of the transport rate in the flume in all but the 3.2 m^3/s flow run over a sand bed. The determination of (dynamic) equilibrium in bedload-transport rates was inferred by observing continuous plots of sediment accumulation in the weigh pans and computing 60-minute averages of sediment flux using the CDAQ system. Although it is possible that Sand Trials 12 and 18 might have occurred before the onset of equilibrium, there is no evidence to support that this potential problem interjected significant bias in the analysis.

6. The variability of bedload-transport data across the pans, in addition to the unknown time interval that bedload passing in the vicinity of the deployed bedload sampler deposited in the slot, were complicating factors in the analyses. The large datasets produced by the pans and use of small, medium, and large time intervals of bedload transport to compare to those determined from the bedload samplers, partly ameliorated this complication.

6Aii. At-a-Point Bedload-Sampler Discrete Data

The data produced by the manual deployment of the bedload samplers were considered to be more reliable than those collected using cable-suspended bedload samplers in the field. This was due in part to sampler stabilization using a tether line, which essentially precluded the addition of gouged bed material despite the slight forward movement of the sampler (in an arc by dint of the tether line's attachment to the upstream flume ceiling) as it descended to the bed. The upstream orientation of the bedload-sampler intake nozzle during each deployment was relatively easy to set, maintain and verify – a distinct advantage over most riverine bedload measurements. In the absence of immersed stabilization for a cable-suspended bedload sampler and (or) without visual evidence, neither the stability nor orientation of a cable-and-reel deployed bedload sampler can be unequivocally confirmed as part of a routine environmental bedload measurement.

6B. Analytical Techniques

The at-a-point bedload-sampler deployment scheme used to collect 2,030 bedload samples using four types of pressure-difference samplers – coupled with the Main Flume pan data – was based on the data-centric requirements of a bedload-sampler calibration model developed by Thomas and Lewis (1993) ("T-L" model) for application to the Hubbell and others (1987) dataset. The T-L model calculated bedload-trapping coefficients for a given bedload sampler on a given bed type by regressing the cube-root transformed bedload sampler transport rate on the cube-root transformed average of trapping-rate measurements from all the (then-seven) weigh pans over the same day as the sampler deployment. The cube-root transform was judged to convert the data to be approximately normally distributed, a requirement for the maximum likelihood method used to evaluate the regression.

The regression of the transformed sampler transport rates on the average transformed pan trapping rates induced significant variation in the variance of the residuals across different flume discharge rates. Consequently, a weighted regression formulation of the maximum likelihood estimation method was specified, the weights being given by a specific formulation of the daily variance of the transformed pan trapping rates. The model did not explicitly require addressing the temporal or spatial variations in bedload transport with respect to the sampler cross-section and the Main Flume slot, a complication that is difficult to address directly, as demonstrated in Thomas and Lewis' (1993) evaluation of the Hubbell and others (1985; 1987) probability matching method.

The StreamLab06 bedload-sampler trapping-efficiency analytical approach was designed to identify and – to the extent possible – normalize the dataset for temporal and spatial bedload-transport variability for all 37 trials, and for the dataset that excluded the trials at the lowest sand- and gravel-bed flows of 2.0 and 4.0 m^3/s, respectively ("truncated dataset"), toward deriving trapping coefficients for each bedload sampler deployed over a coarse sand bed channel (BLH-84, Helley-Smith, and Elwha) and a medium gravel bed (BLH-84, Elwha, and TR-2). This was in part due to the fact that bedload moving past the test section could not be assumed to eventually fall into the weigh pan 8.5-m directly downstream (according to William Emmett, U.S. Geological Survey [retired], written commun., early 21st century, bedload movement tends to deviate by some 9 degrees with respect to the downstream direction). Additionally, the lag in the time that bedload passing the sampler cross-section reached the slot was indeterminate, varying non-linearly with discharge (flow velocity).

The first objective of the bedload-trapping tests was to produce the largest dataset that available resources could support. This objective was addressed through the acquisition of 2,030 bedload samples and some 3.8-millions individual weigh-pan trapping-rate measurements. The second objective was to parse the temporal and spatial combinations of the pan data to ascertain if any affected the evaluated sampler-trapping coefficients.

Four analytical techniques considered to be tractable and technically supportable – albeit representing a range of computational complexity – were selected for trapping-coefficient

determinations. Each of the four techniques was evaluated for two datasets: The first using all 37 trials, and the second for the truncated dataset (the lowest sand- (2 m^3/s) and gravel-bed (4 m^3/s) flows near incipient motion for the bed particles that were considered inadequate for comparing bedload-sampler trapping rates to those at the slot due to the excessive time lag in particle movement between the sampler cross-section and the slot).

Following are descriptions of the methods used to assess potential spatial and temporal complicating factors in the trapping-coefficient analyses.

Spatial Variability Assessments: To identify the potential effect(s) of the expected spatial variations in bedload transport between bedload-sampler deployment section and the slot – and possibly utilize an improved understanding of the spatial nature of bedload – each of the eight analytical combinations (the four analytical techniques and the full and truncated datasets) included comparing transport rates for a given bedload sampler to those determined from one or more of the weigh pans in the cross-channel slot 8.5-meters downstream, as follows:

- The "Home" weigh pan – the trapping-rate data for the pan located directly downstream from the sampler (i.e., the distance from left wall to the pan's center equaled that to the center of the deployed bedload sampler),

- The "Neighbor" weigh pans – the average of the trapping-rate data produced by the home pan and those for adjacent pan(s) (a total of three pans unless the sampler was deployed at either station 1 or 5, in which case the mean trapping rates were computed for the home pan and the single adjacent pan), and

- "All" weigh pans – the average of the trapping-rate data for all five weigh pans.

Temporal Variability Assessments: The temporal bedload-transport monitoring conundrum – the need to synchronize or otherwise link sampler measurement values with those of the appropriate weigh pans – was addressed using a more data-intensive approach than those used by Hubbell and others (1987) or Thomas and Lewis (1993). Statistics for three intervals, or time "windows," of pan-transport data – representing the entire run time series ("infinite" case), and two subsets of the run time series – were computed for comparison and potential selection for use in transport-coefficient estimations. These three-time windows, selected by the author to represent relatively short-, medium- and long-term pan trapping rates, are the:

- **"50N" Window**: The duration that an at-a-point bedload sampler is deployed on the bed to collect a single sample – ranging from 15-180 seconds among the 37 trials – is multiplied by 50 to produce a time window to accumulate and average transport data from one or more pans where the window begins at the time the sampler is deployed. If the window "bumps" against the end of the run, the selected window covers 50 times the deployment interval ending at the end of the run. The pan data, collected on about 1.1-s intervals, were averaged for each

sampler deployment interval for subsequent use in the ensuing analyses. If the pan data are cube-root transformed, the transformation is applied after the deployment-interval averaging of the pan data. Consequently, the pan data are reduced to an average of 50 values of transformed deployment-interval averaged values. If no transformation is applied, the average is taken of 50 untransformed, deployment-interval averages, effectively resulting in the simple average of all the pan data in the specified window.

- **"200N" Window**: This is the same as the description for the 50N case (above) but quadrupling the size of the time window.

- **"Infinite" Window**: All of the data from the pans for a given run were used in this analysis.

The same three pan, and three time window data that resulted in nine pan-window coefficient combinations – along with the all-values and truncated datasets – were used as inputs for each of the four analytical methods. These are described as follows.

6Bi. Ratios of Averages Method

The Ratio of Averages (RA) method was conceived and implemented to approximate bedload-trapping coefficients for each of the four bedload samplers for subsequent comparisons to those produced by the Average of Ratios and the original and modified applications of the Thomas and Lewis (1993) model. It was performed using untransformed bedload-transport data, so no bias correction factor was required in the derivation of trapping coefficients in real space[5].

This method calculated trapping coefficients for each of the 37 trials by developing a ratio of the average trapping rates for a given trial for each of the nine pan-window combinations (the time-window pan data used for this analysis were the same used for the other three analytical methods). The nine coefficients were then averaged to produce a single coefficient for a set (bedload sampler and bed type). The RA is a relatively straight-forward, intuitive, and easily understood analytical approach. However, its use of coefficients based on simple averages of transport rates determined for each of the 37 trials renders it the most general – and therefore likely less precise or reliable – of those produced by the four analytical methods.

The 423 discrete bedload-trapping-coefficient values for the nine pan-window combinations for each of the 37 trials are shown in table 5. These trapping coefficients subsequently were reduced to nine coefficients by averaging the coefficients separately for each of the six sets. Another nine average coefficients for each set were derived for the data subset that excluded the lowest-flow sand- and gravel-bed trials using the following weighting scheme:

1. multiply each trial-average coefficient by the number of bedload samples in the trial,

2. sum the products for all the trials for a given set, and

3. divide this sum by the total number of samples collected in the set.

[5] The bedload-trapping coefficient analyses were performed using cube root-transformed bedload-transport rates (consistent with those used by Hubbell and others (1987) and Thomas and Lewis (1993)) that did not require application of a bias correction when back-transformed to real space because their magnitudes were determined to be inconsequential. The analyses were also performed on non-transformed bedload-trapping data, also referred to as “real-space data.”

Table 5. Bedload-sampler trapping coefficients by bed type, trial number, pan (drum) combinations and time-window combinations[1]

						Home Pan			Neighbor Pans			All 5 Pans		
Sampler	Trial #	Mean Bedload Transport Rate (g/(m*s))	Water Discharge	Station m from left flume wall	N	50N Trapping Coefficient Unweighted for N	200N Trapping Coefficient Unweighted for N (correct 4/11/19)	∞ Trapping Coefficient Unweighted for N	50N Trapping Coefficient Unweighted for N	200N Trapping Coefficient Unweighted for N	∞ Trapping Coefficient Unweighted for N	50N Trapping Coefficient Unweighted for N	200N Trapping Coefficient Unweighted for N (corrected 4/11/2019)	∞ Trapping Coefficient Unweighted for N
BLH-84	S14	5.8	2.0	1.37	120.0	0.85	0.65	0.53	0.68	0.55	0.45	0.61	0.54	0.44
BLH-84	S12	9.3	2.0	1.92	49.0	0.67	0.75	1.06	0.61	0.67	0.97	0.58	0.51	0.71
BLH-84	S16	24.0	2.5	0.82-1.92	120.0	1.11	1.02	0.90	1.07	1.04	0.93	1.05	1.04	0.93
BLH-84	S1	39.2	3.0	1.92	75.0	0.51	0.50	0.52	0.52	0.51	0.51	0.49	0.49	0.50
BLH-84	S5	48.9	3.0	0.82	30.0	0.35	0.35	0.56	0.36	0.36	0.60	0.38	0.38	0.63
BLH-84	S6	63.9	3.0	1.37	30.0	0.47	0.46	0.75	0.48	0.48	0.77	0.49	0.50	0.82
BLH-84	S8	63.9	3.0	2.47	30.0	0.54	0.58	0.95	0.54	0.56	0.89	0.50	0.50	0.82
BLH-84	S7	82.5	3.0	1.92	30.0	0.67	0.69	1.09	0.65	0.67	1.08	0.63	0.64	1.06
BLH-84	S4	85.7	3.0	0.27	30.0	0.79	0.67	1.17	0.70	0.64	1.07	0.68	0.67	1.10
BLH-84	S19	113.3	3.2	1.92	74.0	1.50	1.48	1.33	1.53	1.39	1.29	1.26	1.29	1.25
BLH-84	S9	207.1	3.6	1.92	80.0	1.01	1.05	1.07	1.08	1.11	1.12	1.21	1.19	1.15
Elwha	S13	16.1	2.0	1.92	60.0	4.89	2.82	1.84	2.53	2.56	1.68	1.50	1.54	1.23
Elwha	S17	37.3	2.5	1.92	45.0	1.81	1.21	1.53	1.84	1.22	1.45	1.48	1.14	1.45
Elwha	S3	173.0	3.0	1.92	30.0	6.11	4.39	2.27	4.87	4.21	2.27	4.40	3.90	2.22
Elwha	S10	311.5	3.6	1.92	15.0	2.85	1.73	1.61	2.66	1.74	1.68	2.42	1.68	1.73
Helley-Smith	S15	41.9	2.0	0.82	50.0	3.62	2.64	2.21	3.94	3.27	2.65	4.21	3.87	3.21
Helley-Smith	S18	88.8	2.5	0.82	50.0	3.02	2.51	3.06	3.15	2.90	3.42	3.26	3.01	3.45
Helley-Smith	S2	235.1	3.0	0.82	42.0	4.08	4.20	2.68	4.56	4.77	2.86	5.25	5.33	3.02
Helley-Smith	S11	631.3	3.6	0.82	50.0	10.90	3.10	3.32	7.59	3.39	3.52	5.19	3.45	3.51
BLH-84	G22	4.8	4.3	x-sect.	25.0	0.66	0.68	0.47	0.63	0.64	0.44	0.65	0.65	0.45
BLH-84	G21	4.9	4.0	0.82	51.0	7.77	9.55	4.11	3.12	3.64	2.67	2.84	3.38	1.96
BLH-84	G17	5.5	4.0	x-sect.	25.0	4.13	3.97	2.27	2.99	3.21	1.87	1.88	1.64	2.19
BLH-84	G18	6.3	4.0	x-sect.	25.0	19.18	12.20	5.09	9.90	5.00	3.46	5.07	4.57	2.52
BLH-84	G23	9.2	4.3	x-sect.	25.0	0.59	0.67	0.99	0.53	0.62	0.85	0.56	0.64	0.86
BLH-84	G14	18.7	4.0	x-sect.	25.0	10.11	18.46	10.74	15.25	10.22	8.00	16.92	11.19	7.45
BLH-84	G26	147.6	4.9	x-sect.	25.0	0.82	0.82	0.92	0.81	0.80	0.90	0.81	0.81	0.91
BLH-84	G9	514.7	5.5	x-sect.	25.0	0.65	0.73	0.69	0.61	0.68	0.66	0.60	0.68	0.66
BLH-84	G2	599.5	5.5	0.27	28.0	0.96	0.96	0.94	0.77	0.74	0.75	0.75	0.78	0.76
BLH-84	G12	701.6	5.5	x-sect.	25.0	1.12	0.82	0.88	1.07	0.81	0.86	1.06	0.83	0.89
BLH-84	G6	757.5	5.5	2.47	28.0	1.68	1.22	1.19	1.26	1.02	1.03	1.04	0.93	0.96
BLH-84	G5	766.8	5.5	1.92	28.0	1.09	0.93	0.93	1.19	1.00	0.99	1.09	0.97	0.98
BLH-84	G4	828.9	5.5	1.37	28.0	1.00	0.87	0.96	0.97	0.87	0.94	1.08	0.99	1.06
BLH-84	G8	842.0	5.5	0.82	75.0	0.94	0.76	0.88	1.08	0.92	1.03	1.18	1.03	1.07
BLH-84	G3	896.7	5.5	0.82	28.0	0.94	0.86	0.94	1.08	1.04	1.09	1.16	1.10	1.14
BLH-84	G11	1026.4	5.5	x-sect.	25.0	1.19	1.23	1.31	1.10	1.20	1.28	1.11	1.24	1.31
Elwha	G16	12.6	4.0	1.92	40.0	4.87	1.25	2.36	6.02	2.22	3.66	7.26	3.17	5.03
Elwha	G20	23.8	4.0	0.82	51.0	15.83	12.14	14.51	15.75	14.84	15.02	17.34	16.27	9.69
Elwha	G24	33.3	4.3	1.92	55.0	2.98	2.85	2.30	4.85	4.84	3.39	4.32	4.41	3.12
Elwha	G27	322.7	4.9	1.92	70.0	1.93	1.73	1.82	2.17	1.91	2.15	2.01	1.82	2.00
Elwha	G1	500.8	5.5	5 sample xs	5.0	0.75	0.53	0.61	0.71	0.53	0.60	0.71	0.60	0.64
Elwha	G7	1129.7	5.5	1.92	66.0	1.91	1.50	1.36	1.94	1.53	1.45	1.77	1.47	1.44
TR-2	G15	18.0	4.0	1.92	40.0	6.03	4.71	3.35	9.06	7.42	5.21	10.70	9.20	7.16
TR-2	G19	23.8	4.0	1.92	51.0	15.68	13.22	4.44	14.13	13.73	6.90	16.48	15.94	9.48
TR-2	G25	38.1	4.3	1.92	55.0	3.28	3.14	2.63	5.48	5.41	3.87	4.82	4.92	3.57
TR-2	G28	340.4	4.9	1.92	70.0	2.47	2.17	1.92	2.70	2.43	2.26	2.60	2.28	2.11
TR-2	G10	1008.9	5.5	1.92	40.0	1.40	1.49	1.22	1.43	1.58	1.30	1.39	1.57	1.28
TR-2	G13	1041.8	5.5	1.92	22.0	1.35	1.37	1.26	1.48	1.45	1.34	1.53	1.49	1.33

[1] The "home pan" refers to the weigh pan directly downstream from the deployed bedload sampler; the "neighbor pan" includes the home pan and adjacent pan(s) (three pans if the bedload sampler was deployed directly upstream of any of the three interior pans, or a single additional, adjacent pan if the bedload sampler was deployed directly upstream from a pan adjacent to the flume wall); and "all pans" refers to the average transport rates determined for all 5 pans. Time-window combinations of 50N and 200N refer to the average of all relevant pan transport rates that occurred within 50 and 200 times, respectively, the duration that the bedload sampler rested on the bed (N, in seconds). The Infinity time window used the average transport rate determined for the relevant pans for the duration of the run.

6Bii. Average of Ratios ("AR") Method

The AR method takes greater advantage of the StreamLab06 bedload datasets than that of the RA method by enabling ratios to be computed for a specific window with respect to a given bedload-sampler deployment in a trial. It develops pan-window ratios for every manual bedload sample in a trial. The ratios are then averaged to produce a total of four

trapping coefficients for each set. The AR method was applied only to untransformed (real-space) data.

6Biii. Modified Thomas and Lewis (1993) Bedload-Sampler Calibration Models

As described previously, Thomas and Lewis (1993) developed a model for calculating bedload-sampler coefficients and applied it to the Hubbell and others (1987) dataset. A modified version of the T-L model was applied to the StreamLab06 in real- and cube root-transformed space.

For either application real-space or cube root application, the modified T-L model first averaged real-space transport data at intervals equal to the duration the sampler rested on the bed during a trial. For the cube root-transformed analysis, the interval averages were then cube root-transformed and subsequently averaged according to the specified pan-window combination intervals (the application of the model in real space simply skipped the aforementioned transformation step).

The conceptual approach of Thomas and Lewis (1993) is that the sampler measurement responds to the true bedload transport rate in a linear relation. Let y_i represent the transformed sampler measurement for observation i, which is related to true, transformed bedload, m_i, according to equation 3,

$$y_i = bm_i + e_i, \quad (3)$$

where e_i is a random measurement error, assumed to be normally distributed with mean zero and variance σ_e^2; and b is an unknown coefficient indicative of the trapping efficiency of the sampler. Equation (3) is a simplified version of the equation proposed in Thomas and Lewis in that the intercept of the linear relation is constrained to equal zero.

True, transformed bedload transport at the sampler, m_i, is unobserved. Following Thomas and Lewis, m_i is estimated by a mean value, $\widetilde{m}_i$, this value being related to the true value according to

$$m_i = \widetilde{m}_i + u_i, \quad (4)$$

where u_i is independent of $\widetilde{m}_i$ and assumed to be normally distributed with a mean of zero and a variance of σ_{ui}^2. The variance σ_{ui}^2, referred to as the uncertainty in true bedload transport, is assumed to vary across observations, a consequence of changing variability

at different discharge rates. The use of a mean value in place of the unobserved true value is similar to an instrumental variables approach to model estimation. The means (i.e., instruments) are likely highly correlated to the true transport rates over the range of discharges applied in the experiments, and the mean is uncorrelated with the residual of equation (3).

Applying equation (4) to equation (3), equation (3) can be rewritten as equation 5,

$$y_i = b\tilde{m}_i + e_i + bu_i = b\tilde{m}_i + v_i, \qquad (5)$$

where v_i is a residual, independent of $\tilde{m}_i$, and represents the combined measurement

error uncertainty and the uncertainty in the true bedload transport experienced by the sampler. Consequently, the variance of v_i, σ_{vi}^2, varies by observation, with

$$\sigma_{vi}^2 = \sigma_e^2 + \sigma_{ui}^2.$$

Whereas equation (3) cannot be estimated due to the unobservability of m_i, the second

equality in equation (5) depends on observed values of $\tilde{m}_i$ and therefore can be

estimated. Note, however, that due to variations in the variance of truth uncertainty, the estimable equation has heteroscedastic residuals, a condition that can be controlled using weighted estimation.

The implemented T-L method relates data that have been cube-root transformed, and bases the mean transformed true transport rate, $\tilde{m}_i$, on a window average of the pan data.

The pan data are individually processed according to the time and duration of each sampler measurement, with the data produced by each of the five pans evaluated separately. Initially, the pan data are averaged, without transformation, according to numerous smaller intervals over the full run, with each smaller interval corresponding in length to the length of time the sampler is deployed to generate a sampler measurement. These interval-averages are then cube root-transformed. For the infinity case, all transformed interval averages over the run are averaged. For the 200N window case, an average is taken of the 200 transformed interval averages corresponding to a time window that begins at the time the sampler is deployed for the measurement, subject to the condition that the run extends sufficiently into the future to contain the window; otherwise, a 200N window average is taken consisting of the last 200 intervals during the run. A similar window average is computed for each sampler measurement corresponding to a window that is 50-intervals in duration ("50N"). Also computed is the variance of the transformed interval averages within each window. These variances represent the variance in transformed bedload presumably experienced by the sampler across multiple

measurements, referred to above as the uncertainty in true transport. As explained below, these variances are used to compute weights for a weighted least-squares regression.

The modified T-L method is implemented in a three-step process. In the first step, a simple linear regression is performed with the cube-root-transformed sampler measurement regressed on the corresponding measurement's window average of the transformed, interval-averaged pan data (either the home pan, the home pan averaged with its neighboring pans, or all pans). In performing this regression, the intercept of the regression is constrained to equal zero. The estimated coefficient in this regression is unbiased, but the standard error of the coefficient could be biased because of the heteroscedasticity of the residuals. This bias is corrected through weighted least squares, a procedure that requires a second-step regression.

In the second step, the residuals of the first-step regression are squared and regressed on the variance of the transformed, interval-averaged pan data, computed over all intervals in the specified window. The intercept of this regression is the variance in the residual that does not depend on varying true uncertainty, and thus is assumed to represent the innate measurement error of the sampler.

In the third step, the second-step regression is used to predict the variance of the residual for every observation. The inverse of this predicted variance is used as a weight in the re-estimation of the first-step regression. As a consequence of weighting, the reported standard error of the slope coefficient, the coefficient on the window average of the transformed, interval-averaged pan data, is unbiased.

The modified T-L method described above was also implemented without transformation of the sampler and pan data. The method remains valid as weighted least squares does not require residuals to be normally distributed, or to have any particular distribution. The only requirement for weighted least squares is that the observations are independent and that the weighted residuals are approximately homoscedastic. The implementation of the method without transforming the data has the advantage that no transformation of the estimated calibration coefficient is required.

6C. Selected Observations on the StreamLab06 Bedload-Transport Dataset

Several notable advantages and drawbacks are associated with the dataset produced by the four pressure-different bedload-samplers and weigh pans as part of the StreamLab06 Phases I and II experiments. This section presents the more important of those and indicates how challenges in producing reliable bedload-trapping coefficients were addressed.

6Ci. Selected Considerations for Identifying the Most Relevant Analytical Tools

Method and Dataset Evaluation: Each of the four analytical methods selected – and their application to the full 37-trial and truncated datasets– were associated with a different analytical treatment. Those taking the greatest advantage of the data and available analytical tools were generally considered to be the most reliable.

Considerable inconsistencies resulted in the coefficient(s) developed for a given sampler among the four methods. The following information is proffered to share the author's reasoning in the coefficient analysis:

1. The truncated dataset was considered to be more relevant and applicable than the full 37-trial dataset for coefficient analyses. This conclusion was reached in part based on sediment-transport theory – that bedload movement near incipient motion (referred to as Type-I Transport by Ryan and others, 2002) is an exceptionally slow process compared to that for Type-II transport. Relatively long lag times in bedform movement likely resulted in fewer than the 2-3 bedforms sought for measurement purposes transiting the 8.5-meter upstream reach from the weigh pans. Additionally, anomalous coefficients ranging from values of 7-19 occurred solely during 4.0 m^3/s flows over a gravel-bed channel.

2. Coefficient determinations from the modified T-L model in either real space or cube root space were considered superior to the Average of Ratios or Ratio of Averages methods. This was due in part to the relative strength of the 3-step regression approach that used weighted predictions from the 2^{nd} step adjusting for the square of the variance in the second model step. Also, the internal general agreement in the magnitudes of the computed coefficients was maximal for the modified T-L model.

3. Analytical results consistent with known or estimated sampler-hydraulic efficiencies were considered to lend greater credence to the derived coefficients. This follows from the fact that hydraulic efficiency exerts a considerable influence on trapping coefficients determined from data produced by a properly selected and deployed bedload sampler.

4. Geometrically congruent sampler nozzles with identical nozzle-flare ratios were expected to exhibit similar trapping coefficients. This focused primarily on the TR-2 sampler and its 2/3-scale congruent version, the Elwha sampler. As sampler widths increase with the same intake-nozzle ratio, sampler-trapping coefficients theoretically should converge to the same value.

Spatial and Temporal Relations in Transport Data: If it is possible to unequivocally identify a correlation between bedload-transport rates determined by a bedload sampler deployed in at-a-point fashion to those derived from the data from one, some, or all five weigh pans located in a slot 8.5 meters downstream, it has yet to be shared with the author. Thomas and Lewis (1993) contended that Hubbell and others' (1985; 1987) probability matching method resulted in a biased assessment of bedload-trapping efficiencies. The primary challenge of this analysis was to parse a relatively large but "messy" bedload-transport dataset in an attempt to produce useful statistics for weigh pan combinations and time intervals that showed minimal variations for a given trial or set.

For example, where minimal statistical variations for two or all three weigh-pan time intervals used in a given analysis, it was construed that the average temporal bedload-transport statistics for the given analysis are consistent and could be accepted with relative confidence. The same concept is applicable to the weigh-pan data: If the transport statistics for the pan immediately downstream from the deployed bedload sampler – the "Home Pan" – were similar to the average of the rates determined for the "Neighbor Pans" and for all five pans, it could be inferred that spatial disparities in transport in the weigh pans more or less could be ignored and average values from multiple pans could be reliably used for coefficient determinations.

However, when transport rates differed substantially between the pan combinations, a more nuanced evaluation was required. Based on sediment-transport theory – and more-or-less confirmed by a graph depicting an approximate bell-shaped curve of average transport rates across the then-seven pans in the Main Flume slot (previously unpublished files relating to David Hubbell's 1980s Main Flume experiments (Gray and others, in press)) it was unsurprising that both pans nearest the flume walls typically captured sub-average percentages of total bedload transport. Additionally, some near-incipient motion transport rates in which but a few g/(m×s) were measured, could be considered unimportant artifacts (most low transport-rate values measured by the bedload samplers and the pans were considered of dubious relevance).

Uncertainty Statistics: Consistency in uncertainty statistics for a given data treatment was useful in determining if the statistics were significant, but only confined to a given data treatment. Statistics for cube root-transformed data were internally comparable, but not to those statistics from untransformed data, and vice-versa.

General Unreliability of Coefficients developed at the Lowest Sand- and Gravel-Bed Runs: Most low-flow bedload-transport coefficient calculations for all samplers during sand-bed runs (2 m^3/s) and gravel-bed runs (4 m^3/s) resulted in values that were considered to be largely unreliable for the purpose of defining bedload-sampler trapping

coefficients. This was in part a function of the exceptionally slow rate that bedforms moved from the bedload-sampler section to the slot, such as what appeared to have occurred during these lowest flows for each bed type. These low-flow measurements, made near incipient motion as Phase I transport (Ryan and others, 2002) were not only unlikely to be accurate due to difficulty in gram-level variations in the amount of sequentially left in the sampler bag after its contents were transferred to a sample bag. More importantly, such low-transport rate values were deemed of minimal relevance to a bedload sampler's usefulness for collecting accurate bedload data. Although derivation of more accurate low-transport transport-rate values to help define the slope of a coefficient relation would have been preferred, the author considers the key data to be those that describe transport above low flows, particularly during Type-II transport (Ryan and others, 2002) in which the surficial material is largely mobilized.

Additionally, some of the transport rates measured by the bedload samples under these circumstances were less than 0.03 kg/(m×s). Because small variations in wet masses of bedload that remained in a sampler bag occurred during the iterative bag-empty-and-redeploy sequence, some of the actual bedload rates might have been zero or perhaps double that from the collected-and-weighed sample. Also, grams of bed material could have been dislodged when the sampler was set on the bed that would have been inferred by dint of their presence in the mesh bag as bedload.

Although the low-flow trapping coefficients are somewhat important in determining the slope of a coefficient line, the refinement of trapping coefficients for a sampler above low transport rates is a substantially more important goal. Because the presumed spurious low-flow coefficients tended to interject greater uncertainty in many of the analyses, those analyses performed on the dataset excluding the low-flow coefficients was considered to result in more reliable and useful sampler coefficients.

Consistency in Computed Coefficients With Hydraulic Theory and Other Evidence: According to Hubbell and others (1987), the Helley-Smith – with the largest intake-nozzle flare ratio – also has the largest hydraulic efficiency – 1.54 – of the four sampler types (those quoted for the BL-84 and TR-2 are qualified as "estimated"). Because hydraulic and bedload-trapping efficiencies are positively correlated, the trapping coefficient for the Helley-Smith was expected to be relatively large, particularly in the readily erodible sand bed in which it was deployed.

Bunte and others (2017) provides measured hydraulic-efficiency statistics for the BLH-84, Elwha, and TR-2 (but not for the Helley-Smith) samplers that the author considers to be more reliable than shown as appearing as estimates in Hubbell and others (1987); hence, the Bunte and others (2017) hydraulic coefficients weigh heavily in the ensuing analysis. According to Bunte and others (2017), the BLH-84 has the lowest hydraulic efficiency, ranging from 0.93 - 1.03. Those for the Elwha range from 1.01 - 1.10, and for the TR-2, from 1.08 to 1.15. The relevance of these and the Helley-Smith hydraulic efficiency (Hubbell and others, 1987) are woven into the ensuing analysis.

7. Bedload-Sampler Trapping Efficiencies

The several-hundred bedload coefficients produced by the four analytical methods and two datasets (combinations of bedload-sampler and bed type) were averaged and reduced to eight coefficients for each set (table 6). Standard deviations were calculated for the eight coefficients associated with each sampler. The bar charts that appear in figures 13, 15, 17, 19, 21, and 23 show sampler coefficients calculated for the:

1. Modified T-L method in cube-root space,

2. Modified T-L method in real space,

3. Average of Ratios (AR) method, and

4. Ratios of Averages (RA) method.

Each of those four methods was further evaluated for:

- All nine combinations of three pan configurations and three time windows, and

- Both the full 37-trial transport-rate dataset, and the truncated dataset excluding the runs at the lowest sand-bed (2 m^3/s) and gravel-bed (4 m^3/s) flows, thus retaining the substantial preponderance of analytical data available from the four higher-flow sand runs and the three higher-flow gravel runs.

The line plots that appear in figures 14, 16, 18, 20, 22, and 24 show sampler coefficients calculated for each of the nine combinations of pan configurations and time windows versus transport rates determined from the unweighted-for-N average of the trapping rates for all trials within the set (i.e., Ratios of Averages method).

Appendix 2 shows selected plots generated by the modified T-L model for each set – the both the BLH-84 and Elwha samplers over a coarse-sand and medium-gravel bed; a Helley-Smith over a coarse-sand bed; and a TR-2 over a medium-gravel bed – with the regression line relating the All Pans, Infinity window "true" transport rate to that measured by the respective bedload sampler. All values were derived from untransformed bedload-transport measurements.

Table 6. Summary of bedload-trapping coefficients calculated for the four pressure-difference bedload samplers by the Modified T-L, Average of Ratios, and Ratios of Averages methods, in each case for the full 37-trial bedload-sampler dataset and for that excluding the trials during the 2 m^3/s sand-bed run and 4 m^3/s gravel-bed run. H-S is Helley-Smith; TR-2 is Toutle River-2.

Bedload Sampler	Bed Material	MODIFIED THOMAS AND LEWIS (1993) RESULTS FOR SETS							
		All 37 Bedload-Sampler Trials				No 2 or 4 m^3/s Bedload-Sampler Trials			
		REAL SPACE		CUBE ROOT >REAL		REAL SPACE		CUBE ROOT >REAL	
		MEAN	STDEV	MEAN	STDEV	MEAN	STDEV	MEAN	STDEV
BLH-84	SAND	0.83	0.06	0.52	0.06	0.89	0.05	0.56	0.06
ELWHA	SAND	1.76	0.20	1.59	0.16	1.74	0.17	1.57	0.09
H-S	SAND	3.10	0.49	3.14	0.31	3.14	0.45	3.18	0.26
BLH-84	GRAVEL	0.89	0.15	0.65	0.13	0.86	0.09	0.59	0.06
ELWHA	GRAVEL	1.46	0.21	1.68	0.35	1.44	0.21	1.58	0.29
TR-2	GRAVEL	1.64	0.18	1.84	0.63	1.59	0.18	1.72	0.30
		AVERAGE OF RATIOS FOR SETS				RATIOS OF AVERAGES FOR SETS			
		REAL SPACE				REAL SPACE, WEIGHTED FOR N TRIALS			
		ALL 37 TRIALS		NO 2 or 4 m^3/s Trials		ALL 37 TRIALS		NO 2 or 4 m^3/s Trials	
		MEAN	STDEV	MEAN	STDEV	MEAN	STDEV	MEAN	STDEV
BLH-84	SAND	0.86	0.04	0.80	0.15	0.73	0.08	0.81	0.08
ELWHA	SAND	2.32	0.67	2.11	0.45	2.38	0.74	2.43	0.64
H-S	SAND	3.83	0.90	3.84	0.67	3.00	1.02	3.03	1.02
BLH-84	GRAVEL	2.15	0.57	0.83	0.14	1.34	0.74	0.91	0.03
ELWHA	GRAVEL	4.70	0.73	2.24	0.33	3.02	0.69	1.96	0.29
TR-2	GRAVEL	4.96	1.29	2.50	0.42	2.50	0.63	3.03	1.02

7A. Evaluation of BLH-84 Sand- and Gravel-Bed Trapping Efficiencies

Hydraulic Efficiency: According to Bunte and others (2017), the hydraulic efficiency of an empty BLH-84 (i.e., with an unobstructed collection bag, a caveat relevant to the trapping efficiency of any pressure-difference sampler) ranges from 0.93 to 1.03. Based on the positive correlation between hydraulic and trapping efficiencies, trapping coefficients for the BLH-84 were expected to range from sub-unity at lower transport rates to near unity at higher rates. These trends are reflected in both figures 13 and 14 albeit with the key difference that those shown in figure 14 calculated by the Ratios of Averages method indicate moderately super-unity trapping coefficients at medium- and high-transport rates.

Sand Bed: All 54 coefficients depicted in figure 13 indicate that the BLH-84 traps sand with a sub-unity coefficient. All real-space trapping coefficients range from 0.73 (for the least-reliable Ratios of Averages, All Trials method) to 0.89 for the relatively reliable T-L truncated-dataset analysis with untransformed data. The coefficients of 0.52 and 0.56 based on cube root-transformed data are about two-thirds the magnitude of the real-space data. This general disparity in real space vs. cube root data was also reflected in the coefficients derived for the BLH-84 gravel data (figure 19). No similar bias appeared consistently among the other four sets (combinations of bedload sampler and bed type).

Figure 14 indicates that coefficients are near or less than unity at lower bedload-transport rates, and above unity at higher transport rates. The shape of this plot is somewhat consistent with that shown for the BLH-84 gravel-bed coefficients in figure 20. Aside from the coefficients at transport rates of 50-100 g/(m×s), deviations among the nine pan-window combinations tended to be within a range of about 20-percent.

The disparities between the real-space and cube-root T-L analyses for the BLH-84 led to adding the Average of Ratios method to the analysis. The source of these disparities could not be unequivocally identified.

Due to the relatively consistency of the coefficients developed with real-space data, the coefficients computed using cube-root data were considered inferior and therefore ignored. BLH-84 hydraulic-efficiency data (Bunte and others, 2017) were generally consistent with the trapping-efficiency results. An average of the coefficients developed in real space for the truncated dataset – the T-L model, AR, and RA methods – yielded a sand-bed trapping coefficient for the BLH-84 of 0.83.

Gravel Bed: The coefficients depicted in figure 15 – excluding the anomalously large values for the real-space Average of Ratios method – indicate that the BLH-84 sampled medium gravel sub-efficiently. More or less consistent with results from the sand-bed trapping analysis, all of the real-space trapping coefficients range from 0.91 (for the least-reliable Ratios of Averages, All Trials method) to 0.86 for the most reliable T-L truncated dataset analysis. The coefficients of 0.65 and 0.59 based on cube root-transformed data again are about two-thirds the magnitude of the real-space data.

The plot in figure 16 – with the exception of the Home Pan 50N combination which peaks at a coefficient of about 1.7 – exhibits minimal variations for the pan-window combinations. Its general shape – and inferences from BLH-84 hydraulic-efficiency data (Bunte and others, 2017) – is close to the sampler's bedload-trapping performance in a sand bed (figure 14). The gravel-bed trapping coefficient for this sampler calculated in the same manner as that for the sand bed yielded a trapping coefficient of 0.87.

Conclusion: The preponderance of evidence from the T-L model supports the conclusion that the BLH-84 samples moderately and relatively consistently sub-efficiently. These results support correction of bedload-transport rates by dividing raw sand-trapping rates by a coefficient of 0.83; and dividing raw medium-gravel-trapping rates by a coefficient of 0.87.

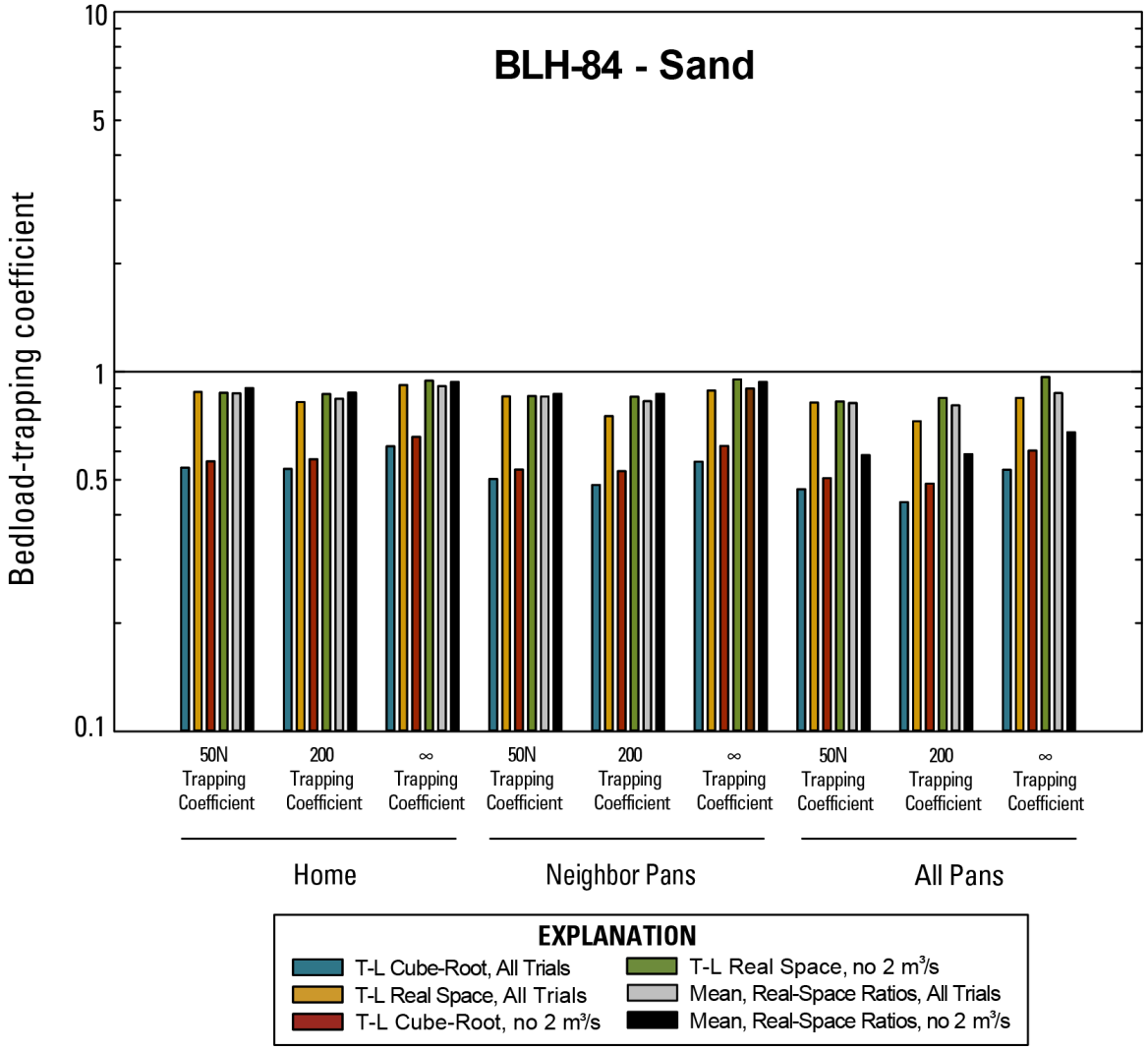

Figure 13. Graph showing BLH-84 sand-bed trapping coefficients calculated for three of the four analytical methods (excluding the Ratios of Averages method). Coefficients for the nine combinations of Home Pan, Neighbor Pans, and All Pans plus the 50N, 200N, and Infinite windows are shown, and include coefficients for both the 37-trial dataset and that without the 2.0 m^3/s run.

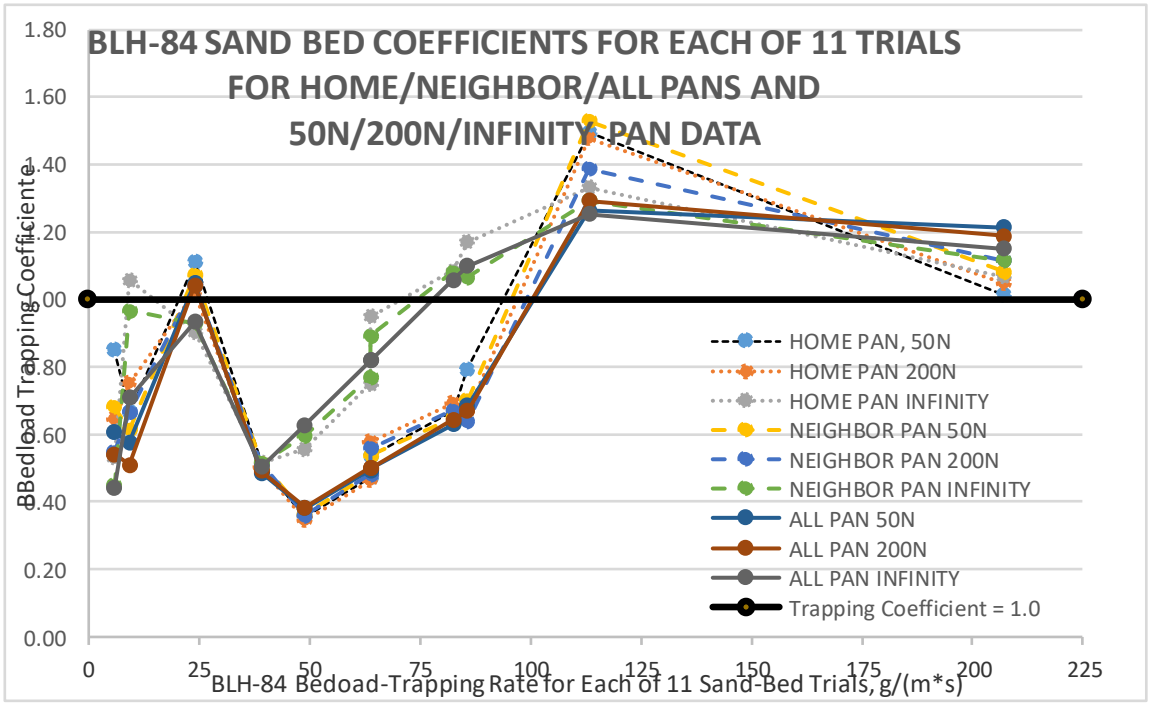

Figure 14. Plot showing BLH-84 sand-bed trapping coefficients versus the mean set bedload-transport rate for the bedload samples computed by the Ratios of Averages (RA) method. Coefficients for the nine combinations of Home Pan, Neighbor Pans, and All Pans plus the 50N, 200N, and Infinite windows are shown.

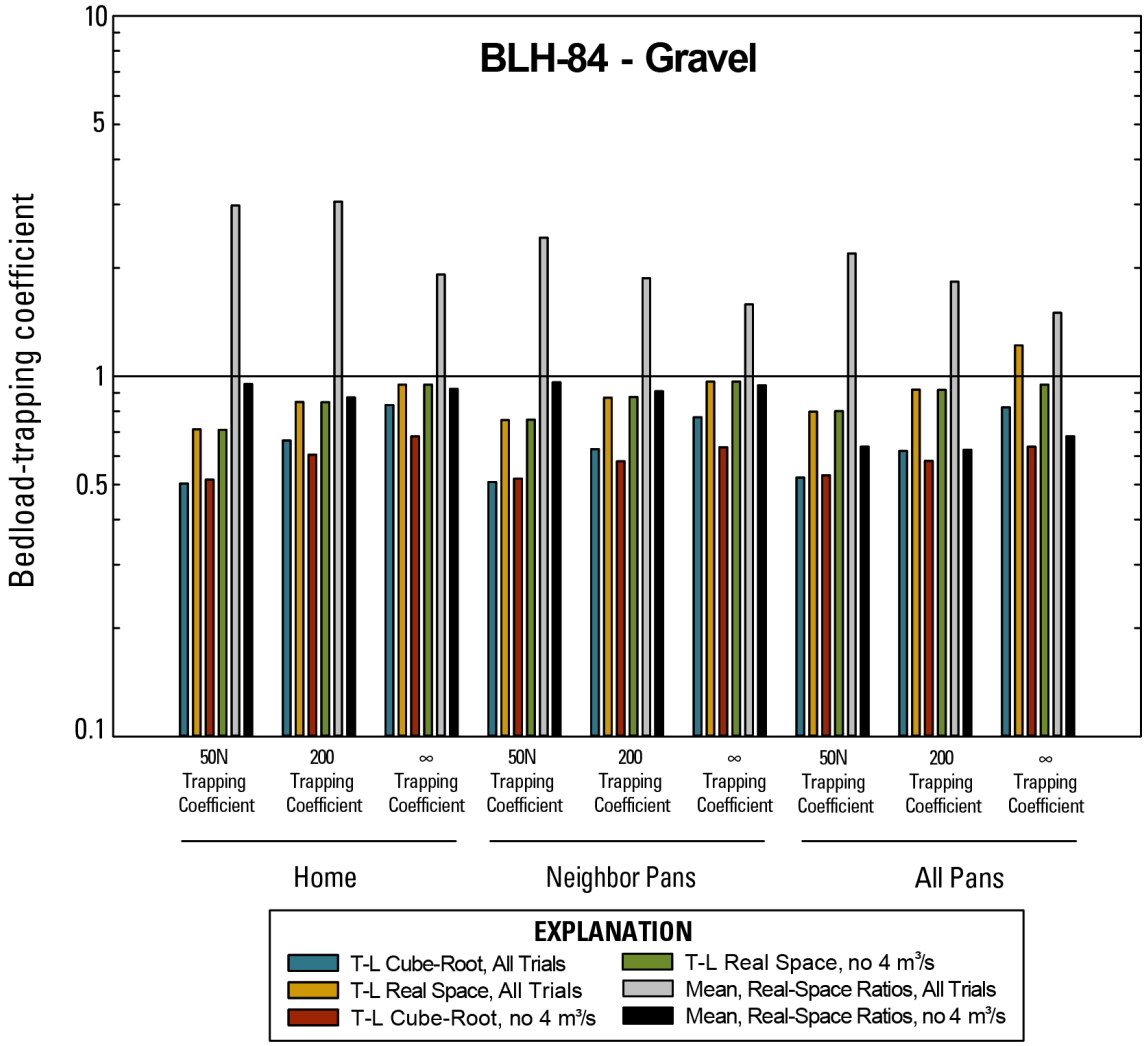

Figure 15. Graph showing BLH-84 gravel-bed trapping coefficients calculated for three of the four analytical methods (excluding the Ratios of Averages method). Coefficients for the nine combinations of Home Pan, Neighbor Pans, and All Pans plus the 50N, 200N, and Infinite windows are shown, and include coefficients for both the 37-trial dataset and that without the 4.0 m^3/s run.

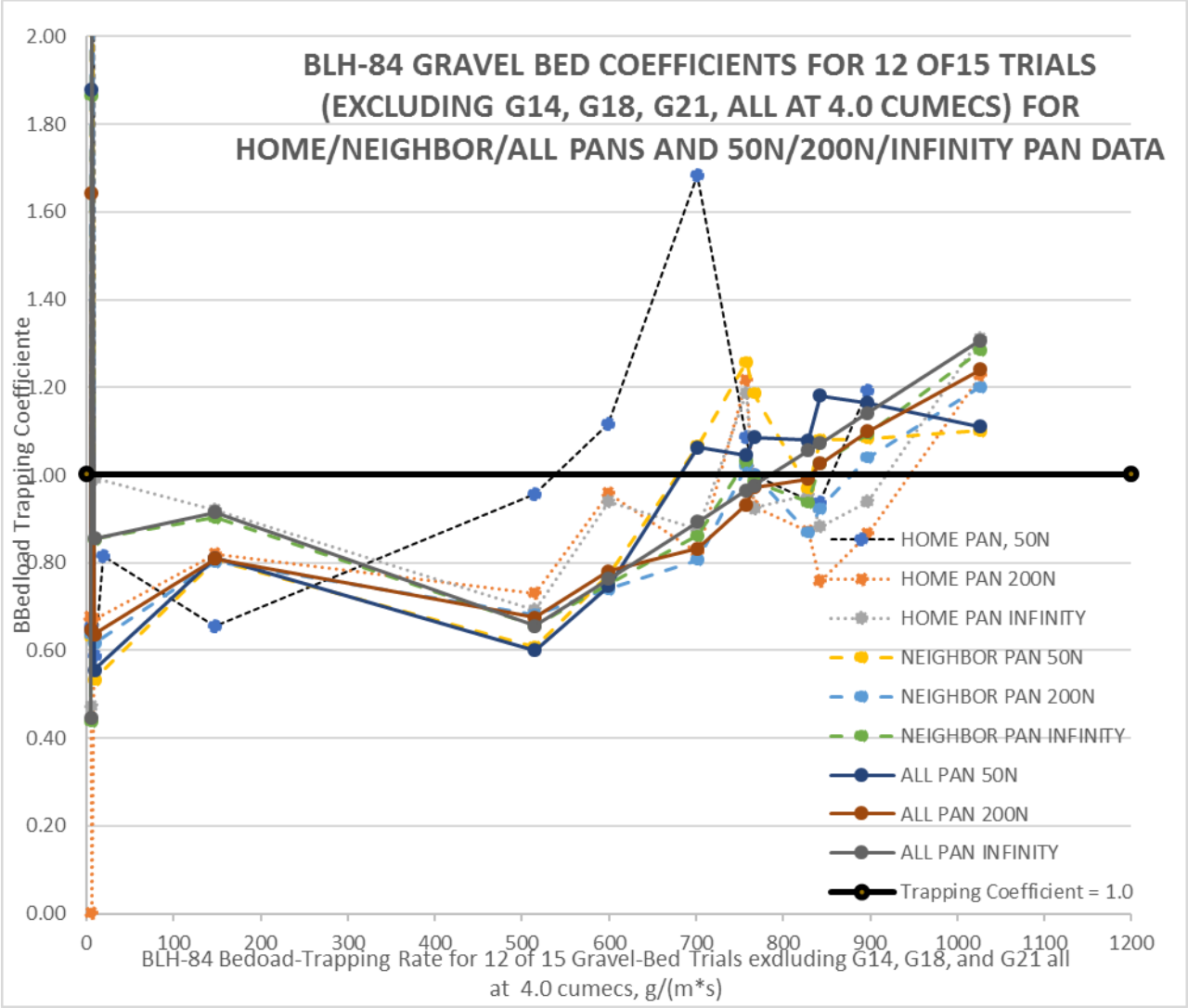

Figure 16. Plot showing BLH-84 gravel-bed trapping coefficients versus the mean set bedload-transport rate for the bedload samples computed by the Ratios of Averages (RA) method. Coefficients for the nine combinations of Home Pan, Neighbor Pans, and All Pans plus the 50N, 200N, and Infinite windows are shown. “CUMECS” are m^3/s.

7B. Evaluation of the Elwha Sand- and Gravel-Bed Trapping Efficiencies

Elwha Hydraulic Efficiency: According to Bunte and others (2017), the hydraulic efficiency of an unobstructed Elwha ranges from 1.01 to 1.10. Based on the positive correlation between hydraulic and trapping efficiencies, trapping coefficients for the Elwha were expected to be uniformly superefficient and to increase concomitant with transport rates. Such expectations are neither unequivocally confirmed nor refuted in this analysis (see figures 17, 18, 19, and 20).

Sand Bed: Figures 17 and 18 indicate that, without exception, the Elwha consistently traps sand super-efficiently. All T-L model results, including the full 37-trial dataset and the truncated dataset, indicate that the cube-root data underperform their real-space counterparts by about 10 percent. Five of the nine real-space Average of Ratios values exceed a coefficient of 2, as do three of the T-L real-space coefficients. However, both the 37-trial and truncated datasets used in the T-L real-space model showed considerable consistency around an average coefficient of 1.67.

The plot in figure 18 includes a major anomaly at a transport rate of about 170 g/(m×s), in which the pan-window coefficient combinations not only diverge substantially but range anomalously from about 2-6. The most stable of the combinations are the three infinity-window cases, implying that the infinity time-window data were more stable (and likewise presumably reliable) versus the 50N and 200N window cases.

Gravel Bed: Consistent with its sand-trapping characteristics, Figure 19 indicates that the Elwha consistently traps gravel super efficiently. The T-L truncated dataset yields the most consistent and reasonable results for this sampler.

Figure 20 indicates for trials greater than low-to-medium flow (exceeding about 300 g/(m×s), the pan-window combinations are relatively consistent. However, the mid-range coefficient dips to an average of about 0.7 but "recovers" to a value of about 1.5 at the highest transport rate. The mid-range anomaly remains unexplained. Regardless, the nine pan-window combinations above low low-transport rates cluster closer to a coefficient of unity than those plotted for the sand set.

The mean medium-gravel-trapping efficiency for the Elwha is 1.54 based on the four T-L analyses.

Conclusion: As with the BLH-84, heretofore unexplainable variations in the shapes of the sand- and gravel-bed coefficient plots produced by the Ratios of Averages method versus bedload-transport rates could not be fully explained. However, the T-L statistics for both indicate that somewhat similar trapping rates were derived for the sampler in both bed types and for the full and truncated datasets.

The nearly uniform super-efficient trapping coefficients are consistent with the hydraulic performance of the Elwha, per Bunte and others (2017). These results support correction of bedload-transport rates by dividing raw sand-trapping rates produced by the Elwha by a coefficient of 1.67; and dividing raw medium-gravel-trapping rates by a coefficient of 1.54.

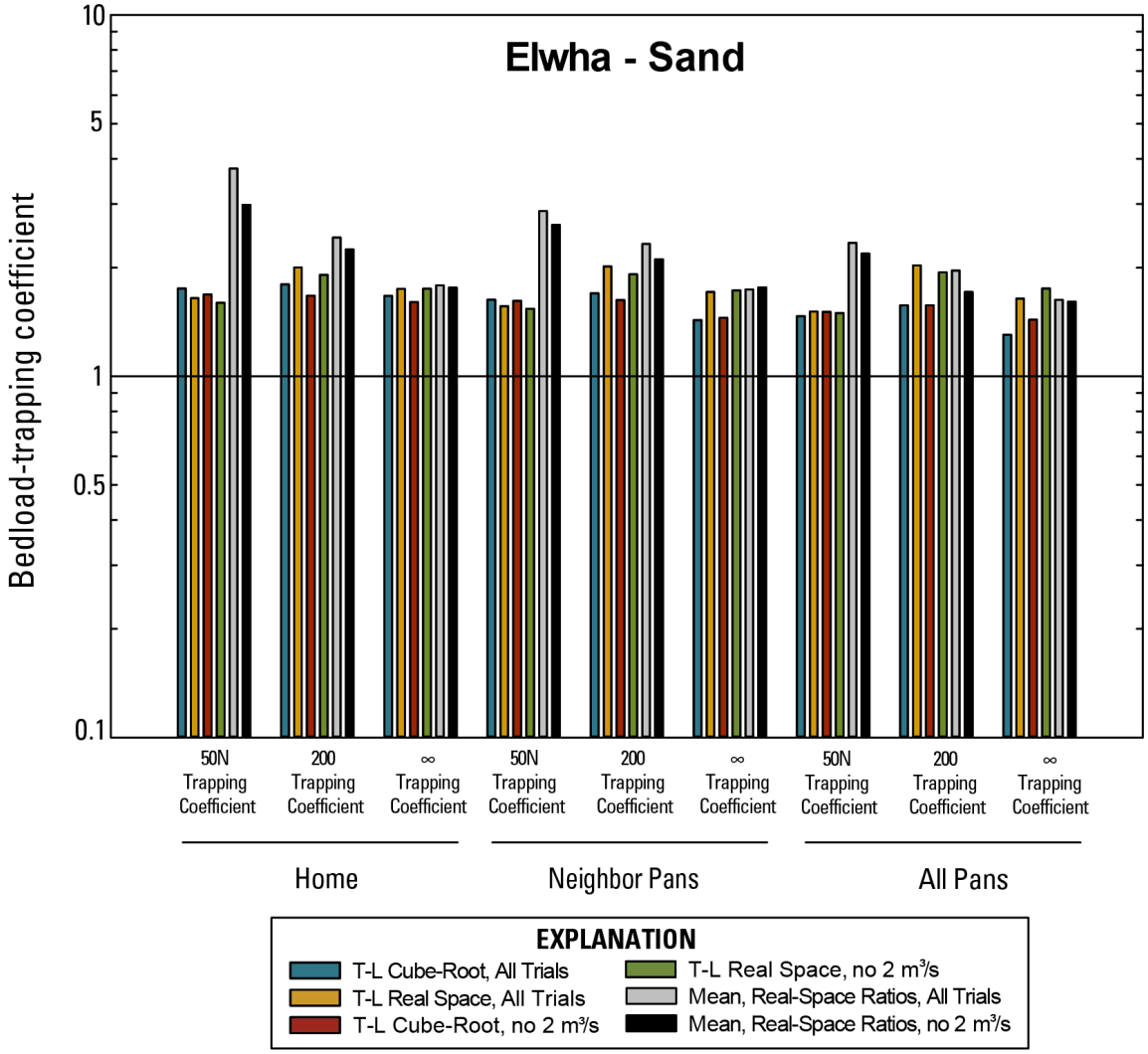

Figure 17. Graph showing Elwha sand-bed trapping coefficients calculated for three of the four analytical methods (excluding the Ratios of Averages method). Coefficients for the nine combinations of Home Pan, Neighbor Pans, and All Pans plus the 50N, 200N, and Infinite windows are shown, and include coefficients for both the 37-trial dataset and that without the 2.0 m^3/s run.

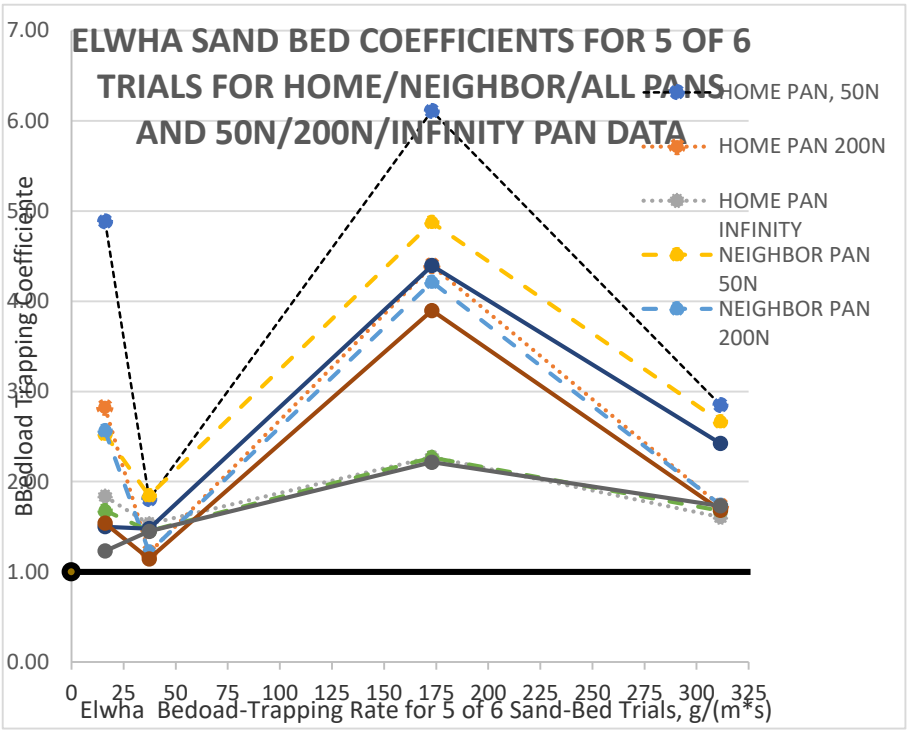

Figure 18. Plot showing Elwha sand-bed trapping coefficients versus the mean set bedload-transport rate for the bedload samples computed by the Ratios of Averages (RA) method. Coefficients for the nine combinations of Home Pan, Neighbor Pans, and All Pans plus the 50N, 200N, and Infinite windows are shown.

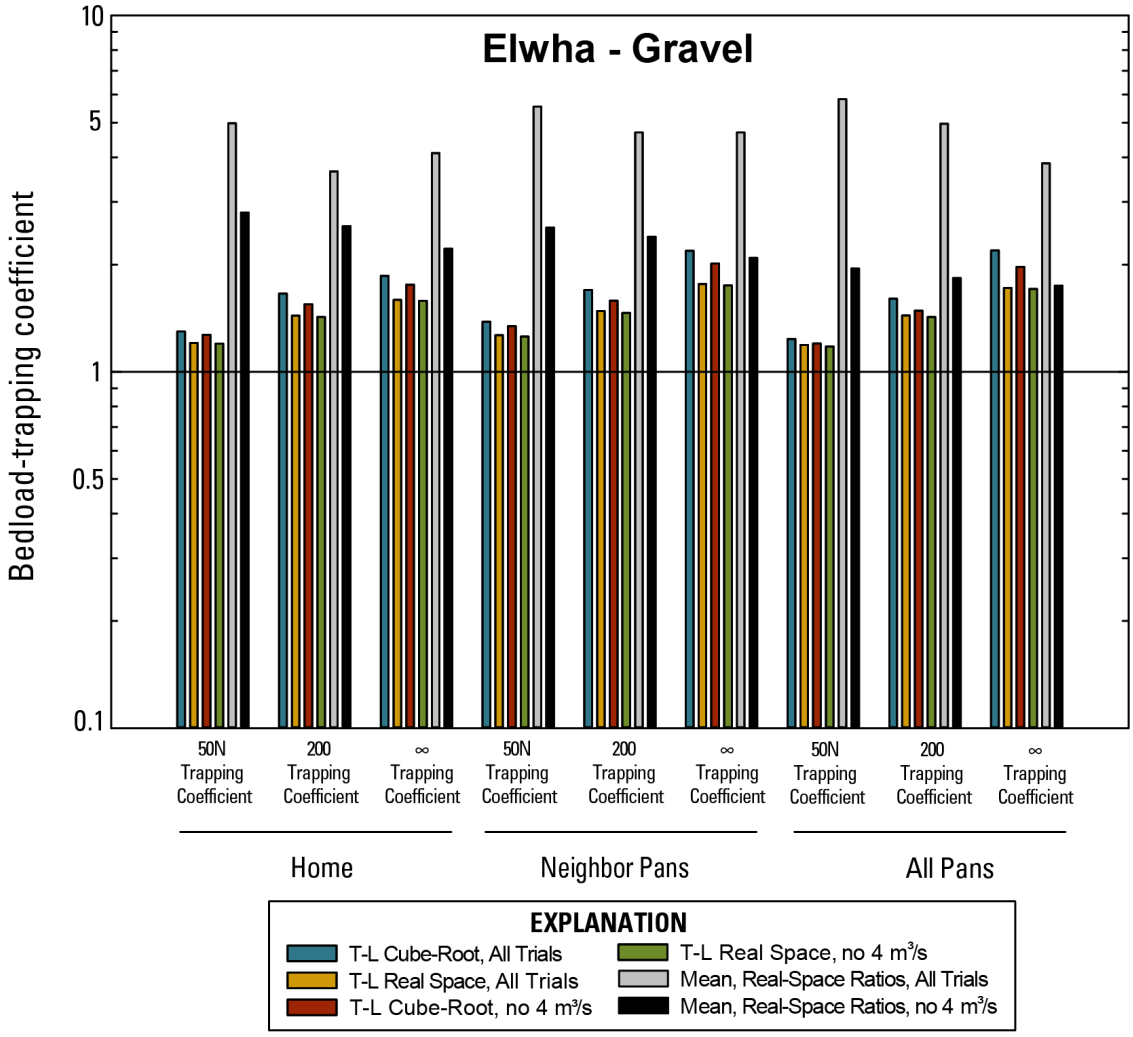

Figure 19. Graph showing Elwha gravel-bed trapping coefficients calculated for three of the four analytical methods (excluding the Ratios of Averages method). Coefficients for the nine combinations of Home Pan, Neighbor Pans, and All Pans plus the 50N, 200N, and Infinite windows are shown, and include coefficients for both the 37-trial dataset and that without the 4.0 m^3/s run.

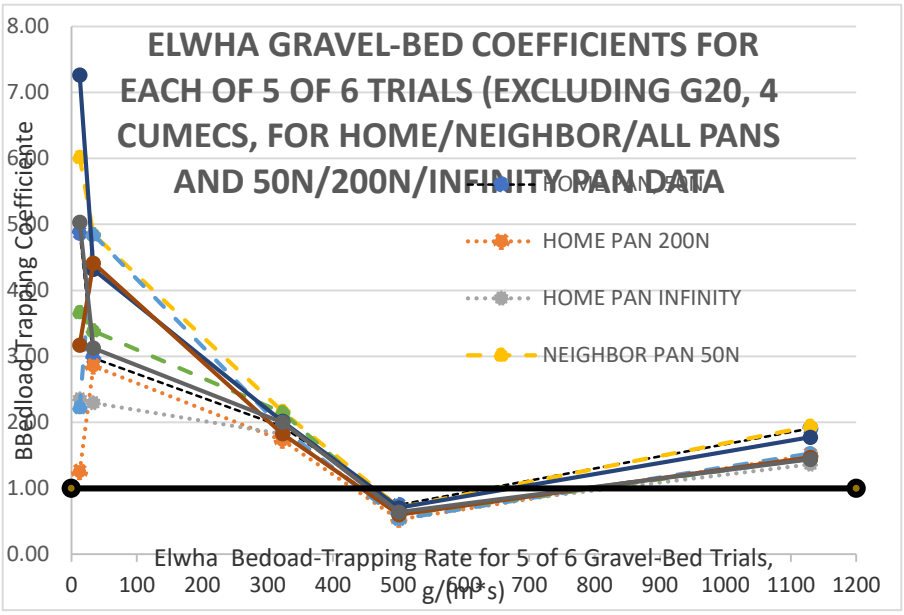

Figure 20. Plot showing Elwha gravel-bed trapping coefficients versus the mean set bedload-transport rate for the bedload samples computed by the Ratios of Averages (RA) method. Coefficients for the nine combinations of Home Pan, Neighbor Pans, and All Pans plus the 50N, 200N, and Infinite windows are shown for 5 of 6 trials (excluding that for the 4 m³/s. run). "CUMECS" are m³/s.

7C. Evaluation of the Helley-Smith Sand-Bed Trapping Efficiency

Helley-Smith Hydraulic Efficiency: Hubbell and others (1987) assign an unqualified (i.e., not estimated) hydraulic coefficient of 1.54 for the Helley-Smith sampler. Although this sampler's hydraulic efficiency was not tested by Bunte and others (2017), hydraulic theory supports the assumption that a 3.22 nozzle-flare ratio would result in larger – and likely substantially so – hydraulic efficiencies than those for samplers with a 1.4 flare ratio. Based on the positive correlation between hydraulic and trapping efficiencies, the trapping coefficient(s) for the Helley-Smith were expected to be more super-efficient than those for either a BLH-84 or Elwha deployed over a sand bed.

Consistent with the aforementioned expectation, figures 21 and 22 indicate that the Helley-Smith traps coarse sand super-efficiently, at about double the rate calculated for the Elwha, and over treble that calculated for the BLH-84. This finding was supported by deformation of the sand dune in the measurement section in the drained Main Flume after Helley-Smith at-a-point deployments; bed material had been sucked into the sampler at a substantially greater rate than the mean bedload-transport rate for the dune bedform based

on a ‘gouge’ in the dune at the sampling point observed after flow ceased and the flume was drained.

Figure 22 indicates the presence of substantial variations at higher transport rates among the 9 pan-window combinations. On the other hand, all four T-L model results indicate relative consistency in the coefficient, albeit in a broad range from about 2.4 to 3.6.

Conclusion: The sand-trapping data are unequivocal, indicating that the Helley-Smith traps bedload super-efficiently at about treble the true rate. These results support correction of raw sand-transport rates produced by the Helley-Smith by dividing raw sand-trapping rates by a coefficient of 3.11.

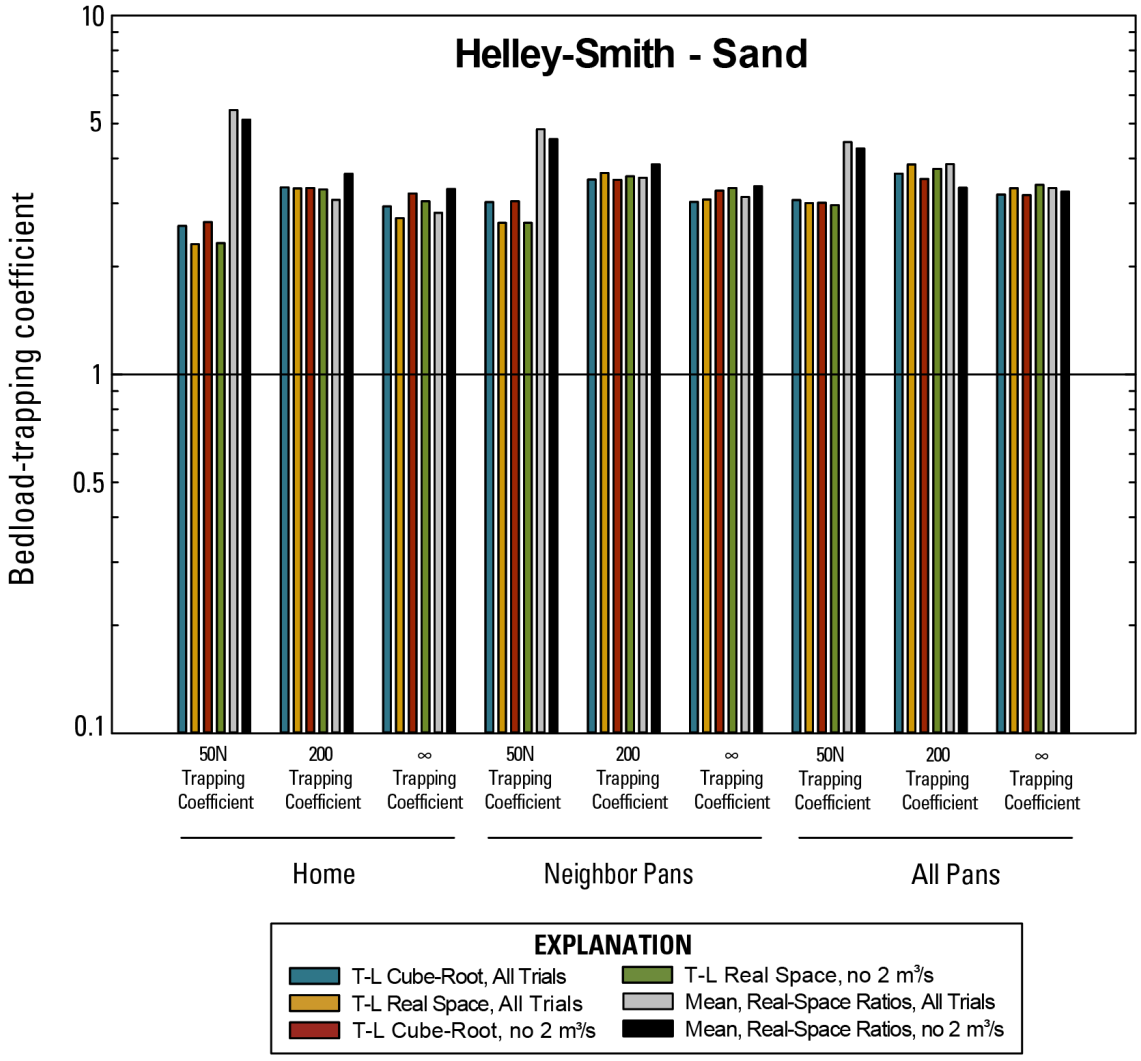

Figure 21. Graph showing Helley-Smith sand-bed trapping coefficients calculated for three of the four analytical methods (excluding the Ratios of Averages method). Coefficients for the nine combinations of Home Pan, Neighbor Pans, and All Pans plus the 50N, 200N, and Infinite

windows are shown, and include coefficients for both the 37-trial dataset and that without the 2.0 m³/s run.

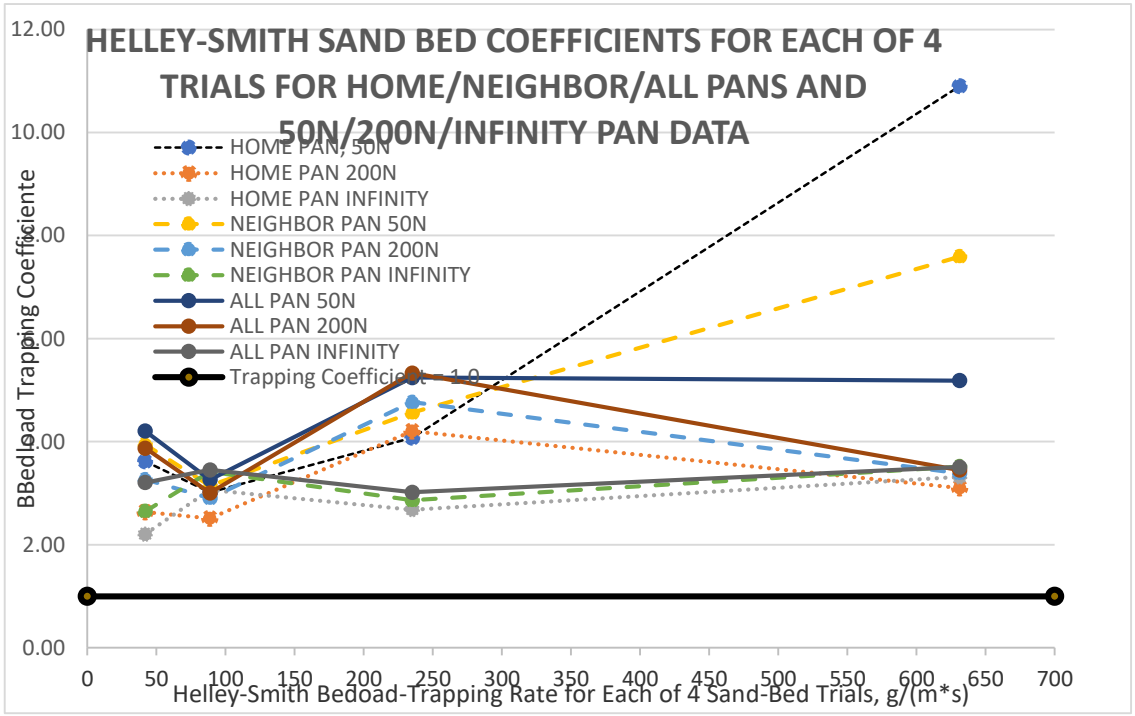

Figure 22. Plot showing Helley-Smith sand-bed trapping coefficients versus the mean set bedload-transport rate for the bedload samples computed by the Ratios of Averages (RA) method. Coefficients for the nine combinations of Home Pan, Neighbor Pans, and All Pans plus the 50N, 200N, and Infinite windows for sand-bed trials shown.

7D. Evaluation of the TR-2 Gravel-Bed Trapping Efficiency

TR-2 Hydraulic Efficiency: According to Bunte and others (2017), the hydraulic efficiency of an empty TR-2 (i.e., with an unobstructed collection bag) ranges from 1.08 to 1.15. Based on the positive correlation between hydraulic and trapping efficiencies, trapping coefficients for the TR-2 over a gravel bed were expected to be superefficient to a somewhat greater degree than those for the smaller but congruently configured Elwha over a gravel bed.

Figures 23 and 24 indicate that the TR-2 consistently traps gravel super-efficiently. The trapping rates for the T-L truncated model tended to be the most stable, with the real-space dataset exceeding that for the cube-root dataset by about 10 percent. All but one of the coefficients from the Average of Ratios method for all 37 trials exceeded a value of 3.3, and none was used in the ensuing analysis due to a lack of consistency with the modified T-L model results.

Figure 24 indicates both a degree of stability in the trend in the coefficients with increasing bedload-transport rates measured by the sampler, and in the relative agreement of the 9 pan-window combinations, infer a level of consistency not evident in the other samplers.

Conclusion: Consistent with the coefficients determined for the congruently configured Elwha sampler, the preponderance of evidence from the T-L model supports the conclusion that the Toutle River-2 (TR-2) samples medium gravel about 70-percent super-efficiently. These results support correcting raw TR-2 medium-gravel transport rates by dividing the raw rates by a coefficient of 1.70.

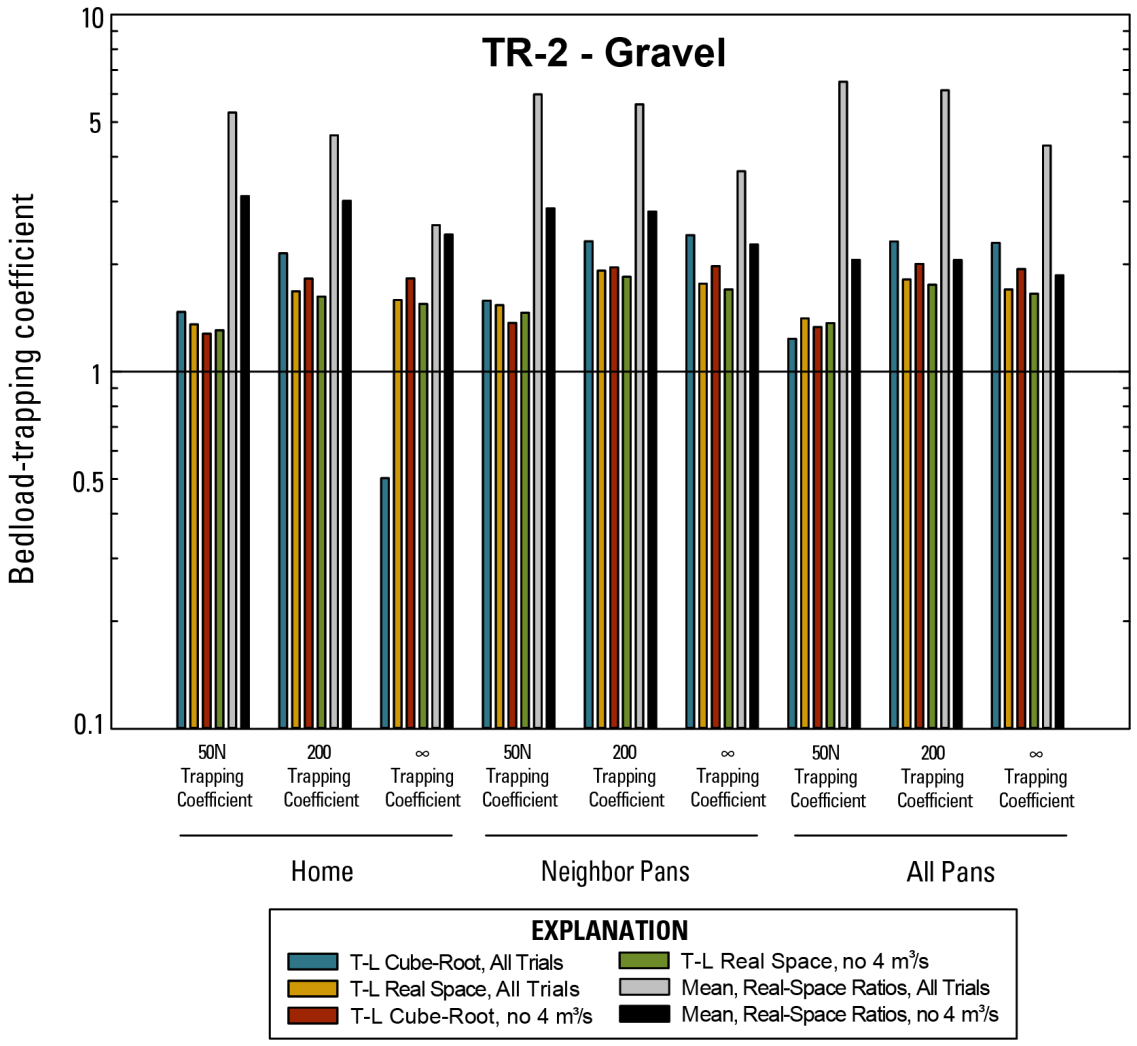

Figure 23. Graph showing Toutle-River 2 (TR-2) gravel-bed trapping coefficients calculated for three of the four analytical methods (excluding the Ratios of Averages method). Coefficients for the nine combinations of Home Pan, Neighbor Pans, and All Pans plus the 50N, 200N, and Infinite windows are shown, and include coefficients for both the 37-trial dataset and that without the 4.0 m^3/s run. One low transport-rate set of coefficients for trial G19, with coefficients ranging from 4.4-15.7, was excluded from the plot.

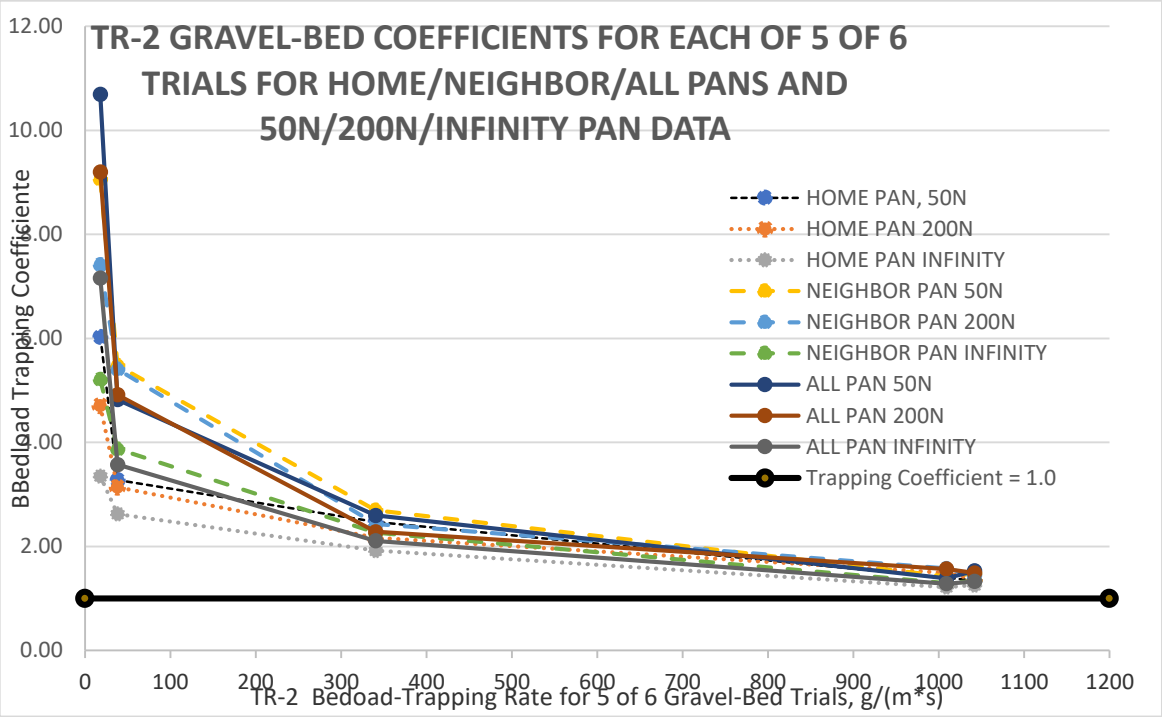

Figure 24. Plot showing TR-2 gravel-bed trapping coefficients versus the mean set bedload-transport rate for the bedload samples computed by the Ratios of Averages (RA) method. Coefficients for the nine combinations of Home Pan, Neighbor Pans, and All Pans plus the 50N, 200N, and Infinite windows for the gravel-bed trials are shown.

7E. Summary of the Trapping-Efficiency Analysis and Comparison to Previous Research

The derivation of single trapping coefficients for each sampler tested and a given bed type as part of the StreamLab06 experiments resulted from application of four analytical techniques ranging from relatively simple and straightforward to computationally complex and intensive. The data exhibited considerable variability and, in some cases, inexplicable inconsistencies. For example, all modified T-L model and AR results for the BLH-84 indicated a slight-to-moderate sub-unity coefficient averaging about 0.85 for both bed types; but figure 14 exhibits coefficients for that sampler in a sand bed as large as about 1.5 at medium transport rates. Trapping coefficients for the Elwha at medium-transport rates over a sand bed ranging from about 2.2-6.1 (figure 18) – calculated by the Ratios of Averages method – were inconsistent with the substantially more stable modified T-L model results (figure 17).

Despite the highly variable data and above-noted analytical inconsistencies, the following factors combined to render the analytical results to be moderately consistent and technically defensible (given the nature of the bedload process), as follows:

1. the large dataset available for analyses, comprised of 2,030 manually collected bedload samples and some 3.8-million time-series individual weigh-pan measurements, including data obtained during flow rates for the sand- and gravel-bed experiments that included low, medium, and high flows,

2. relatively sophisticated modified T-L and Average of Ratios analytical methods that included nine pan-window combinations, and

3. the theoretical positive correlation between hydraulic and trapping efficiencies,

These factors more-or-less consistently supported the conclusion that the BLH-84 samples bedload slightly sub-efficiently. The other three samplers with super-efficient hydraulic efficiencies tend to vacuum the bed sediments over which the respective sampler was deployed, thus resulting in super-efficient trapping coefficients. The BLH-84 and Elwha samplers tend to sample sand and gravel bedload with similar, moderately sub-unity coefficients. The Helley-Smith sampler substantially over-samples sand, but with a relatively stable coefficient of 3.11 that may be used to bias-correct contemporary or historical sand-bedload data collected with this sampler.

Table 7 provides a summary of selected individual sampler analytical results from the StreamLab06 experiments. It also includes results from Hubbell and Stevens, 1986 (i.e., their probability matching method) and the Thomas and Lewis (1993) model. It is notable that all data utilized by these researchers, as with the present analysis, were collected in the SAFL Main Flume.

The Hubbell and others (1987) dataset included bed-material D_{50} sizes of 2.1 mm, 6.5 mm, and 23.5 mm. Although neither the D_{50} values for bed material in the present study – 1.0 mm and 11.2 mm – corresponded directly with those Hubbell and others (1985, 1987) and Hubbell and Stevens (1986), general comparisons were made using a simple mean value from their results for the two larger (6.5mm and 23.5 mm) size values for comparison to the coefficients in this study, and for the finest size fractions.

The average trapping coefficients for the BL-84 from Hubbell and others (1985) and Hubbell and Stevens (1986) for sand and fine gravel all equal or exceed unity and are inconsistent with those from the present study. Their single coefficient reported for the TR-2, 6.5-mm material, exceeds that from the present study by about 50 percent. However, the coefficients reported for the BL-84 by Thomas and Lewis (1993) are reasonably close to those from the present study.

The Helley-Smith's sand-trapping coefficient from the present study is substantially larger than the single values reported by Hubbell and others (1987) and Thomas and Lewis (1993), but is more-or-less consistent with the large hydraulic efficiency reported for this sampler by Hubbell and others (1987).

TR-2 coefficients among the three data sources can best be described as a "hodgepodge" with little consistency or comparability.

In summary, with respect to the comparative data in table 7, there is at best a modicum of agreement between the three coefficients produced for somewhat similar bed-material configurations and sampler types by the three studies. Even results from Thomas and Lewis (1993), that are based on the same dataset produced by Hubbell and others (1987) exhibit little consistency. A resolution of these vexing disparities is, unfortunately, beyond the scope of this dissertation.

Table 7. Summary of estimated trapping coefficients produced by the present study and previous researchers from data collected in the St. Anthony Falls Laboratory Main Flume. Coefficients listed for Hubbell and others (1985, figure 10) and Hubbell and Stevens (1986, figure 3) were estimated from the general slopes of non-linear graphical relations. Those listed for Thomas and Lewis (1993) were calculated by cubing the relevant cube-root coefficients in table 3. All intercept values for the Thomas and Lewis (1993) coefficients are near zero other than that for the TR-2 sampler and 2.1-mm sediment size, the back-transformed value for which was 0.0018.

Gray, 2019					Hubbell and others 1985; Hubbell and Stevens, 1986[3]				Thomas and Lewis, 1993			
Pressure-Difference Bedload Sampler	Bed Type, median diameters: SAND = 1.0 mm; GRAVEL = 11.2 mm	Nozzle-flare ratio[1]	Provisional Calculated coef-ficients[2]	Provisional suggested generalized coefficients	1.4-4.0 mm (median 2.5 mm)	4.0-8.0 mm (median 6.5 mm)	11.3-32.0 mm (median 23.5 mm)	Average of 6.5 mm and 23.5 mm median diameters	Cube Root Back Transformed 2.1 mm median diameter	Cube Root Back Transformed 6.5 mm median diameter	Cube Root Back Transformed 23.5 mm diameter	Average of 6.5 mm and 23.5 mm diameter
BLH-84	SAND	1.4	0.83	**0.85**	1.5	--	--	--	0.78	--	--	--
ELWHA	SAND	1.4	1.67	**1.6**	--	--	--	--	--	-	--	--
Helley-Smith	SAND	3.22	3.11	**3.0**	1.7	--	--	--	0.87	--	--	--
BLH-84	GRAVEL	1.4	0.87	**0.85**	--	1.4	1.0	1.2	--	1.09	0.79	0.94
ELWHA	GRAVEL	1.4	1.54	**1.6**	--	--	--	--	--	--	--	--
Toutle River-2	GRAVEL	1.4	1.70	**1.7**	--	2.6	--	--	0.03	1.64	0.70	1.17

[1]The area of a pressure-difference bedload sampler's nozzle outlet area divided by its inlet area.

[2]Coefficients presented here were derived from the Modified Thomas-Lewis model in real space.

[3]Coefficient values generalized from a non-linear relations.

8. Summary, Discussion and Conclusions

Bedload-trapping coefficients for four types of pressure-difference bedload samplers – a standard Helley-Smith (intake nozzle width and height of 76.2 mm x 76.2 mm), US BLH-84 or BL-84 (76.2 mm x 76.2 mm), Elwha (203 mm x 102 mm) and Toutle River-2 (TR-2; 305 mm x 152 mm) – were calculated from data collected during the Phases I and II of the StreamLab06 experiments in the St. Anthony Falls Laboratory Main Flume during January-March 2006. The bedload samplers were deployed during nine steady flows: five flows ranging from 2.0-3.6 m^3/s over a sand bed (1.0 mm median diameter) during Phase I, and four flows ranging from 4.0-5.5 m3/s over a medium-gravel bed (11.2 mm median diameter) during Phase II. The BLH-84 and Elwha were tested atop both bed types. The Helley-Smith tests were confined to flows over the sand bed. Those for the TR-2 took place solely over the gravel bed.

The four statistical techniques used to analyze the StreamLab06 bedload dataset produced bedload-trapping coefficients that were characterized by substantial variability, both within the dataset and with respect to coefficients produced by previous researchers (tables 5, 6 and 7). However, parsing the data revealed fundamental characteristics among coefficients calculated for the samplers, including:

- Positive correlations between hydraulic versus bedload-trapping efficiencies among the four samplers, with bedload-trapping efficiencies increasing concomitant with hydraulic efficiencies for a given sampler, albeit non-linearly,
- Close agreement in the two generalized sand- and gravel-trapping characteristics calculated for the BLH-84; and for the two calculated for the Elwha,
- Close agreement in the gravel-trapping characteristics of the TR-2 and its congruently configured (two-thirds scale) version, the Elwha, and
- Distinct and substantially different sets of coefficients derived for the BLH-84 versus the Helley-Smith versus those for the congruently configured Elwha and TR-2.

These and other findings were made possible by several factors, chief among them being the production and use of a comparatively large bedload dataset that included 2,030 manually collected bedload sampler measurements, and some 3.8-million discrete weigh-pan time-series measurements. Additionally, enhanced, state-of-the-art data-collection and -analytical techniques yet to be developed in when Hubbell and others (1987) performed their calibration experiments were brought-to-bear in and to the considerable benefit of the present study.

Analyses of these data and related information enabled identification of generally consistent and distinct bedload-trapping coefficients for each combination of sampler and bed type (table 7, and figures 13, 15, 17, 19, 21 and 23), and provided a more-thorough and -detailed understanding of how these samplers perform. The derived coefficients can be used to correct bias in raw transport rates produced by these bedload samples deployed in rivers with bed types and flow velocities similar to those present during the StreamLab06 Phases I and II experiments.

A summary of calculated bedload-trapping coefficients, relying primarily on results from the modified Thomas and Lewis (1993) real-space model, follows (see table 7): the coefficient for the BLH-84 atop the coarse sand bed (D_{50} = 1.0 mm) equaled 0.83; that for the BLH-84 over a medium gravel bed (D_{50} = 11.2 mm) equaled 0.87. The trapping coefficients for the Elwha were 1.67 (sand bed) and 1.54 (gravel bed). A sand-trapping coefficient of 3.11 was derived for the Helley-Smith. The 1.70 gravel-trapping coefficient derived for the TR-2 was close to 1.54 coefficient for the congruently configured Elwha.

For sake of simplicity and consistency, table 7 includes suggested "smoothed" bias-correction coefficients that the Federal Interagency Sedimentation Project, its member agencies, and other domestic and international producers and users of bedload-transport data may consider for adoption based on similarities in bed- and flow conditions during the StreamLab06 bedload-sampler calibration tests (these "smoothed" coefficients appear in two significant figures because any more would imply an unwarranted level of precision).

Among the benefits of formally adopting "smoothed" trapping coefficients for the BLH-84 and Elwha samplers would include rendering selected sampler coefficients more-or-less applicable for correcting raw bedload-transport rates collected in either sand- or medium-gravel bed streams. Additionally, the probability that bedload-transport data produced world-wide by these samplers under similar bed and flow conditions would become comparable if the selected bias-correction coefficients were formally accepted, widely shared and correctly applied.

Selected Streamlab06 bedload-trapping coefficients may also be applied, albeit provisionally, to raw bedload-transport data from the BLH-84, Elwha, and TR-2 samplers deployed atop riverbeds coarser or finer than those in which each sampler was deployed during StreamLab06 phases I and II, and (or) at flow velocities differing substantially from those in which these bedload samplers were tested. The validity of applying these coefficients under conditions differing substantially from those in which the samplers were tested may be inferred but not verified based on these results from the StreamLab06 experiments.

Arbitrarily accepting and applying a bias-correction coefficient of 1.0 to raw data produced by these bedload samplers – with the possible exceptions of the BLH-84 atop a 23.5 mm gravel bed (Hubbell and Stevens, 1986, figure 3, right), and for the BLH-84 associated with near-unity coefficients – has no demonstrable technical basis, regardless of the bed configuration and flow velocities in which the sampler was deployed. This observation stems from a review of the generalized coefficients produced for the four StreamLab06 samplers tested (table 7), none of which fall within 10 percent of unity. It may be worth noting – largely based on the author's 4-decade-long experience in the measurement and analysis of bedload characteristics – that an assumption and de facto application of a 1.0 trapping coefficient is more likely the "rule rather than the exception" for the preponderance of bedload-transport data produced by pressure-difference bedload samplers worldwide.

In conclusion,

1. The data produced, and analysis subsequently performed as part of the StreamLab06 bedload-sampler efficiency experiments consistently infer – under the conditions in which the samplers were tested – that the Elwha (sand and gravel), and TR-2 (gravel) sample at least 50-percent super-efficiently; and that the Helley-Smith traps sand about 300 percent super-efficiently. In contrast, the BLH-84, which collected sand-and-gravel samples sub-efficiently by 15 percent, was the sole sampler tested that trapped bedload with a coefficient relatively close to unity.

2. The data and analytical results herein support the conclusion that raw (uncorrected) bedload-transport rates produced by three of the four samplers tested – the Elwha, TR-2 and Helley-Smith samplers – under the conditions in which each was tested during the StreamLab06 experiments – produce substantially positively biased results that unequivocally require correction for inherent sampler bias to produce results consistent with ambient riverine bedload-transport ("true") rates. The raw data produced by the BLH-84 would also benefit from correction for sampling bias.

3. There is no technically supportable reason to refrain from applying bias-corrections coefficients to the raw data produced by any of these samplers given the availability of selected, technically supportable sampling coefficients produced by bedload-sampler calibration experiments performed in the St. Anthony Falls Laboratory Main Flume. Dividing raw bedload-transport rates produced by these samplers by an appropriate trapping coefficient listed in table 7 should produce relatively unbiased bedload-transport data collected in sand to medium-gravel bed rivers.

9. References Cited

ASTM International, 1998, Terminology for fluvial sediment: ASTM International Designation D 4410–98, 6 p.

Bunte, Kristin, Klema, Matthew, Hogan, Taylor, and Thornton, Christopher, 2017, Testing the hydraulic efficiency of pressure difference samplers while varying mesh size and type: Report Submitted to the Technical Committee of the Federal Interagency Sedimentation Project, 116 p. (https://water.usgs.gov/fisp/research/2016CSU_BedLoadSampler/Testing_the_Hydraulic Efficiency_of_Pressure_Difference_Samplers_While_Varying_Mesh_Size_and_Type.pdf).

Bunte, Kristin, Hogan, Taylor, Klema, Matthew, and Thornton, Christopher, 2019 (in press), Testing the hydraulic efficiency of pressure difference samplers while varying flows and bag properties (mesh size, weave density, fill level): Colorado State University, Poster, SEDHYD, June 24-28, 2019, Reno, NV.

Carey, W. P., 1984, A field technique for weighing bedload samples. Water Resources Bulletin 20(2): p. 261-265.

Carey, W.P. 2005, A brief history of the development and calibration of bedload samplers, *in* National Center for Earth Surface Dynamics: U.S. Geological Survey, Bedload Monitoring Technologies Workshop, Dec. 1–2, 2005, Minneapolis, Minn., papers and manuscripts, 18 p.

Childers, D., 1999, Field comparisons of six pressure-difference bedload samplers in high-energy flow: U.S. Geological Survey Water-Resources Investigations Report 92-4068, 59 p. (http://pubs.er.usgs.gov/usgspubs/wri/wri924068).

Colby, B.R., 1963, Fluvial sediments a summary of source, transportation, deposition, and measurement of sediment discharge: U.S. Geological Survey Bulletin 1181-A, 47 p. (https://pubs.er.usgs.gov/publication/b1181A).

Edwards, T.K. and Glysson, G.D., 1999, Field methods for measurement of fluvial sediment: U.S. Geological Survey Techniques of Water Resources Investigations, book 3, chap. C2, 89 p. (https://pubs.usgs.gov/twri/twri3-c2/).

Edwards, T.K. and Glysson, G.D., 1988, Field methods for measurement of fluvial sediment: U.S. Geological Survey Open-File Report 86-531, 118 p. (https://pubs.er.usgs.gov/publication/ofr86531).

Emmett, W.W., 1980, A field calibration of the sediment-trapping characteristics of the Helley-Smith bedload sampler: U.S. Geological Survey Professional Paper 1139, 44 p. (https://pubs.er.usgs.gov/publication/pp1139).

Emmett, W.W., 1981, Measurement of bed load in rivers, in, Erosion and transport measurement: Proceedings of the Florence Symposium, June, International Association of Hydrological Sciences Publication No. 133, p. 3-15.

Gomez, Basil, 2006, The potential rate of bed-load transport: Proceedings of the National Academy of Sciences, v. 103, no. 46, p. 17,170–17,173.

Gomez, B., Hubbell, D.W., and Stevens, H.H., Jr., 1990, At-a-point bed load sampling in the presence of dunes: Water Resources Research, v. 26, no. 11, p. 2,717–2,731. [Also available at https://doi.org/10.1029/wr026i011p02717.]

Gray, J.R., ed., 2005, Proceedings of the Federal Interagency Sediment Monitoring Instrument and Analysis Research Workshop, September 9–11, 2003, Flagstaff, Arizona: U.S. Geological Survey Circular 1276, 46 p. (Also available at http://pubs. usgs.gov/circ/2005/1276/.) (Appendix 4 is available only online at: http://water.usgs/gov/ osw/techniques/sediment/ sedsurrogate2003workshop/listofpapers.html).

Gray, J.R., Dean, D.J., Czuba, J.A., and Schwarz, G.E, in press, Instruments, Methods, Rationale, and Derived Data Used to Quantify and Compare the Trapping Efficiencies of Four Pressure-Difference Bedload Samplers: U.S. Geological Survey Open-File Report.

Gray, J.R., and Simões, F.J.M., 2008, Estimating sediment discharge; Appendix D of Garcia, Marcelo, ed., Sedimentation engineering—Processes, measurements, modeling, and practice: American Society of Civil Engineers Manuals and Reports on Engineering Practice No. 110, p. 1,067–1,088.

Gray, J.R., Laronne, J.B., and Marr, J.D.G, 2010, Sediment-surrogate monitoring technologies: U.S. Geological Survey Scientific Investigations Report 2010-5091, 37 p. (http://pubs.usgs.gov/sir/2010/5091/).

Gray, J.R., Webb, R.H., and Hyndman, D.W., 1991, Low-flow sediment transport in the Colorado River, *in* Proceedings of the Fifth Federal Interagency Sedimentation Conference, March 18–21, 1991, Las Vegas, Nevada: [Washington, D.C.], Federal Energy Regulatory Commission, Interagency Advisory Committee on Water Data, Subcommittee on Sedimentation, v. 1, p. 4–63 to 4–71 (https://pubs.er.usgs.gov/publication/70120614).

Gray, J.R., and Simões, F.J.M., 2008, Estimating sediment discharge, in, Marcelo Garcia, ed., Sedimentation Engineering – Processes, Measurements, Modeling, and Practice, American Society of Civil Engineers Manual 110, Appendix D, p. 1,065-1,086 (http://water.usgs.gov/osw/techniques/Gray_Simoes.pdf).

Hamamori, A., 1962, A theoretical investigation on the fluctuation of bed-load transport: Delft, The Netherlands, Hydraulics Laboratorium Delft, Report R4, 14 p.

Helley, E.J., and Smith, Winchell, 1971, development and calibration fo a pressure-difference bedload sampler: U.S. Geological Survey Open-File Report 73-108, 18 p. (https://pubs.er.usgs.gov/publication/ofr73108).

Hubbell, D.W., 1964, Apparatus and techniques for measuring bedload: U.S. Geological Survey Water-Supply Paper 1748, 74 p. (https://pubs.er.usgs.gov/publication/wsp1748).

Hubbell, D.W., 1987, Bed load sampling and analysis: In, C.R. Thorne, J.C. Bathhurst and R.D. Hey (eds), Sediment Transport in Gravel-Bed Rivers: John Wiley, Hoboken, NJ, p. 89-118.

Hubbell, D.W., Stevens, Jr. H.H., Skinner, J.V., and Beverage, J.P., 1987, Laboratory data on coarse-sediment transport for bedload-sampler calibrations: U.S. Geological Survey Water-Supply Paper 2299, 31 p. (http://pubs.er.usgs.gov/usgspubs/wsp/wsp2299).

Hubbell, D.W., and Stevens, H.H., 1986, Factors affecting accuracy of bedload sampling: Proceedings of the Fourth Federal Interagency Sedimentation Conference, v. 1, p. 4-20 to 4-29 (https://acwi.gov/sos/pubs/4thFISC/4Fisc-V1/4Fisc1-4.PDF).

Hubbell, D.W., Stevens, H.H., Jr., Skinner, J.V., and Beverage, J.P., 1985, New approach to calibrating bed load samplers: Journal of Hydraulic Engineering, v. 111, no. 4, p. 677–694 (https://pubs.er.usgs.gov/publication/70013202).

Hubbell, D.W., Stevens Jr., H.H., Skinner, J.V., and Beverage, J.P., 1987, Laboratory data on coarse-sediment transport for bedload-sampler calibrations: U.S. Geological Survey Water Supply Paper 2299, 31 p. (https://pubs.er.usgs.gov/publication/wsp2299).

International Standards Organization (ISO), 1992, Liquid flow in open measurement in open channels – Sampling and analysis of gravel-bed material: 9195:1992(E), International Standards Organization, Geneva, Switzerland.

Kuhnle, R.A., 1991, Bedload transport in two small streams: Proceedings of the Fifth Federal Interagency Sedimentation Conference: Interagency Advisory Committee on Water Data, Subcommittee on Sedimentation, Las Vegas, vol. 1, p. 4-141 to 4-146 (https://pubs.usgs.gov/misc/FISC_1947-2006/pdf/1st-7thFISCs-CD/5thFISC/5Fisc-V1/5Fisc1-4.PDF#page=141).

Kuhnle, R.A., 2008, Bed load samplers, in, Sediment transport measurements, in, Marcelo Garcia, ed., Sedimentation Engineering – Processes, Measurements, Modeling, and Practice, American Society of Civil Engineers Manual 110, Chapter 5.4, p. 339-353 (http://water.usgs.gov/osw/techniques/Diplas_Kuhnle_others.pdf).

Leopold, L.B., and Emmett, W.W., 1976, Bedload measurements, East Fork River, Wyoming: Proc. Nat. Acad. Sci, USA, Vol 73, No. 4, p. 1,000-1,004.

Marr, Jeffrey D.G., Gray, John R., Davis, Broderick E., Ellis, Chris, and Johnson, Sara, 2010a, Large-Scale Laboratory Testing of Bedload-Monitoring Technologies: Overview of the StreamLab06 Experiments: U.S. Geological Survey Scientific Investigations Report 2010-5091, p. 266-282; Accessed March 24, 2017, at: https://pubs.usgs.gov/sir/2010/5091/papers/Marr.pdf.

Marr, Jeff, Wilcock, Peter, Hondzo, Miki, Foufoula-Georgiou, Efi, Johnson, Sara, Hill, Craig, Leonardson, Rebecca, Nelson, Peter, Venditti, Jeremy, O'Connor, Ben, Ellis, Christopher, Mullin, James, Jefferson, Anne, Clark, Jeff, 2010b, StreamLab06: Overview of experiments, instrumentation, and data collection -- National Center for Earth-surface Dynamics: St. Anthony Falls Laboratory, 32 p. accessed March 24, 2017 at: http://conservancy.umn.edu/handle/11299/144023.

National Center for Earth-surface Dynamics, 2017, Home Page: http://www.nced.umn.edu/).

Ryan, S.E., Bunte, K., and Potyondy, J.P., 2005, Breakout session II, Bedload-transport measurement – data needs, uncertainty, and new technologies, in, Proceedings of the Federal Interagency Sediment Monitoring Instrument and Analysis Research Workshop, September 9-11, 2003, Flagstaff, Arizona, J.R. Gray, ed: U.S. Geological Survey Circular 1276, p. 16-28, also available at: http://pubs.usgs.gov/circ/2005/1276/.

Ryan, S.E., and Porth, L.S., 1999, A field comparison of three pressure-difference bedload samplers: Geomorphology, volume 30, issue 4, 1 December 1999, Pages 307-322 (http://www.sciencedirect.com/science/article/pii/S0169555X99000598).

Ryan, S.E., Porth, L.S., and Troendle, C.A., 2002, Defining phases of bedload transport using piecewise regression: Earth Surface Processes and Landforms 27, 971–990, DOI:10.1002/esp.387.

Singh, Arvind, Czuba, J.A., Foufoula-Georgiou, Efi, Hill, Craig, Johnson, Sara, Ellis, Chris, Mullin, Mames, Orr, C.H., Wilcock, P.R., Hondzo, Miki, and Paola, Chris, 2013, StreamLab Collaboratory: Experiments, data sets, and research synthesis: Water Resources Research, DOI: 10.1002/wrcr.20142, p. 1,746-1,752.

Singh, Arvind, Fienberg, Kurt, Jerolmack, D.J., Marr, Jeffrey, and Foufoula-Georgious, Efi, 2009, Experimental evidence for statistical and intermittency in sediment transport rates: Journal of Geophysical Research, Vol. 114, F01025, DOI: 10.1029/2007JF000963.

Tacconi, P., and Billi, P., 1987, Bed load transport measurements by the vortex-tube trap on Virginia Creek, Italy, *in* Thorne, C.R., Bathurst, J.C., and Hey, R.D., eds., Sediment transport in gravel-bed rivers: New York, Wiley, p. 583–616.

Thomas, R.B., and Lewis, Jack, 1993, A new model for bed load sampler calibration to replace the probability-matching method: Water Resources Research, Vol, 29, No. 3, p. 583-597.

U.S. Geological Survey, 1990, Programs and plans—Policy and guidelines for the collection and publication of bedload data: U.S. Geological Survey Office of Surface Water Technical Memorandum 90.08 (https://water.usgs.gov/admin/memo/SW/sw90.08.html).

APPENDIX A: Plots of Weigh-Pan Bedload-Transport Rates

Plots of weigh-pan bedload-transport rates in kilograms/(seconds × meter) for each of the nine StreamLab06 Phase I sand and Phase II gravel runs in which bedload samplers were deployed. Each plot provides basic statistics on the mean transport rate and from the run along with the duration of the run. The left and right combinations of each plot are based on the same bedload-transport data.

The left plot for each run shows (top) the average, maximum, and minimum bedload transport rates for all five pans, along with the start-and-end of each bedload-sampler trial; (middle 5) the trapping rates for the individual weigh pans; and (bottom) the water discharge time series in m^3/s.

The right plot shows the accumulation of bedload in each pan and the average accumulation across the five pans expressed as kg/(m×s). The start-and-end of each bedload sampler trial is shown and identified as to the type of sampler deployed.

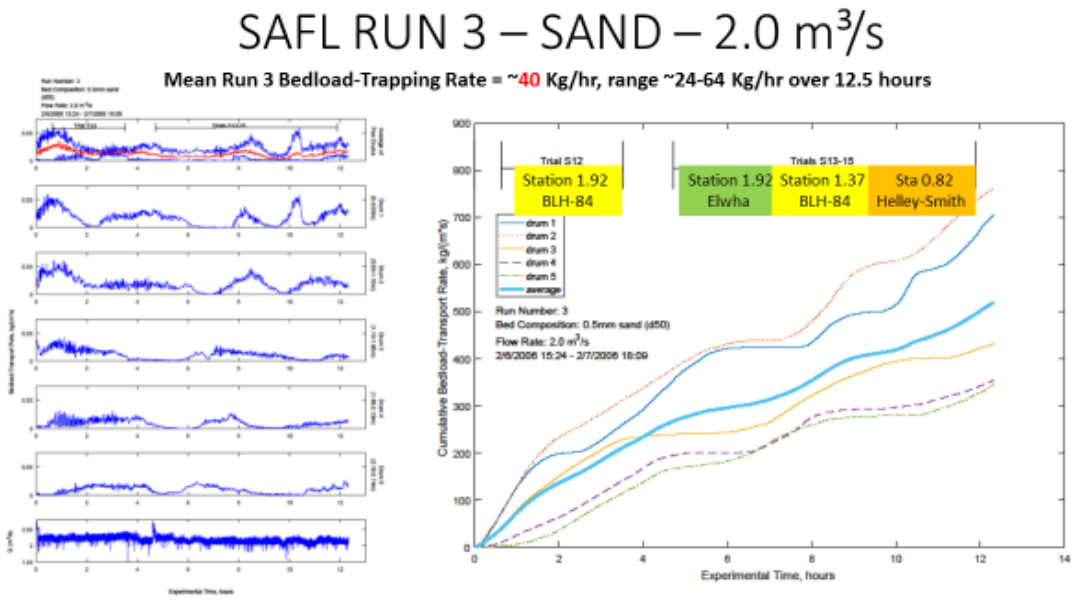

SAFL RUN 4 (2.5m ³/s) & 5 (3.2 m³/s)

Mean Run 4 Bedload-Trapping Rate = ~85 Kg/hr, range ~72-100/hr over 11.1 hours
Mean Run 5 Bedload-Trapping Rate = ~290 Kg/hr, range ~280-340 Kg/hr over 4.7 hours

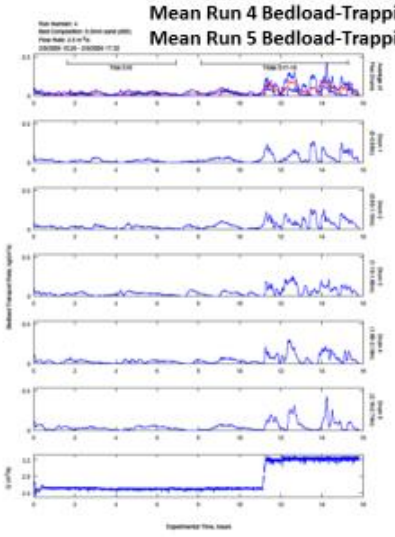

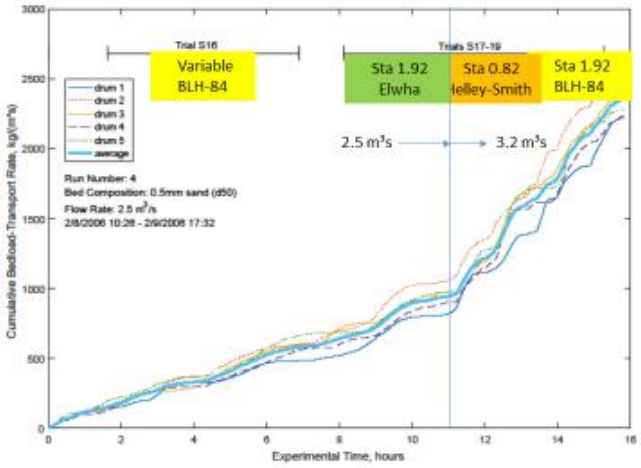

SAFL RUN 1 – SAND – 2.9 m³/s

Mean Run 1 Bedload-Trapping Rate = ~226 Kg/hr, range ~200-260 Kg/hr over 34 hours

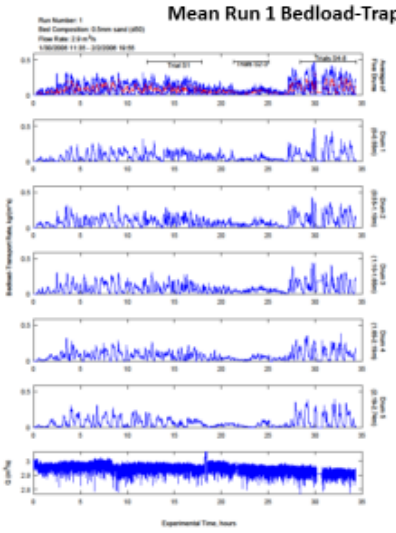

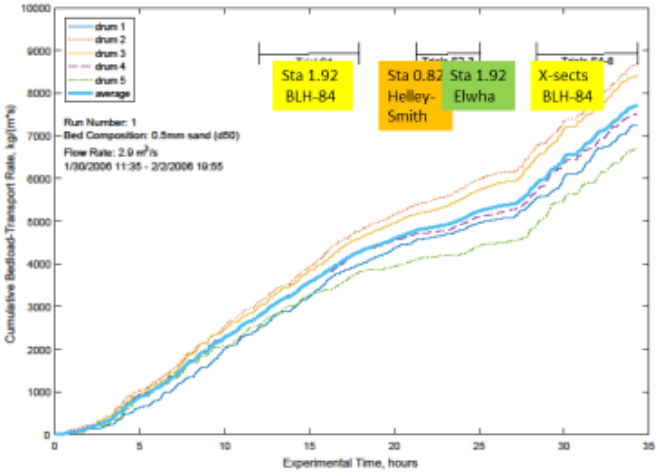

SAFL RUN 2 – SAND – 3.6 m³/s

Mean Run 2 Bedload-Trapping Rate = ~560 Kg/hr, range ~470-600 Kg/hr over 11.5 hours

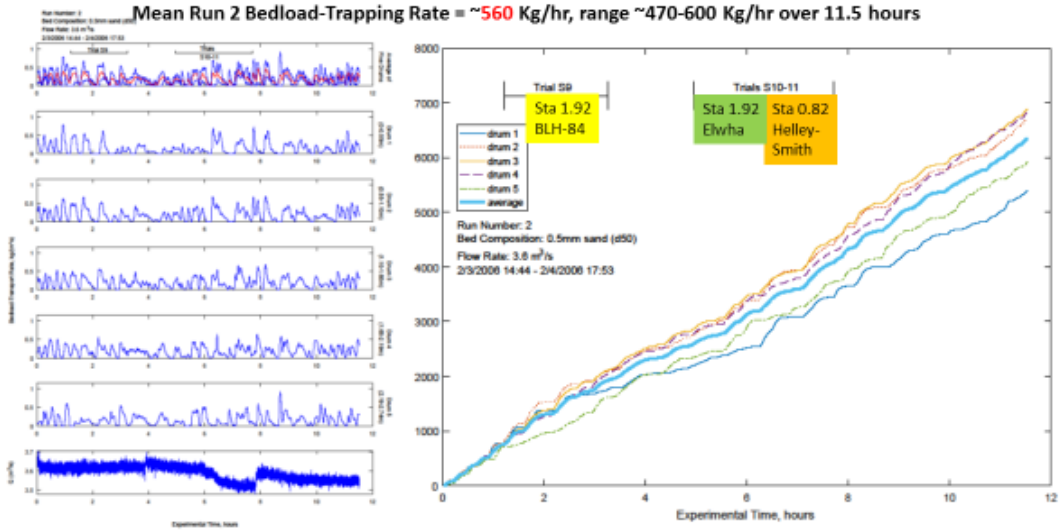

SAFL RUN 10 – GRAVEL – 4.0 m³/s

Mean Run 10 Bedload-Trapping Rate = ~8 Kg/hr, range ~2-18 Kg/hr over 56 hours

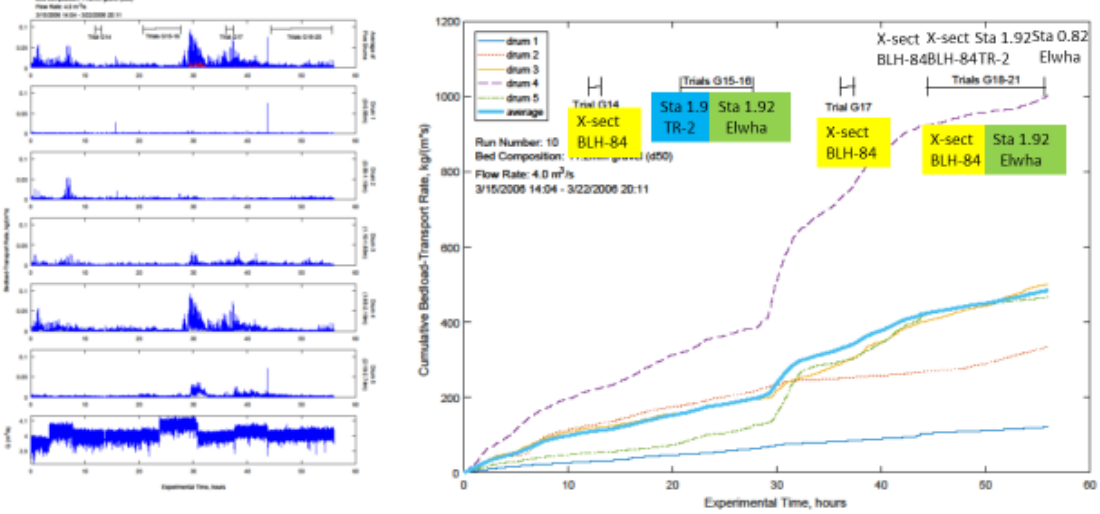

SAFL RUN 12 – GRAVEL – 4.3 m³/s

Mean Run 12 Bedload-Trapping Rate = ~49 Kg/hr, range ~22-56 Kg/hr over 56 hours

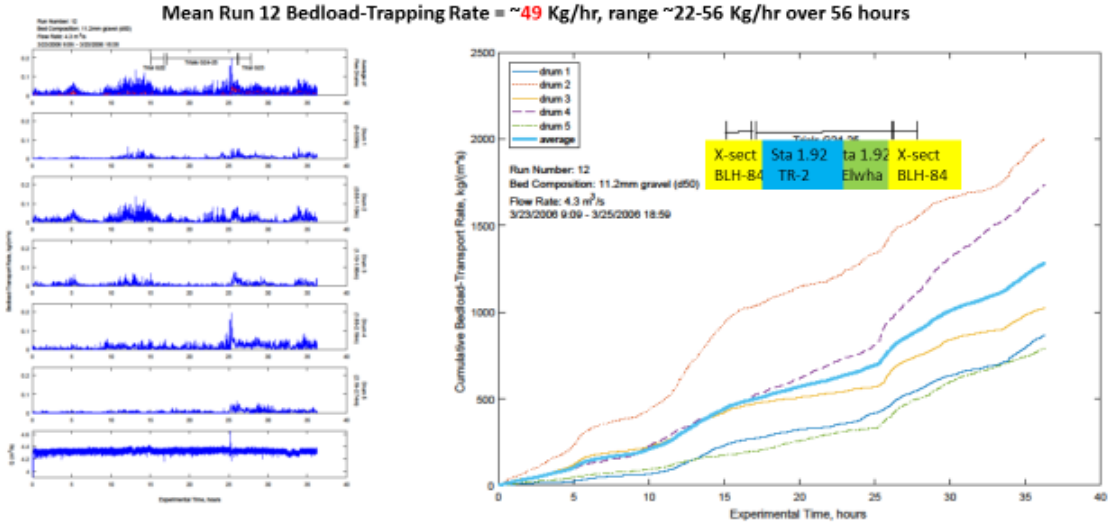

SAFL RUN 13 – GRAVEL – 4.9 m³/s

Mean Run 13 Bedload-Trapping Rate = ~530 Kg/hr, range ~430-680 Kg/hr over 34 hours

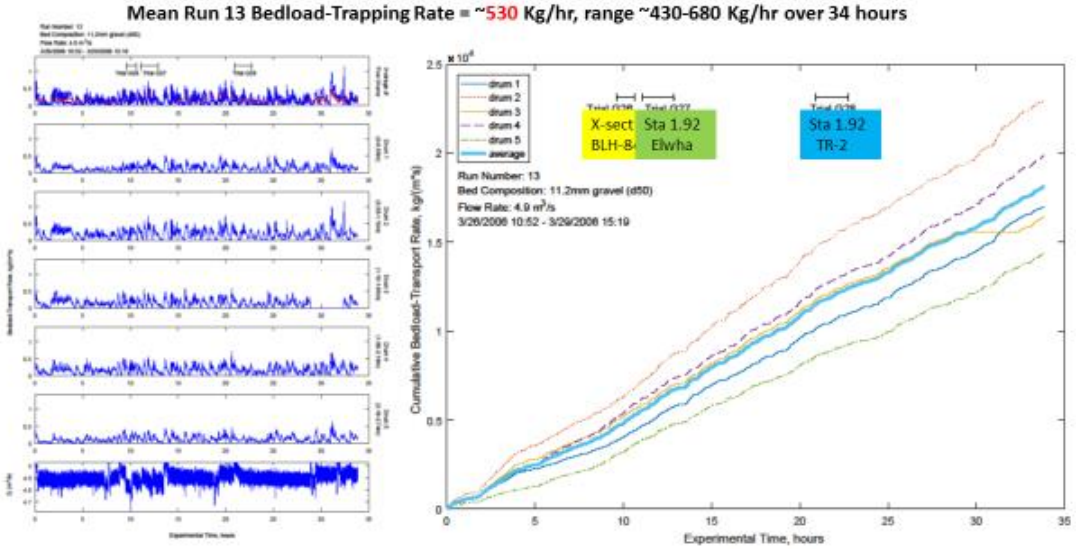

SAFL RUN 8 – GRAVEL – 5.5 m³/s

Mean Run 8 Bedload-Trapping Rate = ~2,600 Kg/hr, range ~2,100-3,200 Kg/hr over 29 hours

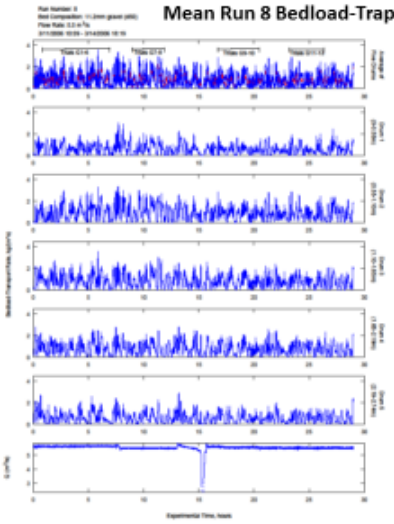

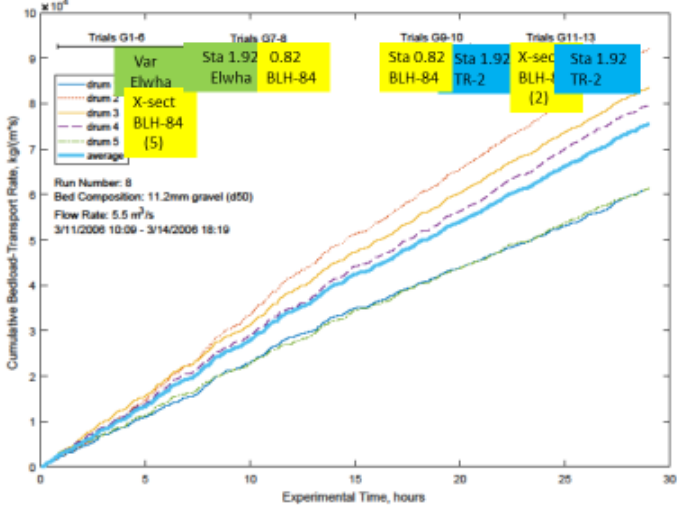

APPENDIX B: Modified Thomas and Lewis (1993) Model Example Plots

Example plots generated using the modified Thomas and Lewis, 1993 (T-L) model in real space for the truncated dataset. They show bedload-sampler transport rates versus All Pan and Infinity window transport rates for each of six sets. A line equal to a value of unity is included. These represent six of the 54-such pan-window combination plots generated from the truncated dataset in real space. Another set of 54 plots were also generated for each of the T-L truncated dataset using cube root data; the T-L all-trials real-space dataset; and for the T-L all trials cube root dataset. Combined, the four T-L analyses resulted in production of 216 plots.

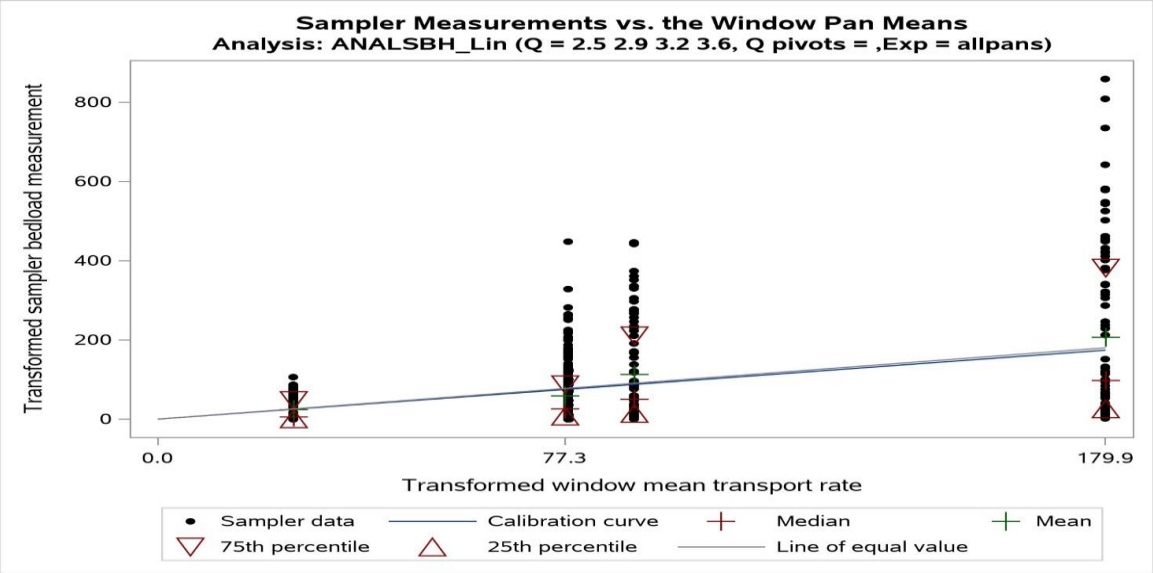

Appendix 2A: Plot depicting data produced by the BLH-84 sampler deployed over a sand bed generated by the modified T-L model using real space data for All Pans and the Infinity Window.

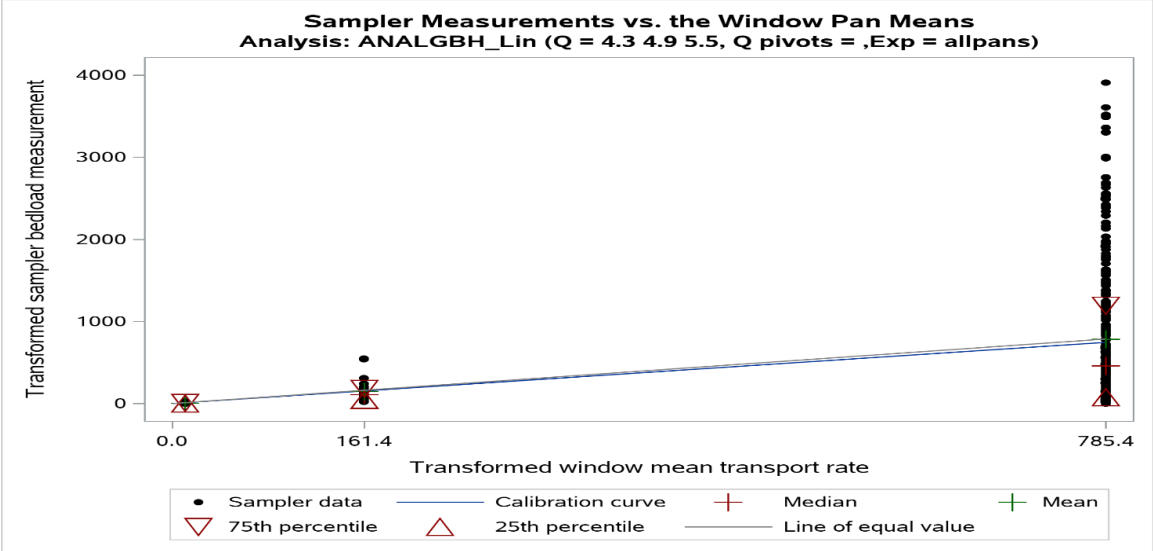

Appendix 2B: Plot depicting data produced by the BLH-84 sampler deployed over a gravel bed generated by the modified T-L model using real space data for All Pans and the Infinity Window.

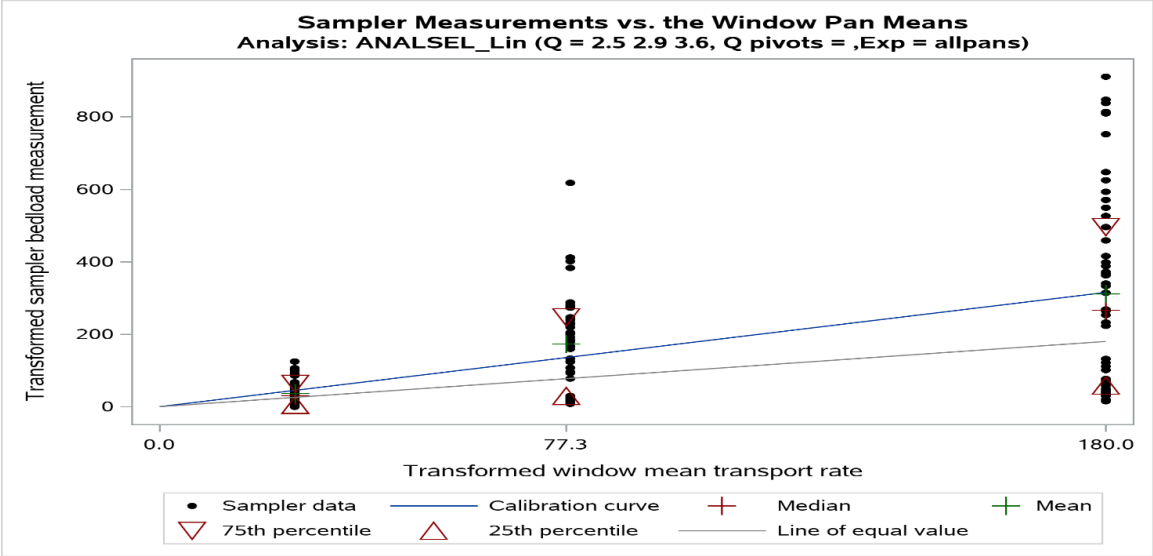

Appendix 2C: Plot depicting data produced by the Elwha sampler deployed over a sand bed generated by the modified T-L model using real space data for All Pans and the Infinity Window.

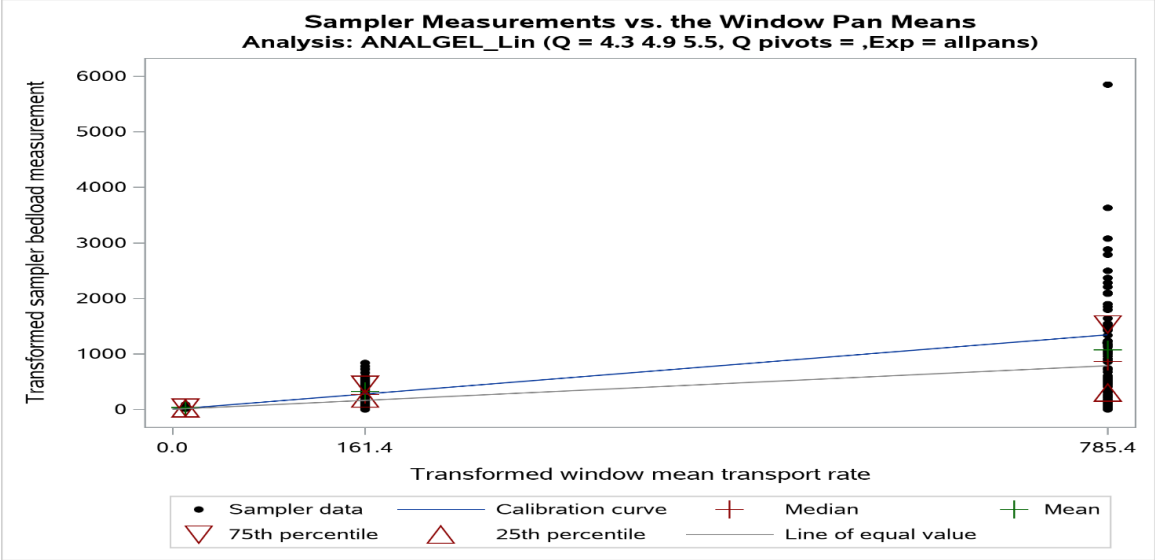

Appendix 2D: Plot depicting data produced by the Elwha sampler deployed over a gravel bed generated by the modified T-L model using real space data for All Pans and the Infinity Window.

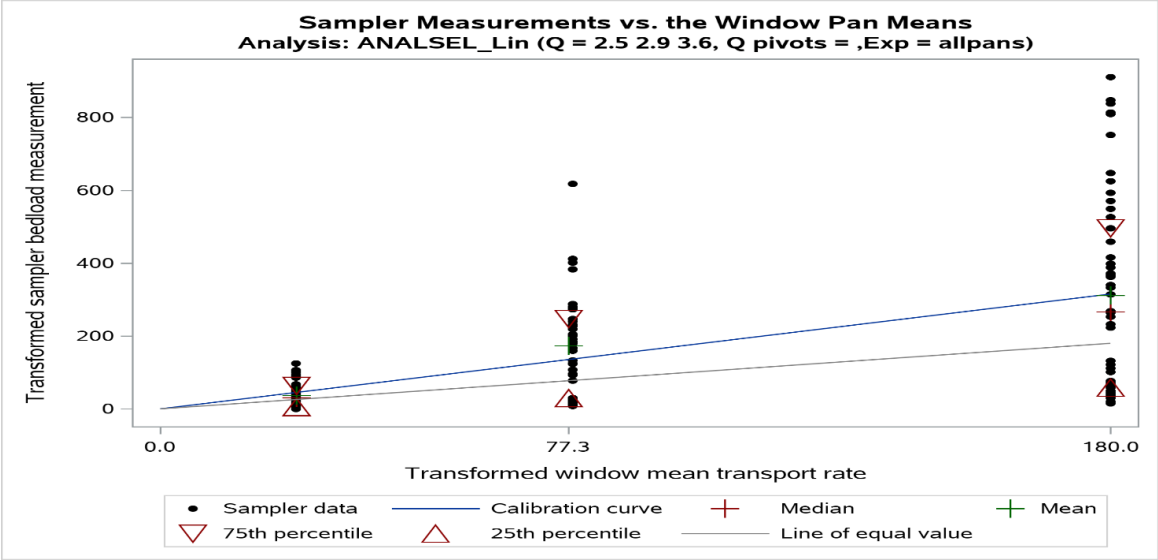

Appendix 2E: Plot depicting data produced by the Helley-Smith sampler deployed over a sand bed generated by the modified T-L model using real space data for All Pans and the Infinity Window.

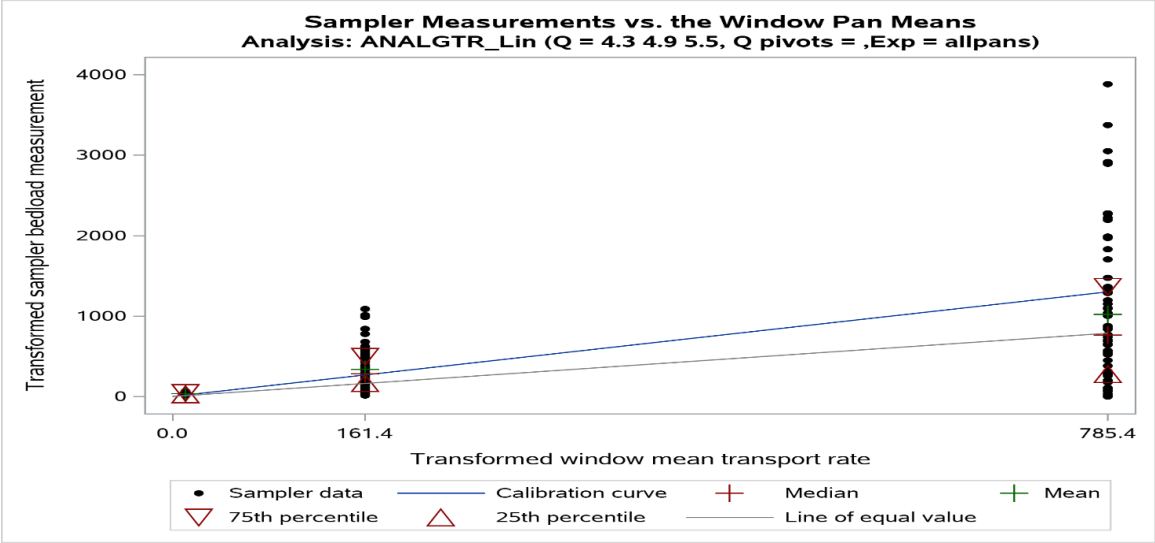

Appendix 2F: Plot depicting data produced by the Toutle River-2 (TR-2) sampler deployed over a gravel bed generated by the modified T-L model using real space data for All Pans and the Infinity Window.